TITLE The Influence of the Dimensional Factors on the Mode of Yielding and Fracture in Medium-Carbon Steel

AUTHOR Julius Miklowitz

UNIVERSITY of Michigan DATE 1948

DEGREE Ph.D. PUBLICATION NO. 1255

THE INFLUENCE OF THE DIMENSIONAL FACTORS ON THE MODE OF YIELDING AND FRACTURE IN MEDIUM-CARBON STEEL

by

Julius Miklowitz
Ann Arbor, Michigan
November, 1948

A Dissertation Submitted in Partial Fulfillment of the Requirements for the Degree of Doctor of Philosophy, in the University of Michigan.

Committee in Charge:

Associate Professor F. L. Everett, Chairman
Professor E. L. Eriksen
Professor J. Ormondroyd
Mr. P. F. Chenea
Professor W. E. Lay
Assistant Professor R. F. C. Bartels

ACKNOWLEDGMENT

Acknowledgment is expressed to Dr. A. Nadai of the Westinghouse Research Laboratories for his guidance in this work. Thanks are extended to Mr. Julius Aronofsky also of the Westinghouse Research Laboratories for his contributions in the testing program and the analysis of the largest round bars. The author appreciates the interest of Professors P. L. Everett and I. Wojtaszak of the Engineering Mechanics Department in the University of Michigan.

The comments of Messrs. W. T. Lankford and T. . Garvey of the Carnegie-Illinois Steel Corporation are appreciated.

Acknowledgment is due the David Taylor Model Basin for permission to publish the test results of Part I and to the personnel there for the help received in the testing of the large bars.

C O N T E N T S

PART I

THE GEOMETRY AND SIZE OF THE FLAT TENSILE BAR

PART II

THE SIZE OF THE ROUND TENSILE BAR

PART I

THE GEOMETRY AND SIZE OF THE FLAT TENSILE BAR

INTRODUCTION

Local necking in the flat tensile bar is a rather unfamiliar subject. As observed in this work, the neck that develops is quite complicated, being characterized by a cross-like depression in the flat sides of the bar. The center of this cross, seen on the face of the bar, has its position on the longitudinal centerline. The greatest depression is a property of the center, the minimum section of the bar passing laterally through this point. Fracture usually starts at the cross center, or in its immediate vicinity. Figure 1 presents a typical case of cross necking in the flat bar. The cross is shown in five stages of its development. The more intense lighting, as necking progresses, is reflective of the higher degree of strain involved in each successive stage. Failure was impending in stage 5.

This part[1] presents the results of a study of this complicated mode of yielding and fracture, focus being on the influence of geometry and size of test bar. The

---

1. The experimental work of this investigation was carried out at the Westinghouse Research Laboratories, East Pittsburgh, Pa. during 1945 and 1946, under a contract with the David Taylor Model Basin of the Navy Department, Bureau of Ships, Washington, D. C.

reader will easily recognize the importance of the two major divisions in the work. The facts, learned in the first part, have been logically extended and used to formulate explanations of the observed phenomena in the second. The first section presents the yielding, that occurs in the bar, reflected in the portion of the stress-strain diagram usually called the uniform strain region.[2] The second section deals with the strain distribution in the neck at fracture. The writer has found that the initiation of necking is highly dependent on the yielding of the uniform strain region, hence the title given the first division. The study of the final stage of necking, fracture, follows not only chronologically, but logically, as will be seen. One would question the absence of the interim yielding, that is, the progressive stages of necking. The volume of data involved in such a study would be enormous. This fact, plus the time factor connected with this investigation have limited this study to the two major divisions discussed.

It is hoped that the results and explanations presented in the body of this paper, plus the attempted correlation with and discussion of the literature, will

---

2. For the medium carbon steel used in this work, this would be the region of the stress-strain diagram from the point just after discontinuous yielding, to the strain coordinate associated with the ultimate load.

do much toward the clarification of the effects of the well-recognized dimensional factors in yielding and fracture in tensile tests.

The summary offers the reader a review of the highlight findings in this work.

TESTING MACHINES, SPECIMENS AND MATERIAL

Since the specimens were of variable size, a good range of load capacity was necessary in the testing equipment. Four tensile testing machines were employed. The largest was the 300 ton hydraulic Baldwin Southwark machine at the David Taylor Model Basin in Washington, D. C. The other three included a 200 ton hydraulic Baldwin Southwark at the East Pittsburgh Works of Westinghouse, and an Amsler Universal and 10 ton constant-strain-rate machine (screw type) at the Westinghouse Research Laboratories. The tests were of slow speed and the strain rates close enough to neglect any possible speed effect.

The specimen type is illustrated in Fig. 2. The thickness h_o was the same in the 6 specimens of a particular series A, B, or C. In each of these series the width-to-thickness ratio $\frac{b_o}{h_o}$ (in the gage length l_o) ranged from 1 to 10. The gage length-to-width ratio $\frac{l_o}{b_o}$ was 5 in all specimens. In each of the series, the gage length-to-thickness ratio $\frac{l_o}{h_o}$ thus varied over the large range 5 to 50. The radius R was made a constant

factor times the width; $\frac{20}{3} b_o$. This latter factor insured perfect geometric similarity in the size variation, even in the heads of the bars in the approaches to the gage length. Series A had specimens all of which were 3/4 in. in thickness h_o; series B had h_o = 3/8 in.; series C had h_o = 3/16 in.[3]

The steel was supplied by the Carnegie Illinois Corporation. It was an open-hearth, silicon-aluminum killed, fine-grained steel of the following composition: C 0.19, Mn 0.77, P 0.021, S 0.026, Si 0.17. No heat-treating except a stress relief was given the supplied 1-in. X 11-in. plates. The War Metallurgy Committee Report of H. W. Gillett and F. T. McGuire (1)[4] was extremely useful in guiding the selection of a proper steel for this work.

STRAIN QUANTITIES AND THEIR MEASUREMENT

Two local conventional principal strains were measured, namely, ε_2, the strain in the lateral direction parallel to the width dimension of the bar, and ε_3, the strain in the direction parallel to the thickness dimension

---

3. The specimens were so marked that the size and shape of the gage cross section was expressed in the number; for example, in specimen 10A, the 10 denotes the $\frac{b_o}{h_o}$ ratio, and the A the 3/4-in. thickness h_o.

4. Numbers in parentheses refer to the Bibliography at the end of the paper.

of the bar. The strain in the axial direction ε_1, was calculated from ε_2 and ε_3 by use of the equation expressing the constancy of volume;

$$(1+\varepsilon_1)(1+\varepsilon_2)(1+\varepsilon_3)=1 .$$

The strain directions relative to the bar are shown in Fig. 3. These directions are valid during uniform straining. Once necking begins, there is a rotation of the principal directions of strain in the neck, the center of the neck being the only point at which the directions, shown in Fig. 3, would hold. The principal directions of strain at any other point of the neck would have to be determined for each particular point.

Fig. 3 shows the specimen grid used for strain measurements. It was mechanically put on the specimen with the use of a scriber before testing. The spacings of the grid lines differed with the size of specimen. At any particular state of strain, the distribution along any lateral grid line could be found by measuring photographically, or directly, the strained elements of the grid. A scale, divided in hundredths of an inch, was used for this purpose. The value for the local strain in the width direction is given by the relation

$$\varepsilon_2 = \frac{dy'-dy}{dy}$$

where dy' is the strained value of the original dy element. Since a particular dy element (which was dy' after straining) was measured along its lateral grid line, the local ε_2 value was roughly the principal strain; the grid

patterns, in a first approximation, were considered to be indicative of the principal-strain directions. The ε_2 values were plotted at the respective centers of the original elements.

The local ε_3 value was calculated, using the entire thickness of the bar as the element; the strain relation is given by

$$\varepsilon_3 = \frac{h - h_o}{h_o}$$

where h is the strained value of the original thickness h_o at any point of the bar. The maximum value of ε_3 along the thickness dimension, occurred at the center of the bar. Actual measurements, in the case of the square bar, led to this assumption. This mean value of ε_3 then, was somewhat lower than the strain at the bar center ($z = 0$) which it represented. At the intersections of the lateral and longitudinal grid lines, the thicknesses h were measured with special micrometers. The ε_3 values were plotted at the original positions of these intersections. From the smoothed plots of the local ε_2 and ε_3 strains, along any particular original lateral section, the data for plotting the local ε_1 curve was computed.

The average value of ε_2 was also the local value, during uniform straining, since there was no appreciable variation of ε_2 along the width dimension during this

part of the test. It is given by the relation

$$\varepsilon_2 = \frac{b - b_o}{b_o}$$

where b is the strained value of the original width b_o.

The average value of the axial strain is given by the relation

$$\varepsilon_1 = \frac{l - l_o}{l_o}$$

where l is the strained value of the original gage length l_o. It was measured along a particular longitudinal grid line, usually the center line.

The square bar presented a special case in that the local strain ε_3 was not taken as its average value. Longitudinal grid lines were put on the edge or side surface of the gage length, as shown in Fig. 3, and the spacings of these lines after stretching were a measure of the local strain ε_3. The value of this strain is given by the relation

$$\varepsilon_3 = \frac{dz' - dz}{dz}$$

where dz' is the strained value of the original element dz. In the case of the square bar, both the local strains ε_2 and ε_3, as measured on the surface, had to be modified slightly in order to represent the strains at the center of the neck.

THE INFLUENCE OF SPECIMEN GEOMETRY ON THE DEFORMATION CHARACTERISTICS DURING UNIFORM STRAINING; THE CONSEQUENT INITIATION OF NECKING

One readily assumes, in ordinary tensile testing, that the initiation of necking, say in a round bar, is associated with a point of stress concentration in the bar. Further, that when the ultimate tensile load is reached, local necking initiates at the cross section of the bar containing the element that produces the stress disturbance. It is assumed, and in many cases shown to be a fact, that this disturbance is a metallurgical structural defect or a geometrical factor, such as an abrupt change in cross section of the bar. The enormous size of the large specimens in the present work, afforded the opportunity of making a detailed study of local strains $\varepsilon_1, \varepsilon_2$ & ε_3. The results of this study gave evidence of another factor, and a most important one, that enters into controlling the position of the local neck, along the gage length of the bar. This factor is a geometrical one, that associated with the restraint on lateral contraction, due to the specimen heads. The subsequent extension to bars of smaller size, both round and flat, is obvious.

Further, as was noted in this work, this factor of restraint offers the extent of its control on the position of necking as early as the beginning of uniform

straining in the bar.

The local measurements on the large bars (series A) decisively exhibited these facts. The plots of these data nicely bring out that necking came approximately at the mid-section of the gage length, the section most remote from the specimen heads, and hence under the lowest degree of restraint due to the heads. The small deviations from this center position can be attributed to structural defects as discussed above, or even slight discrepancies due to machining. The latter is doubted, since the greatest possible care and accuracy were exercised in the specimen preparation.

It should be remarked, at this point, that although the head restraint here seems to offer the predominant control on the position of necking, it might well be, in another type of steel or section, that the metallurgical defect might be the main factor. It must be remembered that the test bars were cut from 1" X 11" plates of a fine grained, silicon-aluminum killed steel. This steel offers a probable optimum in structure for the tensile bar, as far as homogeniety of section is concerned. The best in "killing" methods, it is assumed, has produced a steel free of large blowhole defects, fine grained, with a good dispersion of the non-metallic compounds. The

large reduction through rolling should have insured an even better breaking down of the non-metallic compounds, along with help in the uniformity of the dispersion of these smaller constituents. The reduction of the intensity of the stress concentrations follows, hence their lesser predominating influence in determining the local of the neck.

Mention should also be made of the stress deviations possible, due to section variations produced in machining. This might be an influencial factor in locating the neck. Also, one must realize that a combination of this and the metallurgical factor, might produce a pronounced stress disturbance.

Finally, one must assume that the totality of the role played by all three factors, head restraint, metallurgical defects and machining variations is to increase the stress to the point necessary for the initiation of necking. Metallurgical and machining defects nil, necking would come at the mid-section of the gage length, under the control of head restraint. Deviations from this mid-section would depend on the intensity of the metallurgical and machining defects and their position; that is, the farther from the mid-section, the more intense the defect or combination of defects have to be.

The head restraint is dependent upon the geometry of the bar, as the results of this investigation show.

Pronounced effects on the restraint intensity were found by varying the width-to-thickness-ratio $\frac{b_o}{h_o}$, keeping the gage-length-to-width ratio $\frac{l_o}{b_o}$ a constant. The gage length-to-thickness ratio $\frac{l_o}{h_o}$ varied from 5 to 50, a range large enough so that effects of this variable could be neglected. Work centered about tests on the large specimens, series A. Their size have enabled the writer to bring out the importance of head restraint in uniform straining, and the consequent initiation of necking.

The complete load stress - conventional strain diagrams for series A are shown in Figure 4. As the section approaches the square from $\frac{b_o}{h_o} = 6$, the entire curve seems to give higher stress values for a particular strain. The fracture load stress seems to decrease for this same range of $\frac{b_o}{h_o}$. Table 1 represents the available data on the two smaller geometric series. The results are not complete, but the trends are similar to those seen in Figure 4. A true interpretation of these stress deviations, it is believed, should be studied from true stress definitions. Further, the state of stress for the particular section would have to be investigated, both for the fracture stress trends and the stresses during uniform straining. The present work, primarily devoted to deformation study, did not enter into these detailed stress studies. The author does believe, however, that the de-

Table 1

Ultimate, Fracture Load Stress and Total Strain as Influenced by Geometry

Specimen No.	h_o	$\frac{b_o}{h_o}$	Ultimate Load Stress Lb./In.^{2}	Fracture Load Stress Lb./In.^{2}	Average Strain ε_1
10B	3/8"	10	65,400	56,600	0.25
7B		7	65,900	56,000	----
6B		6	66,900	------	----
5B		5	64,700	52,000	----
3B		3	63,700	49,200	0.33
1B		1	70,300	51,800	0.36
10C	3/16"	10	63,600	54,000	----
7C		7	64,300	53,000	----
6C		6	66,000	54,700	0.32
5C		5	69,500	56,900	0.31
3C		3	65.200	50,500	0.35
1C		1	71,400	50,600	0.42

viations are connected with the variable restraint from section to section and the so-produced differences in the transverse stresses involved.

The total average strain in both Figure 4 and Table 1 is seen to increase as the section approaches the square. It is obvious from the curve shapes, that the differences are primarily due to the necking component of the total strain; a reflection of the more fully developed neck, as the bar section approaches the square. The detailed discussion of this is reserved for the next section of this paper.

Figures 5, 6, 7 and 8, respectively, represent the detailed strain data of specimens 10A, 7A, 6A and 5A, in

their condition at the ultimate load. The ultimate load points on the diagrams in Figure 4 were not well-defined, since the curves were rather flat. Therefore, the value of the strain at the ultimate load had to be approximated. The interpretation of these data led to the conclusions stated here, on the effects of geometry on uniform straining, and was extremely useful in the analogous restraint problem presented by the local neck of a flat bar.

The figures show the variation of $\varepsilon_1, \varepsilon_2, \varepsilon_3$ and ratio $\frac{\varepsilon_2}{\varepsilon_3}$ along the longitudinal axis of the bar. The condition, with respect to the stress-strain diagram, of each of these bars, in their respective Figures, is given in Figure 4. This is the condition recorded at testing. Slight corrections were applied to these recorded average ε_1 values, to make them agree with the calculated local ε_1 plot in Figures 5 and 8. The larger correction necessary in Figure 7 was probably due to erroneous measurements. Since all plots were made at, or in the vicinity of, the ultimate load, the start of local necking has influenced the values at and near the minimum cross section of the bar. However, the variations all along the bar were certainly not a function of local necking alone. The restraint due to specimen heads shows an influence on both ε_2 and ε_3, and the calculated ε_1 and $\frac{\varepsilon_2}{\varepsilon_3}$ ratio. This conclusion results from the obvious strain

gradients in the curves (change of local strain per unit of gage length). The existence of these gradients was noted at the beginning and all during uniform straining. This latter fact led to the conclusion that the position of local necking is predominantly controlled by head restraint. In other words, these tests with large specimens have shown that a minimum section is produced, actually at the beginning of uniform straining, and that this section remains the minimum throughout the test to fracture. One usually assumes that the formation of the minimum section depends upon local necking. These tests have shown that head restraint produces this minimum section, before local necking takes place and that local necking, when it comes, starts at this minimum section as would be expected. Of course, this control is slightly modified by the metallurgical and machining defects, as explained before.

Closer examination and comparison of the curves yield additional valuable information concerning restraint. The ε_2 and ε_3 values are seen to be a function of the width of bar. This follows from the considerations that the thickness h_o and the gage length-to-width ratio $\frac{l_o}{b_o}$ are constants. Hence, the only variable is the specimen width b_o (we are neglecting $\frac{l_o}{h_o}$, since all its values are extremely large and probably do not offer an apprec-

iable influence on the variation of restraint). A comparison of Figures 5, 6 and 8 indicates that as the bar width decreases, the ordinates of both strains increase, at all positions along the gage length. It might be argued that the differences in the average ε_1 conditions of these bars might have produced the noted effect, instead of the width variation. Table 2, however defeats this argument. Comparison of the head values for the specimens 10A and 5A shows that even if the ε_1 curve of 10A were raised 0.025 unit strain, to meet the condition of 5A, the average ε_1 head value would still be substantially below that of 5A (note underlined values in Table). One must also remember that in the region of the ultimate load, changes in the average strain are more likely to affect the portions of the bar that are beginning to neck. Hence, this difference in average strain, in regions away from the minimum section, has even less meaning in the argument.

Table 2

Effect of Width of Specimen on Local Strain Values at Heads

Local Strain	Specimen 10A (Avg. ε_1 = 0.20)			Specimen 5A (Avg. ε_1 = 0.225)		
	Left Head	Right Head	Average	Left Head	Right Head	Average
ε_1	0.15	0.13	0.14	0.19	0.18	0.185
ε_2	0.062	0.053	0.058	0.078	0.070	0.074
ε_3	0.075	0.063	0.069	0.087	0.083	0.085

The effect of width of bar on the lateral strain ε_2 reflects the growth of restraint in the width direction, as the width increases. This can be explained in terms of the existence of a transverse stress that creates the restraint and the growth of this stress, as the width increases. That the regions near the heads of a flat test bar present a case of bi-axial stress, has been pointed out in the past. Nadai (2), for instance, has given this as a case of the plane problem of the second kind: plane stress, where the stress σ_3 in the direction of the bar thickness is equal to zero. Hence, as the ratio of width-to-thickness of the flat specimen increases, in the variation from $\frac{b_o}{h_o} = 1$ to $\frac{b_o}{h_o} = 10$, the portions of the gage length near the heads approach the conditions of a case of plane stress (a growth of the transverse stress). One can think of the restraint originating at the heads in the square bar as comparable to that in the round bar, where the restraint must be created by equal transverse stresses in all directions perpendicular to the longitudinal axis of the specimen. That the two restraining stresses in the square bar are probably equal follows from the equality of its lateral dimensions. In going from the square bar to the very wide flat bar, the restraint is forced into the plane of the bar, since the thickness dimension is now small

compared to the width, the components of stress σ_y, τ_{xy} becoming predominant in causing the restraint originating from the heads. This explains the restraint effects on ε_2 . It can be shown, where ε_2 is completely restricted, that the transverse stress σ_2 in the width direction is half the value of the axial tensile stress σ_1 . The very wide bar approaches this case.

The variation of ε_3 with width dimension is not completely understood. From the outset it would appear that ε_3 acts opposite to the way the plane stress explanation, given above, would predict. But it must be remembered that the effects being described are those exhibited by a change in $\frac{b_e}{h_o}$ from 10 to 5. The bars in this range are all wide enough, probably, to allow one to assume that the restraining stress in the thickness direction is very small. Therefore, the change in $\frac{b_e}{h_o}$, over this range, would not offer enough of a differential of the stress in the thickness direction, to account for any restraining effects in this direction, regardless of the way the stress changed. In any case, the strain ε_3 in regions near the heads of the bar must depend on the actual values of the principal stresses σ_1 and σ_2 , σ_3 being practically zero.

In all cases, the curves in Figures 5, 6, 7 and 8 show that ε_2 lies below ε_3 , at all positions along the

gage length. This produces an $\frac{\varepsilon_2}{\varepsilon_3}$ value below 1.0, and indicates as one would expect, that the bar is more free to strain in the thickness direction. That $\frac{\varepsilon_2}{\varepsilon_3}$ approaches larger values, as the bar width decreases, is just a reflection of the lesser restraint on both ε_2 and ε_3. $\frac{\varepsilon_2}{\varepsilon_3}$ takes on its lowest values in the vicinity of the heads and minimum section. This suggests that the restraint on ε_2 is more severe in the region of the heads. In the vicinity of the minimum section, the start of local necking offers ε_3 its greatest freedom. This latter point will be discussed in detail later. The large average ε_1 condition for bar 6A (Figure 7) would account for its relatively low $\frac{\varepsilon_2}{\varepsilon_3}$ values in the central region of the bar, because of the necking influence on ε_3.

In Figure 9 the ratio $\frac{\varepsilon_2}{\varepsilon_3}$ is a function of the unit conventional strain ε_1. The note explains how the points were obtained. Striking vertical sections through the curves in Figure 9, at $\varepsilon_1 = 0.03$, 0.05, 0.10 and 0.15, gave data for plotting the curves of $\frac{\varepsilon_2}{\varepsilon_3}$ versus $\frac{b_o}{h_o}$, as shown in Figure 10. Starting from a value of 1.0 for the square section $\frac{b_o}{h_o} = 1$, the $\frac{\varepsilon_2}{\varepsilon_3}$ ratio drops, for all values of ε_1, as the bar section becomes wider. That $\frac{\varepsilon_2}{\varepsilon_3}$ decreases with an increase in bar width, is again the effect brought out by Figures 5, 6, 7 and 8. But, the new point, brought out by Figure 10, is that the drop

of $\frac{\varepsilon_2}{\varepsilon_3}$, with an increase in width, is less severe as ε_1 increases. This means, probably, that ε_2 is restrained the most at the beginning of uniform straining, and that as the test progresses, it becomes more and more free of its restraint. This is true for all geometric shapes. The slopes of the curves in Figure 9 approach smaller and smaller values, as ε_1 increases, with the values zero being reached in the neighborhood of $\varepsilon_1 = 0.15$ or 0.16. From this value to $\varepsilon_1 = 0.20$, practically no change occurs in the slope (curves are flat). Beyond $\varepsilon_1 = 0.20$, the $\frac{\varepsilon_2}{\varepsilon_3}$ values are influenced by the local necking, and its resulting larger relative ε_3 values. The important thing brought out by the slopes is that the degree of the freeing of ε_2, through the production of greater ε_1 values, has a limit. This is apparent from the fact that practically no change in restraint occurs between $\varepsilon_1 = 0.15$ and 0.20. Thus, the curves in Figures 9 and 10 suggest that there is another factor, in addition to geometry, that acts to restrain ε_2. This appears to be an anisotropic condition in the steel. This factor is dependent upon the geometry, however. This follows from the greater spread of points on a vertical section through the curves in Figure 10, as the vertical section is moved to higher $\frac{b_e}{h_o}$ values. Important is the fact that this suggested anisotropic effect breaks down as

the uniform straining progresses, and in reaching the limit of its influence ($\varepsilon_1 = 0.15$), leaves what appears to be the restraint factor of purely geometric dependence.

The above possible anisotropic effects add weight to the importance of the geometric restraint factor, in showing that restraint, due to anisotropy, is magnified by an increase in the geometry ratio $\frac{b_o}{h_o}$. The anisotropy could be connected with the fact that the specimens were cut from rolled plates.

THE INFLUENCE OF SPECIMEN GEOMETRY AND SIZE ON THE STRAIN DISTRIBUTION IN THE NECK AT FRACTURE

Further interest in the flat bar centered on the local straining (necking) in all the specimens series A, B and C. The influence of the size expressed itself through the comparisons made of specimens from all three series, $\frac{b_o}{h_o}$ ratios remaining a constant, similarly, the influence of geometry could be viewed in each and any of the individual series. It should be emphasized again that the gage length-to-width ratio was the constant value $\frac{l_o}{b_o} = 5$, in all specimens.

As soon as the load started to drop off from the ultimate, a cross-like highly strained region began to take definite shape. This region became more and more pronounced as necking continued. Noted was the tendency

toward localization of straining to the immediate vicinity of the deepest parts of the cross, as necking progressed. These parts were the centers of the sides of the cross and the vicinity of the cross center. This localization action proceeded throughout the necking so that, just prior to fracture, the local straining was confined to the very center of the cross. Indications were that fracture started at this cross center, or in its immediate vicinity. Specimen 7C, shown in Figure 14, is definite evidence of this. Testing of 7C was stopped previous to fracture. Other tests gave similar evidence, through the observations made.

Interesting were the two portions of the flat bar in the neck, the centers of which were coincident with the minimum section. Under the action of the straining about them, these regions, trapped between the sides of the cross, were moved in toward the center of the cross as the neck developed. The patterns of contour lines, representing equal thicknesses in the neck of specimen 6A, will help the reader understand some of the statements made above concerning the cross. They are shown in Figure 20. Figure 11, the side view of specimen 5A, gives evidence of the cross sides and the trapped region between them.

The necks of the fractured bars are shown in Fig-

ures 12, 13 and 14; respectively the A, B and C series. In each of the series of photographs, the narrower bars have been magnified to facilitate a true comparison of the neck shape (the width dimension just outside of the neck is the same for each photo). These photographs give evidence of a lesser depth of neck with greater width of bar. Table 3 presents the same story for the series A. It is based on calculations using the relation

$$\text{Avg. } \varepsilon_2 = \frac{b - b_o}{b} ,$$

where b is the final width, along the minimum section, at fracture. The increase of average ε_2, with a decrease in bar width, is brought out by the Table. The photographs denote this effect also.

Table 3

The Influence of Geometry on the Average Strain ε_2 at the Minimum Section of the Neck at Fracture

Specimen No.	Average ε_2
10A	-0.244
7A	-0.258
6A	-0.266
5A	-0.268
3A	-0.310
1A	-0.404

Figure 15 is a plot of the data tabulated in Table 4. They present the most significant results of these tests with regards to the final stage of necking, namely, (i) the maximum of ε_2 and ε_3 increase, as the bar size decreases, for any particular $\frac{b_o}{h_o}$ value, (ii) the maximum of ε_2 has its greatest value at $\frac{b_o}{h_o} = 1$ (square sec-

Table 4

The Influence of Geometry and Size of Specimen on the Maximum Strain Values in the Neck of a Flat Tension Bar at Fracture

Specimen No.	h_o	$\frac{b_o}{h_o}$	Maximum ε_1	Maximum ε_2	Maximum ε_3
10A		10	1.84 x	-0.299 x	-0.497 x
7A		7	1.61 +	-0.300 x +	-0.453
6A	3/4"	6	1.60	-0.297	-0.454
5A		5	1.58	-0.300	-0.450
3A		3	1.72	-0.312	-0.467
1A		1	2.43	-0.447 ①	-0.473 x
* 10B		10	1.54 x	-0.275 x	-0.457 x
7B		7	1.70	-0.283 x	-0.483
6B	3/8"	6	1.78	-0.305	-0.482
5B		5	1.92	-0.335	-0.487
3B		3	2.05	-0.360 x	-0.487
1B		1	2.46	-0.453 ②	-0.471 x ④
10C		10	2.09	-0.332	-0.516
7C		7	2.14 +	-0.322 +	-0.528
6C	3/16"	6	1.81	-0.310	-0.483
5C		5	2.03	-0.340	-0.500
3C		3	2.16	-0.343 x	-0.517
1C		1	2.92	-0.513 ③	-0.477

(*) Series B shows nicely the geometric influence on ε_2 & ε_1.

(x) Size trend variations, but if the average of each of these pairs is compared with the remaining specimen of its size series, the size effect is apparent.

(+) Geometry trend does not show, but if the average value of each of these groups is compared with the other members of its geometrical series, the geometrical effect is obvious.

①, ② Pure anisotropic effect.

③ Pure anisotropic effect, but the reverse of that shown at ① and ②. This is probably due to a mistake in directions during machining. The specimen was very small and this could have easily happened, since it was taken from a 1" x 11" bar.

④ These appear to be same, but on basis of ③, ε_3 and ε_2 should be interchanged. Hence, if we take (x) into account, we have size effect here too.

tion), and decreases as $\frac{b_o}{h_o}$ increases to 7, for any particular geometric series, and (iii) the maximum of ε_3 is not affected by $\frac{b_o}{h_o}$ variation, in any of the geometric series. That the maximum of ε_2 is not affected by changes in $\frac{b_o}{h_o}$ to the larger values beyond 7 is also suggested by the curves. Maximum ε_1, being calculated from maximum ε_2 and ε_3, shows the size variation of the latter two and the geometric variation of maximum ε_2. There are a few variations in these trends, as Table 4 brings out, but with the help of the notes in the Table, the reader will conclude that the effects stated are definitely there. It must be stated that the value of $\frac{b_o}{h_o} = 7$, which denotes the limit of geometric influence on ε_2, was derived from a smoothening of plots in Figure 15. The trends in Figure 15 and Table 4 fit those evidenced in the data of Table 3 and the photographs of Figures 12, 13 and 14.

In interpreting the above effects, an analogy has been drawn between the action of specimen head on the material adjacent to it that is straining uniformly, and the action of stagnant material in the neck, on the flowing material adjacent to it. As was noted in the foregoing section, the width dimension had a pronounced effect on the strain ε_2 in its direction; that is, the restraint on strain ε_2 increased as the dimension increased.

This same dimensional influence offers an answer for both the size and geometry variations of strain in local necking. Inferred is the fact that the stress in the direction of the restraining dimension increases with the dimension increase.

Consider the maximum of ε_3 first. As the Figure 15 has shown, for any particular geometric series, maximum ε_3 has no dependence on the width of bar. This makes it evident that maximum ε_3 becomes a purely localized factor with respect to bar width. Its dependence on size of bar, for any particular $\frac{b_o}{h_o}$ value is then, actually a dependence on the thickness dimension. The fact that maximum ε_3 decreases, with an increase in bar thickness, suggests the effect of greater restraint with the greater dimension. It must be remembered that maximum ε_3 was measured at the heart of the cross center and that the suggested restraint acting upon it comes from the material around this center that has become stagnant through localization. This use of the restraint analogy will be more clear to the reader with the aid of the following discussion.

Consider the flat bar neck as shown in Figure 16. It represents a very late stage of necking, where the flowing material is all confined to the region in the vicinity of the cross center (Region A). This region

gets smaller and smaller as fracture approaches. Since the material outside of A is stagnant, it offers restraint on the flowing material within A. In the work dealing with head restraint, the restraint dependence on its dimension was found for a constant gage length-to-width ratio ($\frac{l_o}{b_o}$). Consider two bars like that shown in Figure 16 (a), one twice the size of the other. Then in the larger bar, all linear dimensions will be twice those of the smaller. We can assume that the ratio of areas A are roughly 4:1, and that the ratio of $\frac{d}{h}$ will be approximately a constant for the two bars. This is the ratio of a length across A, to the thickness of region A, at the border between stagnant and flowing material. Reference to Figure 16(b) shows the direct analogy is made between ratio $\frac{d}{h}$ of the specimen-like element p, and the gage length-to-width ratio $\frac{l_o}{b_o}$ of the entire flat bar. An increase in the bar size then, (h increases, $\frac{d}{h}$ remaining constant) would affect the local strain ε_3, just as an increase in width of bar affected ε_2 during uniform straining; that is, as h increases, the dimensional restraint increases and ε_3 decreases. This is what the data has shown for maximum ε_3.

The reader will obviously realize that this is by no means a formal explanation of the dimensional restraint on ε_3. This reasoning stems from the desire to explain in detail the analogy used and to give the reader

a physical understanding of the phenomenon. The specimen-like element p, of course, is under a much more complicated stress and strain system than the freer gage length of the bar. A formal analysis would undoubtedly have to consider all the stresses and strains involved. No attempt of this type has been made in this work. The same remarks apply to the following use of this physical reasoning.

The specimen-like element p has really a random position. A similar discussion would apply concerning restraint on ε_3, for any vertical position of the element p in region A.

The analogy can be further extended to describe the size effect on ε_2. Consider the specimen-like element s in Figure 16(b). An increase of twice the size in the flat bars brings with it an increase of approximately two times in the width r of element s, the ratio of length d_1 to width r (an arc length along the circumference of A) roughly remaining constant. Hence, element s has more restraint on it, due to an increase in r. This is a dimensional restraint in the direction of ε_2. The size effect on maximum ε_2, as brought out by the data, has its possible explanation in these terms. Again, it will be recalled, that ε_1 was calculated from ε_2 and ε_3, and hence, necessarily shows the same trends as the latter two.

The importance of the magnitude of restraining dimension on the degree of restraint is nicely brought out by the vast differences in maximum ε_2 and ε_3. These are the differences in maximum ε_2 and ε_3 for any particular specimen, with the exception of the square bars, which did not exhibit the cross-like neck. Further, these differences indicate that small changes in magnitude of the restraining dimension are much more critical on local straining than the same small changes would be on uniform straining. Consider, once again, Figure 16(b). Actually, the restraining dimension r of element s would be one half the circumference of A. The form of s, as shown, best fit into the foregoing discussion, but certainly its disc shape, now proposed, also applies. This makes the restraining dimension r of element s larger than h of element p. Hence, maximum ε_3, with the smaller restraining dimension, has the larger value.

The geometrical influence on maximum ε_2 adds weight to the importance of the magnitude of restraining dimension. For any particular series in Figure 15, the maximum ε_2 value is seen to decrease, as the width of bar increases ($\frac{b_o}{h_o}$ increases, h_o remaining constant). An increase of width of bar makes dimension r, of the disc interpretation of element s, even larger, with respect to h. This follows because as the bar width increased,

local straining covered a larger area for the same stage of necking. Hence, the even greater difference between maximum ε_2 and ε_3, as the width of bar increases, a reflection of greater restraining dimension.

The fact that geometry ceases to influence maximum ε_2, for values of $\frac{b_o}{h_o}$ greater than 7, is significant. This means that a bar width is reached, whereupon maximum ε_2 becomes a purely localized factor. The progression toward complete localization, for both strains ε_2 and ε_3 was obvious, as fracture approached. Through localization, the strains reach higher values, since this action produces smaller and smaller restraining dimensions. So, localization acts to counter-affect increasing the restraining dimension. The fact that maximum ε_2 is a constant for values of $\frac{b_o}{h_o}$ greater than 7, probably means that through localization, a limiting upper value of restraining dimension for ε_2 (like r of Figure 16(b)) is reached, and a further increase of bar width has no effect on increasing this restraining dimension.

Table 5 brings out the important features of Figure 17. The latter shows the variation, with size and geometry, of the strains ε_1, ε_2, and ε_3 along the width, at the minimum section of the neck at fracture. All the bars are represented in the Figure. The remarkable

Table 5

Geometric Restraint During Necking as Expressed by the Maximum and Minimum Strain Values and Their Differences Over the Minimum Section of the Flat Tension Bar at Fracture

Specimen	Ratio $\frac{b_o}{h_o}$	Strain ε_1 Bar Center	Bar Edge (1)	Bar Edge (2)	Bar Edge Avg.	Diff. Center & Edge	Avg. Diff.
10A		1.84	0.62	0.67	0.65	1.19	
10B	10	1.54	0.67	0.65	0.66	0.88	1.18
10C		2.09	0.54	0.72	0.63	1.46	
7A		1.61	----	----	----	----	
7B	7	1.70	0.70	0.70	0.70	1.00	1.25
7C		2.14	0.62	0.68	0.65	1.49	
6A		1.60	0.63	0.63	0.63	0.97	
6B	6	1.78	0.81	0.76	0.79	0.99	0.98
6C		1.81	0.80	0.85	0.83	0.98	
5A		1.58	0.78	0.76	0.77	0.81	
5B	5	1.92	0.79	0.79	0.79	1.13	1.04
5C		2.03	0.87	0.84	0.86	1.17	
3A		1.72	1.07	0.96	1.02	0.70	
3B	3	2.05	1.07	1.02	1.05	1.00	0.92
3C		2.16	1.03	1.18	1.11	1.05	

NOTE: No data obtained for specimens of the $\frac{b_o}{h_o}$ ratio 1.

Table 5

Geometric Restraint During Necking as Expressed by the Maximum and Minimum Strain Values and Their Differences Over the Minimum Section of the Flat Tension Bar at Fracture

Specimen	Ratio $\frac{b_o}{h_o}$	Strain ε_2 Bar Center	Bar Edge (1)	Bar Edge (2)	Bar Edge Avg.	Diff. Center & Edge	Avg. Diff.
10A		0.30	0.21	0.23	0.22	0.08	
10B	10	0.28	0.21	0.21	0.21	0.07	0.11
10C		0.33	0.15	0.15	0.15	0.18	
7A		0.30	----	----	----	----	
7B	7	0.28	0.22	0.22	0.22	0.06	0.09
7C		0.32	0.20	0.20	0.20	0.12	
6A		0.30	0.21	0.21	0.21	0.09	
6B	6	0.31	0.24	0.24	0.24	0.07	0.09
6C		0.31	0.20	0.22	0.21	0.10	
5A		0.30	0.23	0.25	0.24	0.06	
5B	5	0.34	0.27	0.27	0.27	0.07	0.08
5C		0.34	0.23	0.23	0.23	0.11	
3A		0.31	0.29	0.25	0.27	0.04	
3B	3	0.36	0.27	0.25	0.26	0.10	0.07
3C		0.34	0.26	0.28	0.27	0.07	
1A		0.44	0.35	0.32	0.34	0.10	
1B	1	----	----	----	----	----	0.10
1C		----	----	----	----	----	

Table 5

Geometric Restraint During Necking as Expressed by the Maximum and Minimum Strain Values and Their Differences Over the Minimum Section of the Flat Tension Bar at Fracture

Specimen	Ratio $\frac{b_o}{h_o}$	~ Strain ε_3 ~ Bar Center	Bar Edge (1)	Bar Edge (2)	Bar Edge Avg.	Diff. Center & Edge	Avg. Diff.
10A		0.50	0.22	0.22	0.22	0.28	
10B	10	0.46	0.25	0.25	0.25	0.21	0.25
10C		0.52	0.22	0.29	0.26	0.26	
7A		0.45	----	----	----	----	
7B	7	0.48	0.25	0.25	0.25	0.23	0.26
7C		0.53	0.24	0.24	0.24	0.29	
6A		0.45	0.22	0.22	0.22	0.23	
6B	6	0.48	0.25	0.27	0.26	0.22	0.21
6C		0.48	0.30	0.30	0.30	0.18	
5A		0.45	0.25	0.25	0.25	0.20	
5B	5	0.49	0.25	0.25	0.25	0.24	0.21
5C		0.50	0.30	0.30	0.30	0.20	
3A		0.47	0.32	0.32	0.32	0.15	
3B	3	0.49	0.35	0.35	0.35	0.14	0.15
3C		0.52	0.33	0.37	0.35	0.17	
1A		0.46	0.35	0.35	0.35	0.11	
1B	1	----	----	----	----	----	0.11
1C		----	----	----	----	----	

feature of any particular one of these curves is the difference in maximum (at center) and edge strain value particularly in the calculated ε_1 curves. Table 5 brings this out. Note, for example, specimen 10A. Its maximum ε_1 is three times the edge value. 10C shows an even larger difference. These differences, of course, are reflective of the stagnant trapped material between the cross sides. The Figure 17 brings out the differences in ε_2 and ε_3, for a particular specimen, all along the width of the minimum section; that is, that ε_3 has greater values.

Table 5 brings out a significant point, in fact, a verification of a previous statement, that the restraining dimension of ε_2 reaches an upper limiting value at $\frac{b_o}{h_o} = 7$. This was another way of saying that the area affected by local straining, for a particular stage of necking, increases as $\frac{b_o}{h_o}$ increases from 1 to 7, but beyond this value the area remains practically the same. (Area references here are to those of the later stages of necking; like region A in Figure 16). The data of center and edge values of ε_3, and the variation of these average differences with $\frac{b_o}{h_o}$ brings this out. First consider the meaning of the difference. Since maximum ε_3 does not vary with geometry $\frac{b_o}{h_o}$, a greater difference means a lower edge value. The edge value represents a

measurement made at the outer most point of the stagnant trapped material. That these portions of material had no sharp definition, in the local action, is obvious from the curve shapes in Figure 17. The definition, however, was sharper as the bar became wider. This is also apparent in the curves from their flattening at the outer portions, with the greater the bar width. The extent of the localized region, this not being sharply defined, is however, reflected in the intensity of the ε_3 strain at positions along the width, at the minimum section. With this in mind, consider the ε_3 differences for the bars $\frac{b_o}{h_o} = 10$ and 7. They are the same, as Table 5 shows. Now as $\frac{b_o}{h_o}$ decreases from 7 to 1, the ε_3 differences decrease, which means that the edge is closer and closer to the heart of the local action. This is reflective of the limiting dimension of the region of localization (a reminder again, this is a region like A of Figure 16). The fact that the bars of $\frac{b_o}{h_o} = 7$ and 10 show no variation in their ε_3 differences is proof that this late localization has not affected the edge values of either. This suggests that the limiting dimension of the localization region could have been measured approximately, taking bars of $\frac{b_o}{h_o} = 10$, 7 and 6 into consideration. This has not been done, however.

The ε_2 differences in Table 5 bring out the same

effect as ε_3 concerning localization but rather obscurely. The reason is that the restraint factor enters into the picture. As $\frac{b_o}{h_o}$ increases from 1 to 7, the ε_2 differences seem unaffected. But in this case, maximum ε_2 varies with $\frac{b_o}{h_o}$. This is a restraint phenomenon as discussed before. If the edge values for ε_2 are noted, it will be seen that they follow the same trend as maximum ε_2, that is they increase with a decrease in $\frac{b_o}{h_o}$. Hence, the ε_2 differences remain approximately constant. However, the reflection of the limits of localization is in the ε_2 data of Table 5, if one notes that the edge values increase as $\frac{b_o}{h_o}$ decreases and that the average of edge values for the bars of $\frac{b_o}{h_o} = 10$ varies little from that of the bars of $\frac{b_o}{h_o} = 7$.

It must be remarked that the Table 5 has been constructed from Figure 17 and Table 4, hence, only two figures were used in the strain values. Several additional curves have been plotted for specimens 10A and 6A, to cover the distribution of the three strains in the entire neck at fracture. The three sets of curves for specimen 10A are shown in Figures 18a, 18b, and 18c; those of 6A in Figures 19a, 19b and 19c. The ε_2 and ε_3 values are plotted as a function of the original width dimension. A sketch of the distorted grid has been inserted in each of the figures to facilitate location of the proper curve

for a particular section of the neck. Interesting are the maximums in the ε_2 and ε_3 curves on each side of the longitudinal centerline of the bar. They are reflective of the cross-shaped depression. As the sections get farther away from the minimum section, the respective curves denote the approach to the uniformly distributed strain. The curves of bar 10A show that one of the cross sides is deeper than the other. In both specimens, however, a good degree of symmetry with respect to the minimum section and longitudinal centerline of the bar is evident.

The ε_1 curves have been plotted as a function of the original length dimension. The sketch of the distorted grid shows that one-half of the bar has been considered. For symmetry reasons, the other half was not reproduced.

Figure 20 is a perspective representation of the variation of the axial strain ε_1 in the neck of specimen 6A. The strains have been plotted over the bar in its final fractured condition. A quarter section of the bar is shown giving the flat middle surface on its top face and the distorted surface on its lower face. The figure shows the effects of the cross depressions by bringing out the movement of the strain peaks toward the cross center (intersection of the minimum section and longi-

tudinal centerline "FF"). Figure 20 gives the reader a picture of the axial strain distribution at fracture in this flat tension bar. The breaks in the curves are necessary since the fracture causes a gap in the strain distribution. As previously stated, a pattern of contour lines representing equal thicknesses in the neck is also shown in Figure 20. The features of the cross-like depression are nicely brought out by these lines.

In the square bar the values of ε_3 were no longer taken as an average strain over the entire thickness. The local ε_3 strain was plotted as a function of the thickness dimension. The variations of ε_2 and ε_3 in bar 1A, with their respective directions in the minimum section of the neck are shown in Figure 21. The bar maximum ε_1 was calculated as before, from the maximums of the other two strains, which were at the center of the bar. The minimum section at fracture (inserted in figure) shows the highly strained centerlines "EE" and "NN". Measuring lines were put on the outside surfaces of the bar in the longitudinal direction. After straining, the spacings of these lines laterally, which were a measure of strain, were reduced by the factor

$\frac{0.444}{0.467} = 0.95$ in the width, and $\frac{0.427}{0.452} = 0.95$ in the thickness. These were the ratios of the lengths of center lines "NN" and "EE" to the respective outer

dimensions "JJ" and "II". The maximum strain calculations for 1B and 1C, the smaller square bars, were made on the basis of the strains found in 1A. That is, the average ε_2 and ε_3, along sections corresponding to "NN" and "EE" for 1B and 1C, were multiplied by the 1A ratio of the maximum to average strain. In the square bars, the maximum ε_2 approached the value of ε_3 (see Table 4), in fact, in the case of 1C, the ε_2 value was a little larger. These small differences in ε_2 and ε_3, in the square bar are attributed to a probable anisotropic effect in the material. This effect is in the same direction as the anisotropy noted in the work dealing with uniform straining. However, since it was explained that the latter type of anisotropy broke down at the larger values of uniform strain ε_1, it must be assumed that the anisotropy evidenced here, on the maximum strains ε_2 and ε_3, is of another type, possibly connected with large strains. Both anisotropic effects are probably connected with the plate rolling. The fact that specimen 1C shows its difference in an opposite direction to that of bars 1A and 1B is probably due to an error in the orientation of dimensions during machining. This has been explained in note (3) of Table 4.

The fractures, shown in Figures 12, 13 and 14 were interesting. In the cases where $\frac{b_o}{h_o}$ was 5 or above, the

fracture was of a shear type, the noted angle being between the surface of failure and the flat sides of the bar. The intersections of this surface with the faces of the bar were rough lines, the mean of which were approximately at right angles with the tensile axis. Even in the bars which had $\frac{b_o}{h_o}=3$, the signs of shear failure were present, but a tensile-like tear was mixed with it. The square bars showed fractures similar to the usual cup and cone fracture in a round bar. The bars 5A and 6A showed tensile (cleavage type) breaks in the outside portions of the fracture (through the "trapped" regions of the cross). Figure 12 shows that the fracture of specimen 10A (shear type) progressed into a cross side. Specimen 10C exhibits a similar fracture (Figure 14). Bar 10B, however, showed the shear type failure straight across the bar (Figure 13).

Figure 22 is an example of the typical grid distortion associated with necking in the flat bar.

CORRELATION WITH AND DISCUSSION OF THE LITERATURE

Evidence of interest in the size and geometry of specimen in tensile testing dates back to the latter part of the nineteenth century. Some of the results stated above have been found by other investigators, but the literature in general suffers from the lack of detail, especially in the earliest works. This detail was most helpful, in the present work, in the formulation

of the stated interpretation of the effects of size and geometry. The object of the following discussion is not only to bring out the important earlier findings, but an attempt to correlate these findings with the analogous findings of the present work. This has been done even in the cases where the interpretations given would not indicate verification of the conclusions arrived at in this paper.

The real early work in this subject represented, not a focus of attention on local strains, as in the present work, but that on the overall mechanical properties of the bar. Attention was concentrated on determining the shortest possible gage length of specimen of a given cross section, that would not cause a reduction of elongation at fracture. Work by Rudeloff, Martens and others was primarily devoted to this subject. It was found then, that the elongation depended upon, for one thing, the ratio of the gage length to the square root of the cross sectional area of the bar, later given the name "slenderness ratio". Barba, Unwin and Martens found this independently. Later, Moore (3) and Nichols, Taylerson and Whetzel (4) found the same thing. The latter, working with a large number of low carbon sheet steel specimens, report a decrease of from 45 to 30 percent in total elongation at fracture, for an increase of approximately five times in the slenderness ratio. The results of the

present "A" series check these figures rather closely, but with the knowledge of the recent findings in this subject, one must conclude that the slenderness ratio is a rather meaningless quantity, in flat bar work. It completely covers up the essential features of dimensional effects, that is, the effects of varying the $\frac{l_o}{b_o}$ and $\frac{b_o}{h_o}$ ratios. It therefore takes into account no restraint effects of cross sectional shape, to which the writer and others have attached importance. In these early works, the slenderness ratio was a variable that reflected local ductility, but rather obscurely. The higher values of total elongation, at the smaller slenderness ratios, just reflected that local necking is a major factor in strain contribution for the shorter gage lengths. This is the obvious explanation of curves like Figure 3 of the quoted work (4), which shows the leveling off of the elongation value, as the slenderness ratio becomes great, and a rapid increase of the elongation, as the smaller slenderness ratios are approached.

Unwin (5) reports some early findings of Barba (6); namely, that geometrically similar bars of different size deform similarly under equal stress systems, and are geometrically similar after deformation. This later became known as Barba's law of similitude. The results here would disagree. Another early report of Barba (7) shows he found the ultimate strength was not affected by

the $\frac{b_o}{h_o}$ variation from 1 to 8. Over this range the maximum extension came at $\frac{b_o}{h_o}=6$. These results were found for bars of constant gage length. The variation of the width therefore introduced the variation of $\frac{l_o}{b_o}$, which decreases as $\frac{b_o}{h_o}$ increases, for a constant gage length l_o. The ratio $\frac{l_o}{b_o}$ was not a factor in the present work. That this ratio is another important variable in the restraint problem has been noted by others. The above results of Barba, which have the $\frac{l_o}{b_o}$ ratio incorporated in them, do not agree with the more confirmed findings of others. It is of interest to note these.

First consider that the total elongation at fracture is composed of two parts; namely, the elongation due to uniform straining up to the ultimate load and that due to local necking from ultimate to fracture loads. With this in mind, one must conclude, on the basis of more recent works, the findings of Barba on elongation show an opposite effect to the expected. Gensamer (8), for instance, in work with thin gage sheet metal, points out the extreme variation from simple tension deformation, when a flat specimen begins to neck. He notes the large decrease in reduction of area at fracture, due to an increase in width and the resulting necking differences. Little influence was found on the uniform strain. Assuming then constant uniform strains

in Barba's work, the necking differences should have produced an opposite effect to what he found. Further, work by Mac Gregor (9) shows this same trend. On flat bars of $\frac{b_o}{h_o} = 2$, where l_o was varied from 2 to 8 inches, both the true fracture strain[5] and true local necking strain were reduced when the length became less. A similar phenomenon of restraint in round bar work, has been called the "notch effect". MacGregor (10) shows experiments with annealed SAE 1112 steel, in which the gage length was varied from that of a $\frac{1}{4}$" U notch to $3\frac{1}{2}$ inches, bar diameter remaining constant. He noted a considerable decrease in reduction of area at fracture, as the length became smaller. That the restraint effect enters, is clear. Both quoted works (9) and (10) agree with (8), in that this "notch" type of restraint influenced only the local strain. Wood, Duwez and Clark (11) also offer results along these lines. Their work, with small specimens of cold rolled steel, showed for a gage length-to-diameter variation of from 6.7 to 26.6, an increase in the percent reduction in area at fracture of from 53 to 64 percent.

One can deduce from the above discussion, the factor of notch restraint gives the slenderness ratio an even

---

5. Definition of this term and other stress-strain terms of logarithmic character, can be found in quoted paper (9).

greater degree of obscurity, in ductility work. We would logically expect that differences in notch restraint, produced by variations in the slenderness or $\frac{l_o}{b_o}$ ratio, would be of the same order since the two quantities are dimensionally analogous. One must realize, however, that unless proper values for either (very low values) are selected, the notch restraint will not show up in plots of total elongation against the ratio. Covering up this effect will be the fact that for short gage lengths (but long enough for a well-developed neck) the strain due to necking is a large portion of the total strain. In other words, although the restraint increases, as the slenderness or $\frac{l_o}{b_o}$ ratio decreases, if these ratios are in a range such that local necking is a large factor in the total elongation, the usual plot of the latter against the ratio will show an increase in total elongation, as the ratio decreases. Hence, notch restraint would be completely covered up.

These facts are brought out nicely by a comparison of the results of (4) with those of (8) and (10). In the latter, extremely small $\frac{l_o}{b_o}$ and $\frac{l_o}{d_o}$ ratios were used (d_o is diameter). The $\frac{l_o}{b_o}$ ratio in (8) was as low as 1/6, whereas in (4) values of the slenderness ratio were 5 and above. The quoted work (11) brings out that the notch restraint is present even in real large gage

lengths, but as would be expected, the variation over the range of the large values is small. The elongation values are also given in the work (11) for this same variation of $\frac{l_o}{d_o}$ (6.7 to 26.6). They are seen to decrease from 9.0 to 3.4 percent. This would be the effect presented by an elongation-slenderness ratio plot, and if solely presented could give no indication of notch restraint.

One sees, then, as has been realized more recently, the need for more detailed ductility indices. The shape of section, its particular dimensions, along with the gage length, are important in restraint influences, as has been noted in this work and by others. The breaking down of the total elongation into its uniform and local strain components is fundamental.

A few of the other early works deserve mention. Unwin (5) in his work with ship and boiler plates found an increase in elongation for a greater width, thickness constant. Here again, a constant gage length was employed. The effect is opposite to the expected. In the same group of tests, he found for bars of constant width, an increase of uniform elongation, when the bar thickness was increased. Since the increase in thickness means a decrease in $\frac{b_o}{h_o}$, and since there is a constant $\frac{l_o}{b_o}$ ratio in these latter tests, they indicate similar trends as shown here. Beare and Gordon (12), working with mild steel and rolled copper, found for

$\frac{b_o}{h_o} > 2$, a greater reduction of area in the neck at fracture, as the bar became smaller. They also note a decrease in reduction of area, as $\frac{b_o}{h_o}$ increases up to 7. Beyond this value, small effects were found. Beare and Gordon were not clear as to their treatment of $\frac{l_o}{b_o}$ however. Templin (13) ran tests on flat bars of soft aluminum sheet. $\frac{b_o}{h_o}$ was varied from 1 to 50. A 25 percent reduction in elongation, over this range, was found, as $\frac{b_o}{h_o}$ became greater. In hard aluminum, an even greater reduction was found, 75 percent over the range. The $\frac{l_o}{b_o}$ was constant here. The results are in line with the present findings. Lyse and Keyser (14) found definite effects on the elongation and reduction of area due to size and shape of specimen. The reduction of area values, plotted over the $\frac{b_o}{h_o}$ range 1 to 4, showed a decrease as the $\frac{b_o}{h_o}$ ratio became larger. The greater reduction of area for smaller specimen of a particular $\frac{b_o}{h_o}$ ratio, was also shown. The material was a structural steel. The elongation plots were mixed with the effect of the constant gage length, and the fact that elongation values were calculated on the basis of a length one-half of this gage length, placed symmetrically about the fracture position. These are really local strain values then, reflective of necking. That they show an increase as $\frac{b_o}{h_o}$ increases from $\frac{1}{4}$ to 4 is easily understood. Noted in the present work was the

fact that the intense localization region increased as $\frac{b_o}{h_o}$ increased up to 7. Hence, Lyse and Meyser were measuring elongation values that had more and more local strain character, as $\frac{b_o}{h_o}$ increased to 4.

The more recent investigations give evidence of greater detail in ductility study. A great deal of work during the past war was devoted to studies of this nature. Dorn and Finch (15) show a plot of percent reduction against width for the width, thickness and area values. The greater widths had more of an effect on width reduction than it did on thickness. Less reduction for greater width followed the trends stated here. The fact that reductions in width were greater than in thickness for any particular width is not understood, unless the magnesium material offers the explanation.

MacGregor has contributed several papers in which he has stressed the importance of local ductility indices. In his work with flat bars of low carbon steel (9), the $\frac{b_o}{h_o}$ was varied from 1 to 26. He noted that the type of fracture changed from a typical transverse tensile fracture to a shear fracture inclined at an angle of 25 degrees to the perpendicular of the tensile axis, at approximately $\frac{b_o}{h_o} = 6$. That the flat bar presents a bi-axial state of stress with transverse restraint was stated in MacGregor's work. The value $\frac{b_o}{h_o} = 6$ was given

special significance. The ductility value trends are given for the group $\frac{b_o}{h_o} < 6$ and $\frac{b_o}{h_o} > 6$. The variations in local strains found for both of these groups are in line with the present findings, that is, a decrease in local strain for an increase in $\frac{b_o}{h_o}$. That an increase in $\frac{b_o}{h_o}$ from 8 to 26 had no effects on the localized axial strain at fracture, was noted. The results of the present work indicate no special significance for $\frac{b_o}{h_o} = 6$ in the fracture mode. No abrupt change from a tensile to shear type fracture at the 25 degree angle was noted for this value. Most of the shear surface angles were visible only on the bar edges. The bars 10A and 10C of this work showed signs of the shear angle noted in the quoted work.

Low and Prater (16) have noted the differences in strains ε_2 and ε_3 during uniform straining in their flat bars of sheet aluminum. They have stated that the natural strains ε_2 and ε_3 are respectively $0.4\,\varepsilon_1$ and $0.6\,\varepsilon_1$ up to the point of necking. They observed that during necking, very little change took place in width dimension and further reduction in area resulted mainly from thickness changes. Where considerable necking took place previous to fracture, they found ratios as low as 0.1 for $\frac{\varepsilon_2}{\varepsilon_1}$ (natural strains). A study of effect of specimen dimensions on elongation to fracture is presented. For several widths, curves of lateral contraction along the gage length are shown. The curves

show the effect of head restraint for several $\frac{l_o}{b_o}$ ratios. However, the data is scattered, and the writers have assumed that the head restraint influences only a short portion of the gage, that adjacent to the heads. An average value of lateral contraction is plotted for the supposedly free part of the gage length. The restraint could have been interpreted as affecting the whole gage length, had a smooth curve been drawn through the scattered points. The writers conclude that the percent of uniform lateral contraction is independent of width, which is not in agreement with the present work. They note that a greater percentage of the gage length is under restraint influence when $\frac{l_o}{b_o}$ is amaller; the variation of $\frac{l_o}{b_o}$ from 0 to $\frac{1}{2}$ leaves no part of the gage length unrestrained. At $\frac{l_o}{b_o} = 4$, they claim 0.8 of the gage is free from restraint. The results of the authors' tests indicate a farther reaching restraint influence.

Bibber's (17) work with flat bars of ship steel commands notice. He tested wide bars of very short and very long gage lengths. He found a cross-like depression in the neck similar to the one exposed here. A contour plot for one of his long specimens showed only one cross side. He noted failure in a short specimen came about by shear at the center and a tension type break at the outer parts of the bar width. This was noted in a few cases here.

Gensamer, Lankford and Prater (18) have contributed data on the size effect in ship plate. They used an 8 inch gage length of $1\frac{1}{2}$ x $\frac{1}{2}$ inch cross section and reduced this to $\frac{1}{4}$ and 1/20th size, geometric similarity in all dimensions remaining. They discuss the variations encountered due to the metallurgical difficulties in producing true size specimens. They do show data based on reduction of area values that would confirm the size effect as written here, if one can rely on equal hardness values as reflective of the elimination of the effects of heat treatment and rolling.

From what has been presented, it seems that the more free type of neck would come about by making the $\frac{l_o}{b_o}$ ratio of the flat bar, or $\frac{l_o}{d_o}$ ratio of the round bar larger. At times this is not possible, since the form and size of material, or size of specimen and testing equipment, may be such as to prevent making the ratio large. The latter was the reason for selecting the value 5 here. This is one half the value of the German standard adopted several years ago. Even with a ratio of only 5, the largest specimen in this work reached the length of approximately 11 feet.

SUMMARY

The body of this paper brings out the extreme importance of the head restraint in a flat tensile bar, as a factor in controlling the position of the local neck along the gage. The fact that this control is exercised at the beginning of and throughout uniform yielding is emphasized. The data here indicates that with metallurgical and machining defects absent, the head control places the local neck at the middle of the gage length.

It has been found that the head restraint is dependent upon the width dimension of the bar; that is, it becomes more intense as the width increases. The large bars used have shown that the increase in width has reduced the lateral strains during uniform straining, in both the width (ε_2) and thickness (ε_3) directions of the bar. It has been argued that this, in the case of the strain in the width direction, is due to a building of the transverse stress, an implication of the approach to the plane stress problem. The greater freedom of strain in the thickness direction over that in the width is apparent. The ratio $\frac{\varepsilon_2}{\varepsilon_3}$ shows lesser values for greater widths. The fact that $\frac{\varepsilon_2}{\varepsilon_3}$ shows its lowest value at the lowest uniform

strain (axial ε_1), for any particular geometric shape (width-to-thickness gage ratio $\frac{b_o}{h_o}$), and that this value builds steadily as the uniform straining increases, suggests a possible anisotropic restraint factor on ε_2, which is broken down through yielding. The greater variation of $\frac{\varepsilon_2}{\varepsilon_3}$, it is noted, due to this effect of anisotropy, comes with an increase in bar width. This suggests dependence of the anisotropic restraint on the width.

The local neck in the flat bar work here was complicated, but symmetrical in shape. The details of this cross-like depressed region have been reviewed. A detailed study of the local strains in this neck at fracture has been made, together with the progressive localization tendencies of these strains prior to fracture. The maximum values of the strains ε_2 and ε_3 and the dependent ε_1 value (calculated from ε_2 and ε_3), in the neck, at fracture, showed an increase, as bar size decreased. Further, the maximum ε_2 decreased, as the bar became wider, up to a $\frac{b_o}{h_o}$ ratio of 7. Beyond this value no effects were noted. Maximum ε_3 showed no dependence on bar width. Maximum ε_1 necessarily showed the geometry trend of ε_2. The effect of the magnitude of the restraining dimension on the head restraint in uniform straining has been analogously extended and used to explain the variations stated above for the

local strains. A direct analogy has been made between the head restraint on uniform strain in the gage length, and that in the neck of the stagnant material on the flowing material adjacent to it. An increase in the stress, in the direction of the restraining dimension, with an increase in the magnitude of the dimension is implied. A detailed explanation for the variations in local ε_2 and ε_3, due to size and geometry of the bar, has been worked out on the basis of this restraining dimension variable. The importance of the restraining dimension is stressed in the huge differences of maximum ε_2 and ε_3, the latter always greater, and the difference increasing with increase of bar width. That the magnitude of restraining dimension is more critical in local straining than in uniform straining, follows from the recognition of these differences.

The progressive localization of straining toward the heart of the neck, as the neck developed, has been studied. Localization acts against the size and geometry variations in that it tends to produce smaller restraining dimensions. This fact has proved helpful in explaining the limiting value of geometrical variation $\frac{b_o}{h_o} = 7$. In explaining this, use has been made of the variations of local ε_2 and ε_3 with bar width, at the minimum section of the neck.

Curves have been included that represent the strain distribution for ε_1, ε_2 and ε_3, in the entire neck

for two large bars, one of $\frac{b_o}{h_o} = 10$, and another of $\frac{b_o}{h_o} = 6$.

A critical review of the literature in this subject is included. Correlation is attempted wherever possible. The lack of detail in the early ductility studies, together with the uninforming interpretations that resulted are discussed. Another restraint variable, not treated in the present work is mentioned. It is that connected with the variation of gage length-to-width ratio $\frac{l_o}{b_o}$. This is related to the "notch" restraint effect noted in round bar work.

PART II

THE SIZE OF THE ROUND TENSILE BAR

INTRODUCTION

Part I of this investigation was devoted to a study of the effects of geometry and size variation on the mode of yielding and fracture in flat tension bars of medium-carbon steel. This work was further extended to include a group of tests on round tensile bars of the same steel where size was varied under geometric similarity.

The local necking phenomenon associated with the fracture of a round tension bar is well-known. It was the purpose of this work to investigate the effects of size variation on this fracture process.

The body of this part reports observations and calculations made on the stress and strain values associated with the progressive necking process and fracture. The size range covered was 16 to 1; the largest specimen reaching a diameter of 3 inches.

TESTING MACHINES, SPECIMENS AND MATERIAL

The testing machines have been discussed in Part I.

The round tensile piece is shown in Figure 1. A series of 10 of these specimens (2 of each size) was used. Later, two additional large bars (specimens No. 11 and 12) were tested. The diameters ranged from 3 to 3/16 inches, a factor of 16, with each specimen being half the size of the one larger than it. Geometric similarity was kept in all by making the gage length 5 times and gage radius 4.25 times the diameter. The larger specimens were undercut 1 per cent in the diameter at the center of the gage length to control the fracture location. To prevent unnecessary stress concentration, the profile of the undercut was made a large circular arc.

The round bars were cut from the same heat of material as the flat specimens of Part I. Billets $4\frac{1}{2}$ x $4\frac{1}{2}$ inches in cross section served the purpose.

THE STRESS AND STRAIN QUANTITIES AND THEIR MEASUREMENT

In the round tensile bar the average true stress in the axial direction on a particular cross section is given by the relation $\sigma = \frac{P}{A}$, where P is the tensile load and A the area of the section when the bar

is under this load. The data for the stress was easily obtained by measuring with micrometers, the particular diameters of interest, after the load was "dropped off" a little from the value recorded. The data on diameters was also useful for calculating the unit conventional strain in the axial direction, since this is given by the relation $\varepsilon = \frac{A_o}{A} - 1$, where A_o is the original area of the strained section A (d_o is the diameter of section A_o). The sections along the bar were circularly marked to facilitate measuring them.

Figure 2 is a copy of Figure 7 of the Davidenkov and Spiridonova paper (1) showing the distribution of the stresses in the minimum section of the neck of a round tension specimen. The maximum-true stress in the axial direction, it can be seen, comes at the center of the bar, the peak of the parabolic function. The relation representing this function is given as

$$\sigma_m = \sigma\left[\frac{R + 0.5a}{R + 0.25a}\right],$$

where a is the radius of the minimum section of the neck and R the radius of curvature, at and near the minimum section, of the contour of the neck in the meridional section. This relation was used in the present work; a and R were measured photographically.

In figure 2, the octahedral shearing stress is seen to be a constant over the entire section. The

octahedral shearing stress is usually defined by the relation

$$\tau_8 = \frac{1}{3}\sqrt{(\sigma_1-\sigma_2)^2+(\sigma_2-\sigma_3)^2+(\sigma_3-\sigma_1)^2}$$

where σ_1, σ_2 and σ_3 are the principal stresses. In the quoted work (1) it was found that at any point in the minimum section, the radial and tangential stresses are equal. The relation for octahedral shearing stress therefore becomes

$$\tau_8 = \frac{1}{3}\sqrt{2(\sigma_1-\sigma_2)^2} \quad ,$$

where σ_1 is the axial and σ_2 the radial or tangential stress. The quantity $(\sigma_1-\sigma_2)$ is called the effective stress and is a constant over the minimum section of the neck. If we denote the effective stress by σ_e, we have $\tau_8 = 0.47\,\sigma_e$. The effective stress is given by the relation

$$\sigma_e = \frac{\sigma}{1+\frac{a}{4R}} \quad .$$

The octahedral shearing stresses in the present work were calculated using these relations.

STRESS AND STRAIN IN THE NECK AS INFLUENCED BY THE SIZE OF BAR

The results of the tests are presented in Table 1. The quantities in this table are plotted in function of the size of specimen (diameter) in Figures 3 and 4. As shown by the large differences in the values of Table 1, the size of test bar influenced the local necking process and the accompanying stress and strain

Table 1

The Size Influence on Stress and Strain in the Minimum Section of the Neck of a Round Tension Bar

Spec. No.	Size (Dia. in.)	Average True Stress at Ultimate Load* Value Lb./In.^{2}	2 Spec. Avg.	Average True Stress at Fracture Value Lb./In.^{2}	2 Spec. Avg.	Maximum True Stress at Fracture** Value Lb/In.^{2}	2Spec. Avg.
5	3/16	81,600	82,100	144,000↑	147,000↑	173,000↑	175,500↑
6		82,600		150,000↑		178,000↑	
3	3/8	78,700	78,700	137,000↓	135,800↓	162,500↓	160,000↓
4		78,700		134,500		157,500	
1	3/4	83,700	84,500	136,000↓	134,500↓	159,500↓	158,300↓
2		85,200		133,000↓		157,000↓	
7	1-1/2	80,200	80,500	***	113,000↑	***	127,000↑
8		80,700		113,000↑		127,000↑	
9	3	79,800	80,100	90,500↑	90,500↑	93,200↑	93,200↑
10		80,300		90,500↑		93,200↑	
11****	3	84,500	84,500	133,800	133,800	155,500	155,500
12****		84,500		(97,800)		(144,200)	

* These stresses were calculated at an axial strain value of 0.22.

** These stresses were calculated by the use of the relations derived by Davidenkov and Spiridonova[1].

*** Specimen 7 was not broken. The comparison of 7 and 8 at the necking load of 100,000 lbs. (just before fracture) is as follows:

	Average True Stress in Min. Section of Neck
Specimen 7	105,500 lbs./in.^{2}
Specimen 8	107,000 lbs./in.^{2}

**** Later tests by Julius Aronofsky.

Table 1

The Size Influence on Stress and Strain in the Minimum Section of the Neck of a Round Tension Bar

Spec. No.	Size (Dia. in.)	Octahedral Shearing Stress at Fracture** Value Lb./In.^{2}	2 Spec. Avg.	Unit Axial Strain at Fracture Value	2 Spec. Avg.
5	3/16	54,200	55,800	1.70 ↑	1.75 ↑
6		57,400		1.80 ↑	
3	3/8	52,600	52,600	1.83 ↓	1.80 ↓
4		52,600		1.76	
1	3/4	53,000	52,100	1.58 ↓	1.52 ↓
2		51,200		1.46 ↓	
7	1-1/2	***	46,700	***	1.05 ↑
8		46,700		1.05 ↑	
9	3	41,300	41,300	0.47 ↑	0.46 ↑
10		41,300		0.45 ↑	
11****	3	51,600	51,600	1.28	1.27
12****		(38,000)		1.26	

** These stresses were calculated by the use of the relations derived by Davidenkov and Spridonova(1)

*** Specimen 7 was not broken. The comparison of 7 and 8 at the necking load of 100,000 lbs. (just before fracture) is as follows:

	Unit Axial Strain in Min. Section of Neck
Specimen 7	0.82
Specimen 8	0.86

**** Later tests by Julius Aronofsky.

features. Over the size increase of 16 times, the variance in average true stress at the ultimate load is slight and no general trend is evident. Since the stress-strain curves were very flat in the vicinity of the ultimate stress, a choice in strain had to be made to compare the stresses at the ultimate load. A unit conventional axial strain of 0.22 was used for the values appearing in Table 1.

Table 1 and Figures 3 and 4 show that with an increase of bar size, the average-true and maximum-true stress at fracture and the unit axial strain at fracture decrease. The octahedral shearing stress at fracture decreases slightly.

These stress and strain values (with the exception of the octahedral shearing stress) have been influenced by the position of the specimen in the original cross section of the billet from which the specimens were cut. Figure 5 shows the cutting plan. Specimens No. 1 and 2 (3/4 in. dia.) and 3 (3/8 in. dia.) were cut from the outside parts of the billet, whereas specimens No. 4 (3/8 in. dia.) and 5 and 6 (3/16 in. dia.) were cut from the central parts. As a check on position, bars A and B, shown in Figure 5 were pulled to fracture. Table 2 gives the results.

Table 2

Influence of Position of Specimen in Original Billet on Stress and Strain in the Minimum Section of the Neck of a Round Tension Bar

Specimen Number	Size (Dia. in.)	Avg. True Stress at Fracture (lb/in.^{2})	Max. True Stress at Fracture* (lb/in.^{2})	Octahedral Shearing Stress at Fracture* (lb./in.^{2})	Unit Axial Strain at Fracture
A (Bar center)	0.357	137,000	155,500	56,000	1.58
B (Bar center)	0.357	140,000	162,000	55,000	1.80

If we assume that the average of values given in Table 2 of specimens A and B are the values of a specimen unaffected by position in the billet, (this specimen lying between A and B) then the stress and strain values at fracture of each of bars 1, 2 and 3 are somewhat high and bars 5 and 6 low. Bar 4 lying between A and B probably was not affected by position. If the values in Table 1 were corrected for position, specimens 5 and 6 would have higher and 1, 2 and 3 lower stresses and strains. A further check on position is given by the specimens 3, 4, 5 and 6. Comparing 3 and 4 in Table 1, 3 shows the higher values; not a great difference, but one that is in line with the tendency shown by position specimens A and B. Comparing specimens 5 and 6, 6 shows the higher values which again is in the right direction.

* Calculated according to Davidenkov and Spiridonova (1).

At a first glance, the differences in the strain values for the 3/8 in. (3 and 4) and the 3/16 in. diameter specimens (5 and 6) might be attributed to the position effect, but if this were so, specimens 1 and 2 (also from the outside of the billet) would have to show larger values than specimens 5 and 6. A glance at the rest of the table verifies the size effect. On the basis of the position influence, specimens 7, 8, 9 and 10 show somewhat low values since they were cut from the center of the $4\frac{1}{2}$ x $4\frac{1}{2}$ billet. Bar 8, being only $1\frac{1}{2}$ in. in diameter as against 3 in. for bars 9 and 10, would be affected more. The position influence is indicated in Table 1. There is an arrow alongside each value indicating how the value should be corrected for position. An upward arrow (↑) signifies a higher and a downward arrow (↓) a lower value. The Table 1 corrected for position shows, in a much more pronounced form, the size effect on stress and strain values. In Figures 3 and 4, arrows similar to those in Table 1 are shown.

The testing of specimens 11 and 12 was contributed by Julius Aronofsky[1] almost 2 years after the

---

1. Research Engineer, Westinghouse Research Laboratories, East Pittsburgh, Pa.

tests on the identical specimens 9 and 10. Premature fracture of the latter two was the reason for additional tests on the largest size bars. As Table 1 shows, enormous differences were found in the stresses and strains between the earlier and later tests. The fractures were entirely different. This will be discussed later. Specimens 11 and 12 came from the same heat of steel as did 9 and 10. The specimen preparation was identical. No position indications are given for specimens 11 and 12. It should be mentioned that the load observations made for 12 are believed to be erroneous, hence the probably incorrect stresses.

The position influence, it was felt, was associated with a non-homogeniety of structure in the billet cross section. The premature fracturing of specimens 9 and 10 gave convincing evidence of this. Figure 6 shows the fracture surfaces of these two large bars. In specimen No. 9, particularly, a lighter ring-like outer region surrounds a dark central region of seemingly different structure. The same, but not as large, central region is shown by specimen No. 10. It was not the purpose of this investigation to enter into the metallurgical details involved, but the outstanding discrepancies, such as the position effect and the abnormal fractures in bars 9 and 10, suggested some research along metallurgical lines.

Schane (2) noted central "dark spots" as they were called, similar to those exhibited by bars 9 and 10, in fractures of smaller specimens of structural steel. It was shown that this condition and the accompanying low ductility were due to a course grain size in the steel in its as-rolled condition.

The perfect cup-and-cone fractures exhibited by bars 11 and 12 (11 is shown in Figure 7), along with their large maximum strain values in the neck at fracture, suggested the search for possible metallurgical causes for the differences observed in the fractures of bars 9 and 10 and the later tests 11 and 12. Comparisons of bars 10 and 11 were made. Cross-sectional slices, taken from points of the gage length of these bars which had undergone 0.20 unit conventional axial strain, served as specimens for producing macroetches. The results are shown in Figure 8(a) and 8(b). A comparison of the sulphur prints of Figure 8(a) reveals a faint square-shaped segregation zone in the case of specimen 10. (The large white spots are due to air bubbles and should not be taken into consideration by the reader). Figure 8(b) exhibits the same slices after they were subjected to another method of etching. The same segregation zone for specimen 10 is evident.

Mention should be made of the fact that the fracture surface of 10 was coincident with a machined line (on specimen for measuring purposes). The possibility that a stress concentration, induced by this machined line, influenced the premature fracture exists. However, specimen No. 9, which had a similar machined line on its gage surface, also broke prematurely and at a strain almost equivalent to that of 10. The line seemingly did not influence the fracture of 9. To eliminate the possibility of influence by machined lines, a photo-grid was used on bars 11 and 12. The author attaches much more importance to the non-uniformity of structure due to segregation as the reason for the premature fractures in bars 9 and 10.

That segregation is an important factor in ductility studies has been pointed out by others. Recent O. S. R. D. work by Mehl, Wells and Fetters (3) and a second report by the first two authors (4) contain information along these lines. Their work entailed a study of the ductility associated with different type fractures in tensile bars of steel used in gun tubes (alloy steels). They defined 4 types of fractures, which, in order of decreasing ductility are the cup-and-cone, angular, irregular and laminated-brittle. The

specimens 11 and 10 of this work would fall into the first and last respectively of the quoted categories. Bar No. 8 of this work, which showed a comparatively low strain value (see Table 1), would probably fit into the "irregular" fracture type. No record of this exists, however. They state that the brittle fracture is commonly caused by the presence and segregation of extraneous refractory inclusions. Mention is made that the inclusions tend to localize into one part of the ingot and are responsible for low ductility.

This then, seems to be a possible explanation for the square-shaped segregation zone and its influence in specimen 10. The shape of the zone was evidently produced by the rolling of the billet. The large number of tests made by the authors (3), (4), showed that only 60 per cent of the tests produced a pure cup-and-cone fracture. Hence, the suggestion that a large number of tests should be made in an investigation of the size effect and that only specimens exhibiting cup-and-cone fractures (optimum ductility) should be compared. In the present work, then, only specimens 11 and 12 (cup-and-cone fractures) along with the smaller sized specimens, have been considered in the plots of Figures 3 and 4.

The distribution of the axial strain in the neck as a function of size is brought out by Figure 9. If

the curve of specimen 1 and that of bars 11 and 12 are compared, the size of specimen seems to influence the strain values all along the gage length (in the vicinity of the deepest portions of the neck) in a manner similar to its influence on the maximum values; the smaller the bar, the higher the strains.

The progressive axial strain diagrams for the specimens 1, 8, 9, 11 and 12 are shown in Figures 10, 11 and 12. The numbered curves in each of the Figures reflect the successive stages of necking. The abscissae of the smaller specimens have not been increased in these Figures. The curves indicate, like in the flat bar work of Part I, that head restraint produces a minimum section before the ultimate load is reached. They also show the localization phenomenon; that is, the straining tends more and more to become restricted to the immediate vicinity of the minimum section of the neck as the necking process continues.

Figures 13(a) and 13(b) show the fractured necks. The smaller specimens have been magnified.

That the size effect is a recognized factor in the plastic flow and fracture of metals has been brought out by others. In a recent survey for the Navy Department of the literature on the fracture problem, Gensamer, Saibel, Ransom and Lowrie (5) mentioned the more important approaches toward explaining size pheno-

mena. Significance is attached to a statistical theory explanation. A paper by Brown, Lubahn and Ebert (6) has a detailed discussion of the pros and cons of several attacks on this work. This, together with a paper by Davidenkov, Shevandin and Wittman (7) do much toward establishing the "Statistical Theory" as the most probably explanation for the size effect. In the quoted paper (6) a complete description of the "Statistical Theory" is presented.

It will be recognized in reading the above literature, that the focus of attention in size phenomena has been directed toward notched bar testing (both bending and tensile) in which a stress gradient is dealt with. Brittle materials under high speeds of testing form the bulk of the work. The paper (6) emphasizes that the size effect is a property of ductile material also.

The present work has brought out a size effect in ordinary uniform tension bars of a ductile material. On the basis of what was learned in Part I, of this paper, the writer favors explaining this influence of size in an analogous manner to that presented for flat bars in Part I. The localization of straining more and more toward the vicinity of the minimum section of the neck, as necking progressed, was brought out by Figures 10 and 11. The production of a thinner

and thinner disc of flowing material at the heart of the neck is probable. Intimation, then, is that the contraction of this disc diameter depends greatly on the lateral stresses in the plane of the disc, which are created by the restraint of the adjacent stagnant material on the disc and which increase with the increase of diameter of the bar (diameter of adjacent stagnant material depends on this bar diameter).

The curves in Figures 3 and 4 seem to indicate that the greatest change due to size variation is in the range of smaller specimens. An actual limit of dimensional influence is suggested by each curve, except the octahedral shearing stress which is only slightly affected in its entirety.

On the suggestion of Dr. A. Nadai, the advice of the metallurgists of the Carnegie Illinois Steel Corporation in Pittsburgh was requested. Messrs. W. T. Lankford and T. M. Garvey of the Carnegie Illinois Steel Corporation expressed the opinion that the size effect, as exhibited here, might have been due to the presence of a small quantity of occluded hydrogen gas in the steel. Mr. Lankford quoted Korber[2], who discussed the possibility that a decrease in hydrogen content with time might be the cause of an increase

---

2. A.S.T.M. Proceedings, Part A, 1937.

in ductility. According to Messrs. Lankford and Garvey, the specimens tested a short time after the steel rolling had a low ductility because of their relatively high hydrogen content. After some time, hydrogen diffused out of the steel and the ductility increased. They believe that the hydrogen diffused out of the smaller specimens with sufficient speed to enable these to show high ductility while the hydrogen in the two 3 in. diameter bars (nos. 9 and 10) had not yet escaped at testing. Contrastingly, the similar specimens Nos. 11 and 12, tested after a time interval of two years, had lost the occluded hydrogen. Statement is made that the time necessary to reach maximum ductility varies roughly as the square of the linear dimensions of the bar cross section.

THE LITERATURE

The amount of literature on the size effect in the static testing of round uniform tension bars is small. As has been stated, most of the work in size phenomena has been directed toward notched bar testing, static and dynamic. Reference (6) covers a great deal of the literature on this.

Lyse and Keyser (8) report early findings of Bach (9) concerned with the size effect in uniform tension testing in round bars. Bach noted that (a)

strength decreased slightly with a diameter increase, (b) elongation was independent of diameter and gage length as long as the gage length-to-diameter ratio remained constant, and (c) reduction in area was independent of diameter. These, of course, are not in line with the present findings. Lyse and Keyser (8) report on their own results that the reduction of area remained constant when bar diameter was varied.

Duwez, Wood and Clark (10) working with annealed copper wires report that stress-strain curves for different sized wires indicate an increase in ultimate strength as wire size decreases. In fact, all stress ordinates along the curves show the same trend. The elongation was not affected by size. The range of wire sizes was from 0.20 to 0.05 in. (4-1).

In a second paper by these authors (11), static tests were run on geometrically similar specimens of annealed SAE 1020 steel. The gage length-to-diameter ratio was 26.6. They varied the size by a factor of 2 only. For comparable hardness values (approximately 73 Rockwell B) they found that (a) ultimate strength increased, (b) elongation decreased, and (c) reduction in area decreased, as bar diameter decreased. The latter two are evidence of a trend opposite to that in the present work. It suggests that perhaps the absolute length of specimen is the important variable.

In other words, with greater size, geometric similarity remaining, the absolute length is larger and possibly this means less restraint due to the heads, over the major portion of the gage length. The authors mention their belief in attributing size variations to a non-uniform distribution of impurities in the different sections. Mention is also made of the possibility that surface characteristics might be more influential in the small specimens (possible greater strength at surface).

SUMMARY

The size of the round uniform tension bar was found to have an influence on the local necking process and its accompanying stress and strain characteristics. Specifically, the test results indicated that the axial conventional strain in the minimum section of the neck at fracture increased as the specimen size decreased (original specimen geometric similarity remaining). The average-true stress in this section and the maximum-true stress at the center of this section at fracture also increased with a specimen size decrease. The octahedral shearing stress, a constant over the section, showed a trend, but not as great, similar to the other stresses. The stress and strain values were influenced by the specimen's original position in the cross section of the billet from

which the specimens were cut. The above-mentioned stress and strain values, with the exception of the octahedral shearing stress were found to be higher in the specimen cut from the outer portions of the billet cross section. Taking this fact into account strengthened the observed size effect.

Metallurgical considerations are taken into account in explaining this position influence. The size effect on the axial strain in the minimum section of the neck at fracture is attributed to a restraint influence of stagnant material in the neck on the localized plastically flowing material adjacent to it. Inferred in this is the reasoning that the stagnant material creates restraining lateral stresses in the plane of the thin plastic disc at the heart of the neck and these lateral stresses increase with an increase in the diameter of stagnant material (or flowing material; at boundary both are same and depend on bar size). The thin disc is produced through localization of straining; that is, the tendency of the straining to become more and more restricted to the immediate vicinity of minimum section.

A review of the available literature on this subject has been included.

BIBLIOGRAPHY - PART I

1. "Behavior of Ferritic Steels at Low Temperatures, Parts I and II," by H.W. Gillett and F.T. McGuire, War Metallurgy Committee Report No. W-78, 1944.

2. "Plasticity," by A. Nadai, McGraw-Hill Book Company, Inc., New York, N.Y., 1931, p. 182.

3. "Tension Tests of Steel with Test Specimens of Various Size and Form," by H.F. Moore, Proc. A.S.T.M., vol. 18, Pt. I, 1918, p. 403.

4. "Tension Test Specimens for Sheet Steel," by J.T. Nichols, E.S. Taylerson, and J.C. Whetzel, Proc. A.S.T.M., vol. 27, Pt. II, 1927, pp. 259-267.

5. "Tensile Tests of Mild Steel; and the Relation of Elongation to Size of the Test Bar," by W.C. Unwin, Proc. Inst. Civil Engr., vol. 155, 1904, p. 170.

6. "Résistance des Matériaux. Epreuves de résistance à la traction. Étude sur les allongements des métaux après rupture," by J. Barba, Mémoirs de la Société des Ingénieurs Civils, Pt. I, 1880, p. 682.

7. Comission des Méthodes d'essai des Matériaux de Construction, by J. Barba, vol. iii, sect. A, Rothschild, Paris, 1895, p. 5.

8. "Strength and Ductility," by M. Gensamer, Trans. A.S.M., vol. 36, 1946, p. 30.

9. "The True Stress-Strain Tension Test - Its Role in Modern Materials Testing - Part I," by C.W. MacGregor, Journal Franklin Inst., vol. 238, 1944, p. 111.

10. "The Tension Test," by C.W. MacGregor, Proc. A.S.T.M., vol. 40, 1940, p. 508.

11. "The Influence of Specimen Dimensions and Shape on the Results of Tensile Impact Tests," by D.S. Wood, P.E. Duwez, and D.S. Clark, O.S.R.D. Report No 3028, 1943.

12. "The Influence of the Width of Specimen Upon the Results of Tensile Tests of Mild Steel and Rolled Copper," by T.H. Beare and W. Gordon, Engineering (London), vol. 112, Sept. 9, 1921, p. 389.

BIBLIO. - Part I cont.

13. "Effects of Size and Shape of Test Specimen on the Tensile Properties of Sheet Metals," by R.L. Templin, Proc. A.S.T.M., vol. 26, Pt. II, 1926, p.378.

14. "Effects of Size and Shape of Test Specimen Upon the Observed Physical Properties of Structural Steel," by I. Lyse and C.C. Keyser, Proc. A.S.T.M., vol. 34, Pt. II, 1934, p. 202.

15. "Properties and Heat Treatment of Magnesium Alloys: Part I- The Effect of Size Upon Tensile Properties of Specimens of Magnesium Alloy Sheet," by J.E. Dorn and D.M. Finch, O.S.R.D. Report No. 1818, 1943.

16. "Final Report on Plastic Flow of Aluminum Aircraft Sheet Under Combined Loads - II," by J.R. Low and T.A. Prater, O.S.R.D. Report No. 4052, 1944.

17. "A Study of the Tensile Properties of Heavy, Longitudinally Welded Plate Specimens Simulating Deck and Shell Joints," by L.C. Bibber, Trans. The Society of Naval Architects and Marine Engineers, vol. 52, 1944, pp. 210-264.

18. "Correlation of Laboratory Tests with Full Scale Ship Plate Fracture Tests," by M. Gensamer, W.T. Lankford Jr., and T.A. Prater, O.S.R.D. Report No. 5380, 1945.

BIBLIOGRAPHY - PART II

1. "Mechanical Methods of Testing - Analysis of the Tensile Stress in the Neck of an Elongated Test Specimen," by N.N. Davidenkov and N.I. Spiridonova, Proc. A.S.T.M., vol. 46, 1946.

2. "Effects of McGuaid-Ehn Grain-Size on the Structure and Properties of Steel," by Phillip Schane Jr., Trans. A.S.M., vol. 22, 1934, pp. 1038-50.

3. "Steel for Gun Tubes - Progress Report," by R.F. Mehl, C. Wells, and K.F. Fetters, O.S.R.D. Report No. 731, July 1942.

4. "Final Report on Steel for Gun Tubes, Part I - The Significance of Angular Fractures," by R. F. Mehl and C. Wells, O.S.R.D. Report No. 1009, Nov. 1942.

BIBLIO. - Part II cont.

5. (a) "Report on Fracture of Metals - Part I," by M. Gensamer, E. Saibel and J.T. Ransom, Welding Research Supplement of the Journal of the American Welding Society, vol. 26, n. 8, 1947, pp. 443s-472s.

(b) "Report on Fracture of Metals - Part II," by M. Gensamer, E. Saibel and R.E. Lowrie, Welding Research Supplement of the Journal of the American Welding Society, vol. 26, n. 8, 1947, pp. 472s-484s.

6. "Effects of Section Size on the Static Notch Bar Tensile Properties of Mild Steel Plate," by W.F. Brown, J.D. Lubahn and L.J. Ebert, Welding Research Supplement of the Journal of the American Welding Society, vol. 26, n. 10, 1947, pp. 554s-559s.

7. "The Influence of Size on the Brittle Strength of Steel," by N. Davidenkov, E. Shevandin, and F. Wittman, Journal of Applied Mechanics, vol. 14, n. 1, 1947, pp. A63-67.

8. "Effects of Size and Shape of Test Specimen Upon the Observed Physical Properties of Structural Steel," by I. Lyse and C.C. Keyser, Proc. A.S.T.M., vol. 34, part II, 1934, p. 202.

9. "Elastizitat und Festigkeit," by C. Bach, Fifth edition, Julius Springer, Berlin, 1905.

10. "Factors Influencing the Propagation of Plastic Strain in Long Tension Specimens," by P.E. Duwez, D.S. Wood and D.S. Clark, O.S.R.D. Report No. 1304, March, 1943.

11. "The Influence of Specimen Dimensions and Shape on the Results of Tensile Impact Tests," by D. S. Wood, P.E. Duwez and D.S. Clark, O.S.R.D. Report No. 3028, Dec. 1943.

FIGURES 1 - 22 PART I

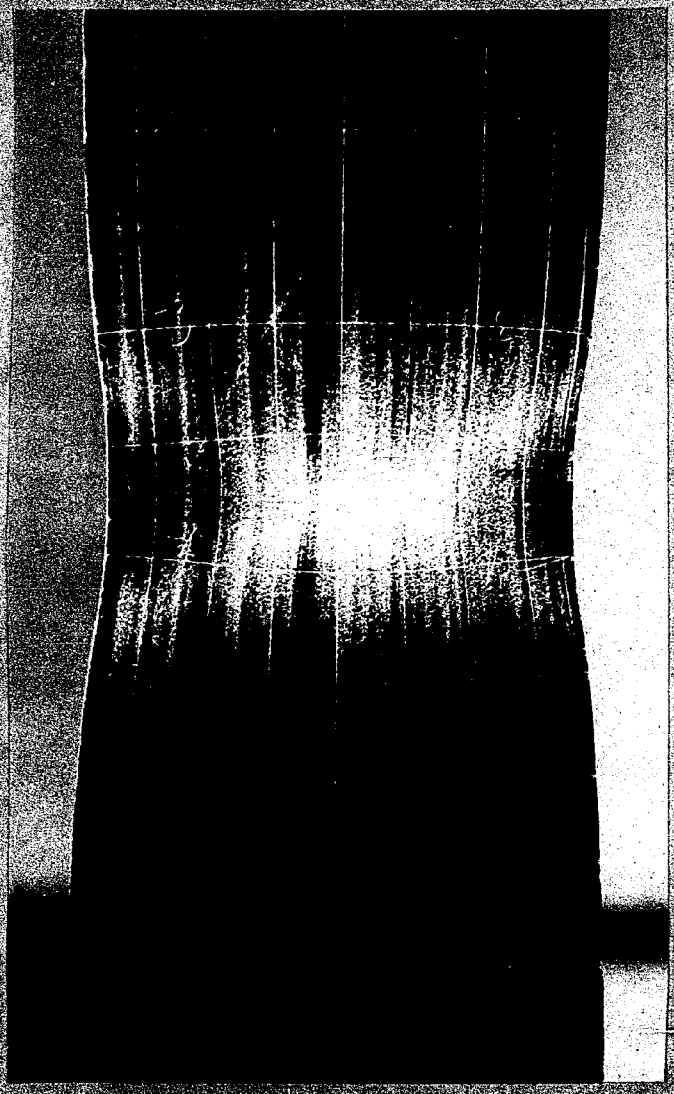

CLOSE UP OF 5

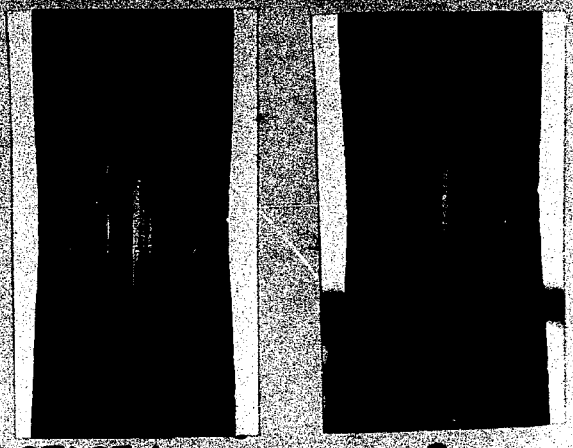

STAGE 1 2

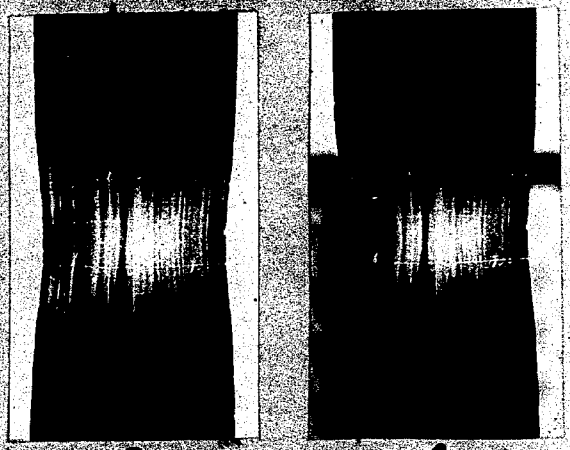

3 4

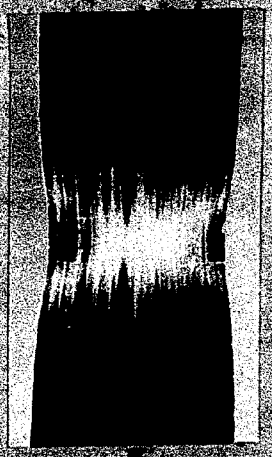

5

STAGES OF CROSS DEVELOPMENT

FIG. 1 THE CROSS NECKING PHENOMENON IN THE FLAT TENSION BAR

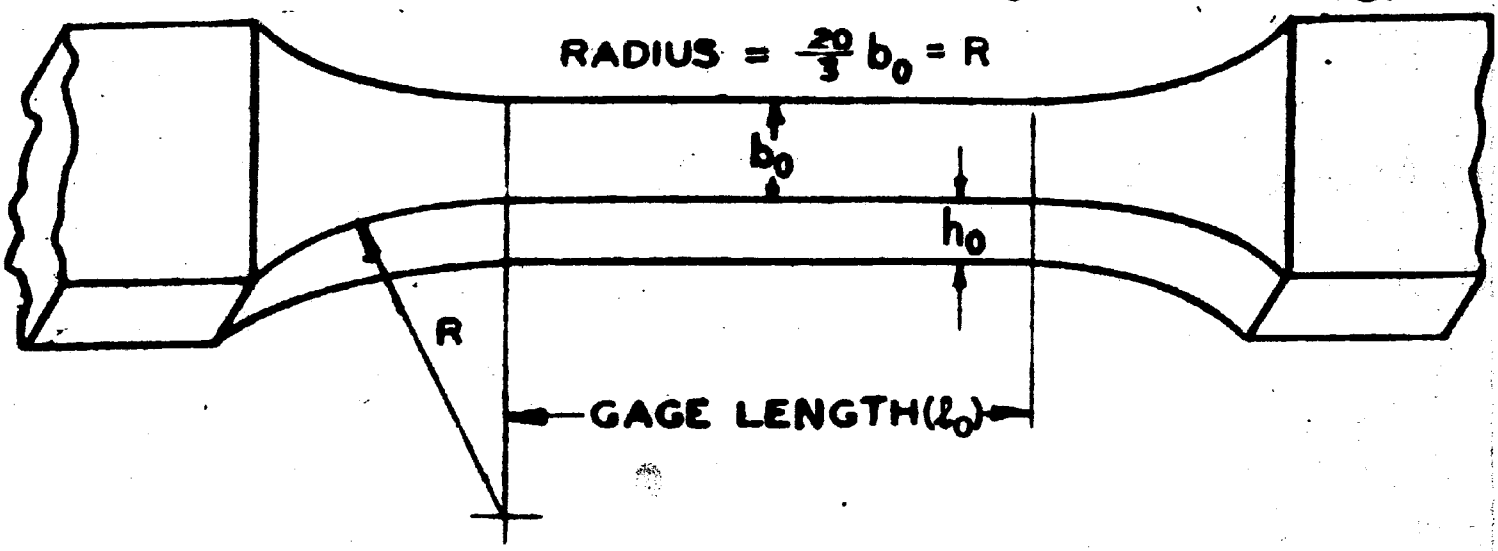

SERIES	SPEC. NO.	DIMENSION (INCHES)				b_0/h_0	l_0/h_0
		h_0	b_0	l_0	R.		
A	10 A	0.750	7.500	37.50	50.00	10	50
	7 A		5.250	26.25	35.00	7	35
	6 A		4.500	22.50	30.00	6	30
	5 A		3.750	18.75	25.00	5	25
	3 A		2.250	11.25	15.00	3	15
	1 A		0.750	3.75	5.00	1	5
B	10 B	0.375	3.750	18.75	25.00	10	50
	7 B		2.625	13.13	17.50	7	35
	6 B		2.250	11.25	15.00	6	30
	5 B		1.875	9.38	12.50	5	25
	3 B		1.125	5.63	7.50	3	15
	1 B		0.375	1.88	2.50	1	5
C	10 C	0.188	1.875	9.38	12.50	10	50
	7 C		1.313	6.56	8.75	7	35
	6 C		1.125	5.63	7.50	6	30
	5 C		0.938	4.69	6.25	5	25
	3 C		0.563	2.81	3.75	3	15
	1 C		0.188	0.94	1.25	1	5

Fig. 2 Dimensions of Flat Bars Used in The Size-Geometry Tensile Tests

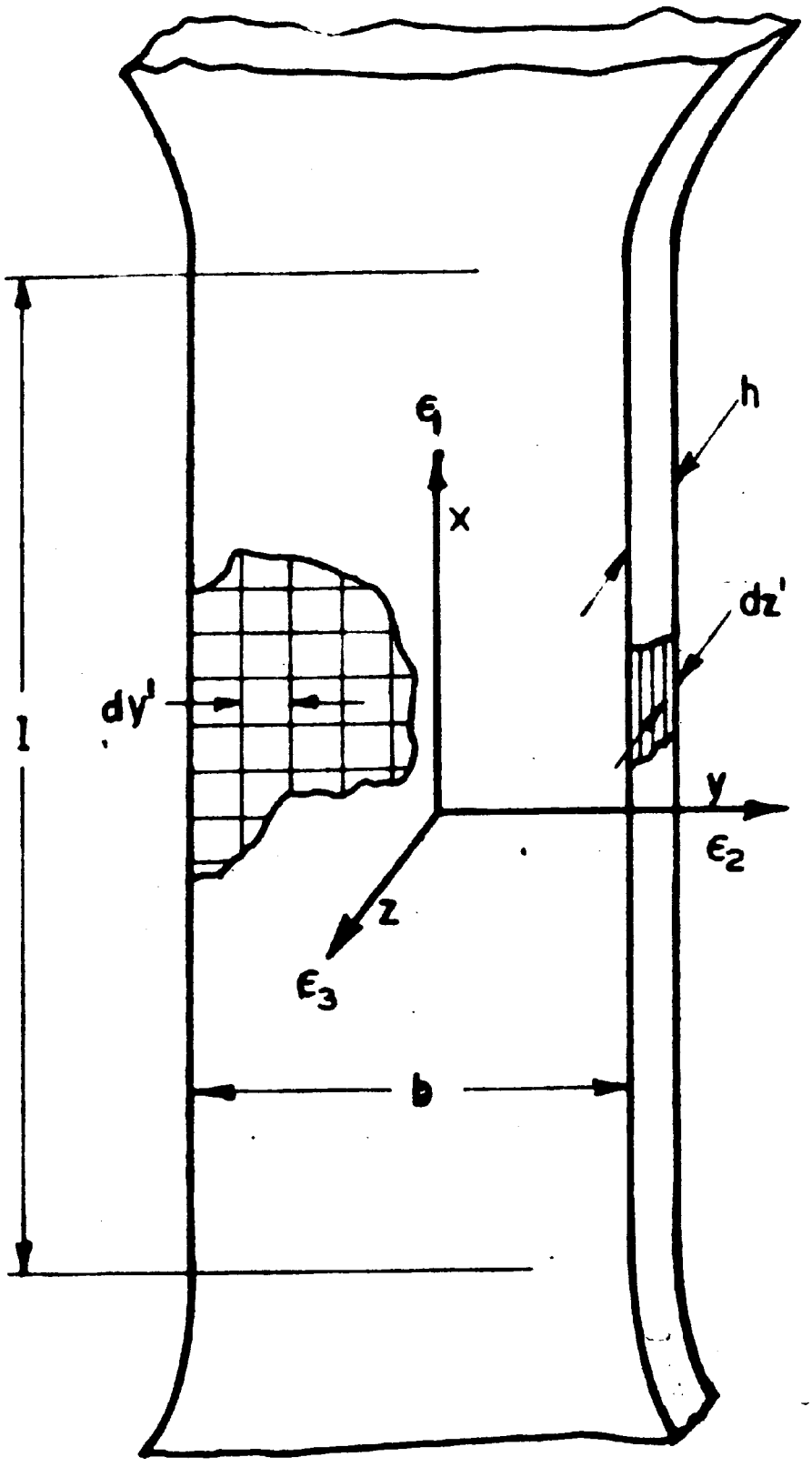

RELATIONS

LOCAL STRAINS:

$$\epsilon_2 = \frac{dy' - dy}{dy}$$

$$\epsilon_3 = \frac{dz' - dz}{dz}$$

$$\epsilon_1 = \frac{1}{(1+\epsilon_2)(1+\epsilon_3)} - 1$$

AVG. STRAINS:

$$\epsilon_2 = \frac{b - b_o}{b_o}$$

$$\epsilon_3 = \frac{h - h_o}{h_o}$$

$$\epsilon_1 = \frac{l - l_o}{l_o}$$

WHERE dy', dz', b, h AND l ARE THE STRAINED VALUES OF dy, dz, b_o, h_o, & l_o RESPECTIVELY.

Fig. 3 Conventional Strain Directions in the Flat Tensile Bar

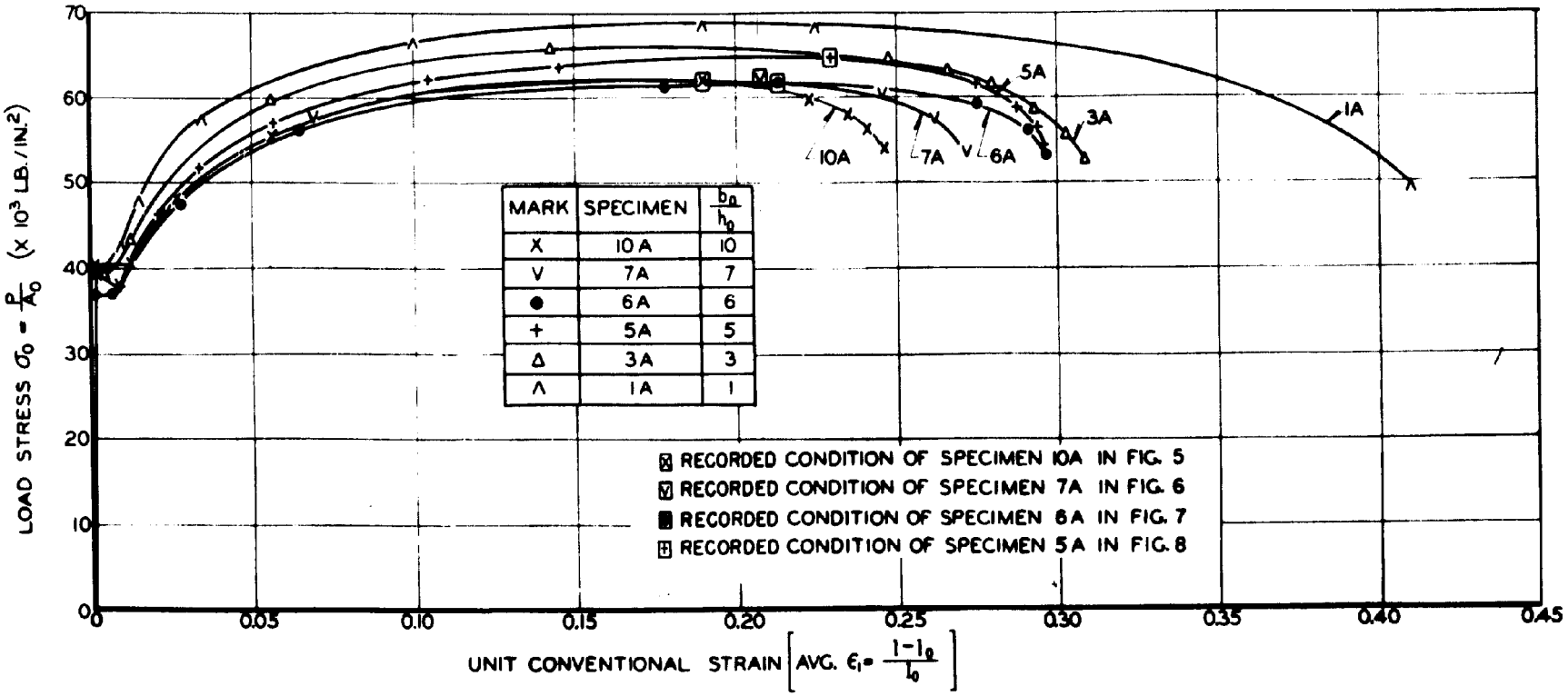

FIG. 4 THE ORDINARY STRESS-STRAIN DIAGRAM AS INFLUENCED BY THE GEOMETRY OF THE FLAT TENSION BAR

(SERIES "A" $h_0 = \frac{3}{4}$", b_0 FROM $\frac{3}{4}$" TO $7\frac{1}{2}$")

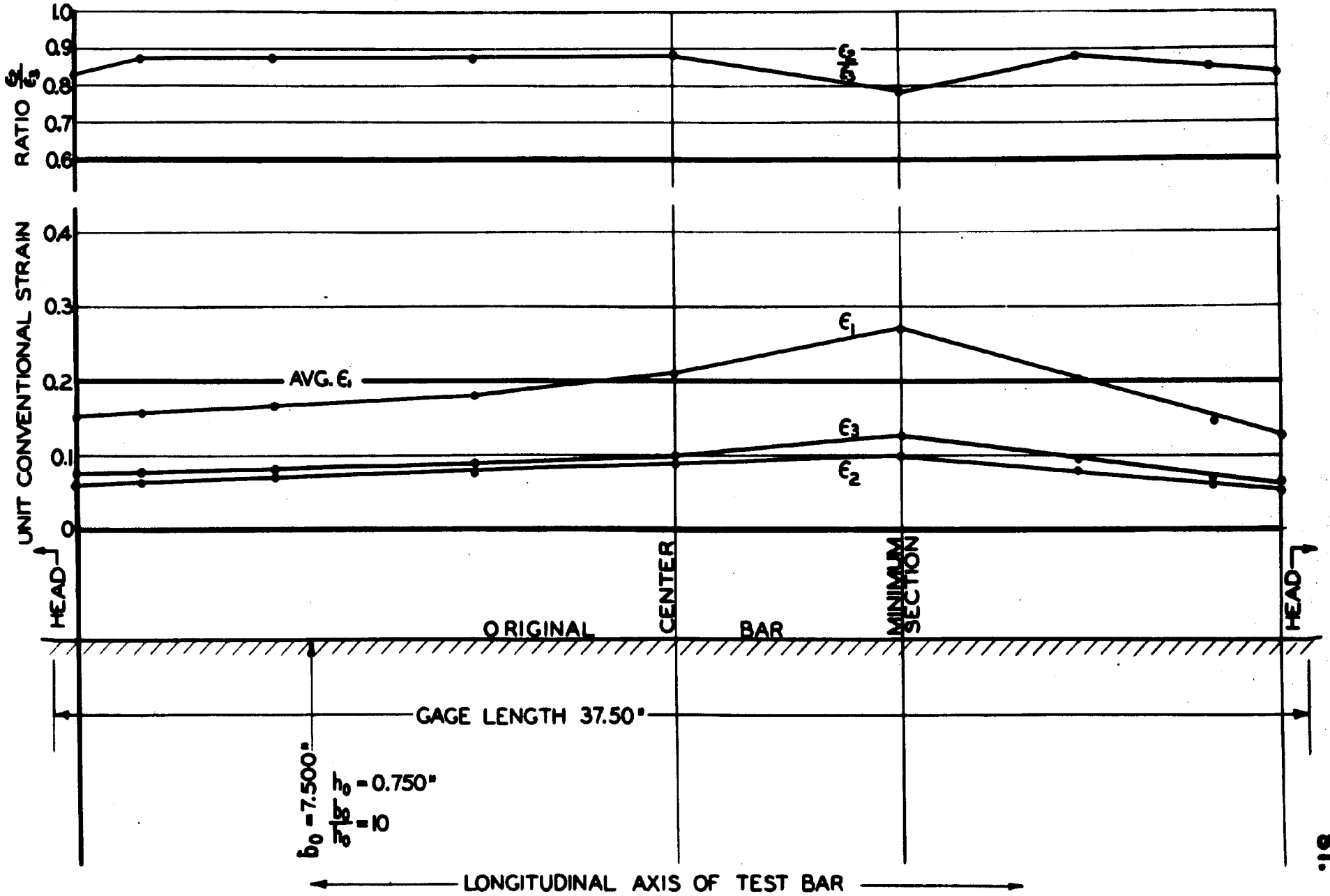

FIG. 5 VARIATION OF $\epsilon_1, \epsilon_2, \epsilon_3$, AND $\frac{\epsilon_2}{\epsilon_3}$ WITH LONGITUDINAL AXIS OF TENSILE BAR.

[SPECIMEN 10A. VALUES COMPUTED FOR BAR AT AVG. $\epsilon_1 = 0.20$ (ULT. LOAD)]

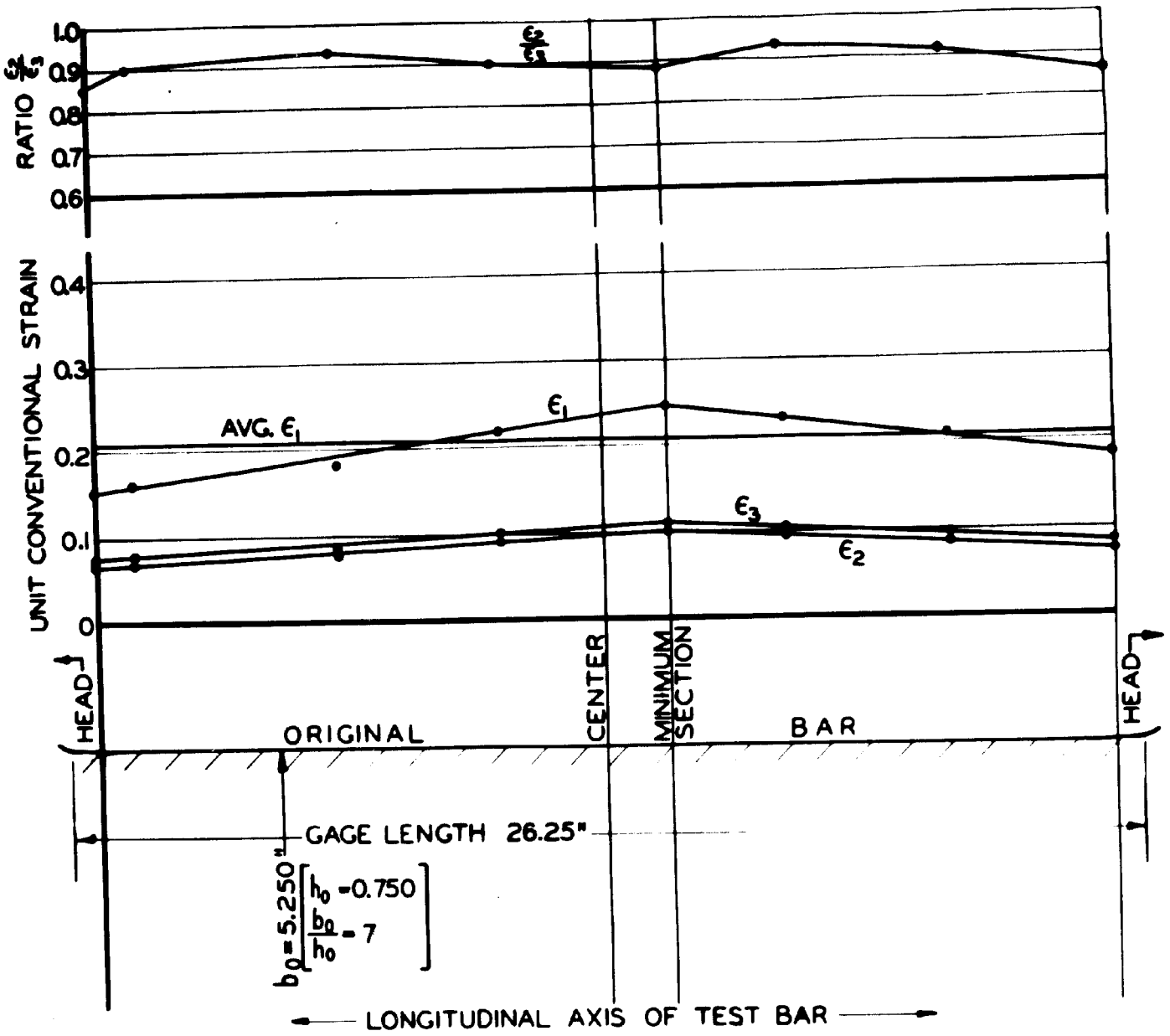

FIG. 6 VARIATION OF $\epsilon_1, \epsilon_2, \epsilon_3$, AND $\frac{\epsilon_2}{\epsilon_3}$ WITH LONGITUDINAL AXIS OF TENSILE BAR

[SPECIMEN 7A. VALUES COMPUTED FOR BAR AT AVG. ϵ_1 = 0.21 (ULT. LOAD)]

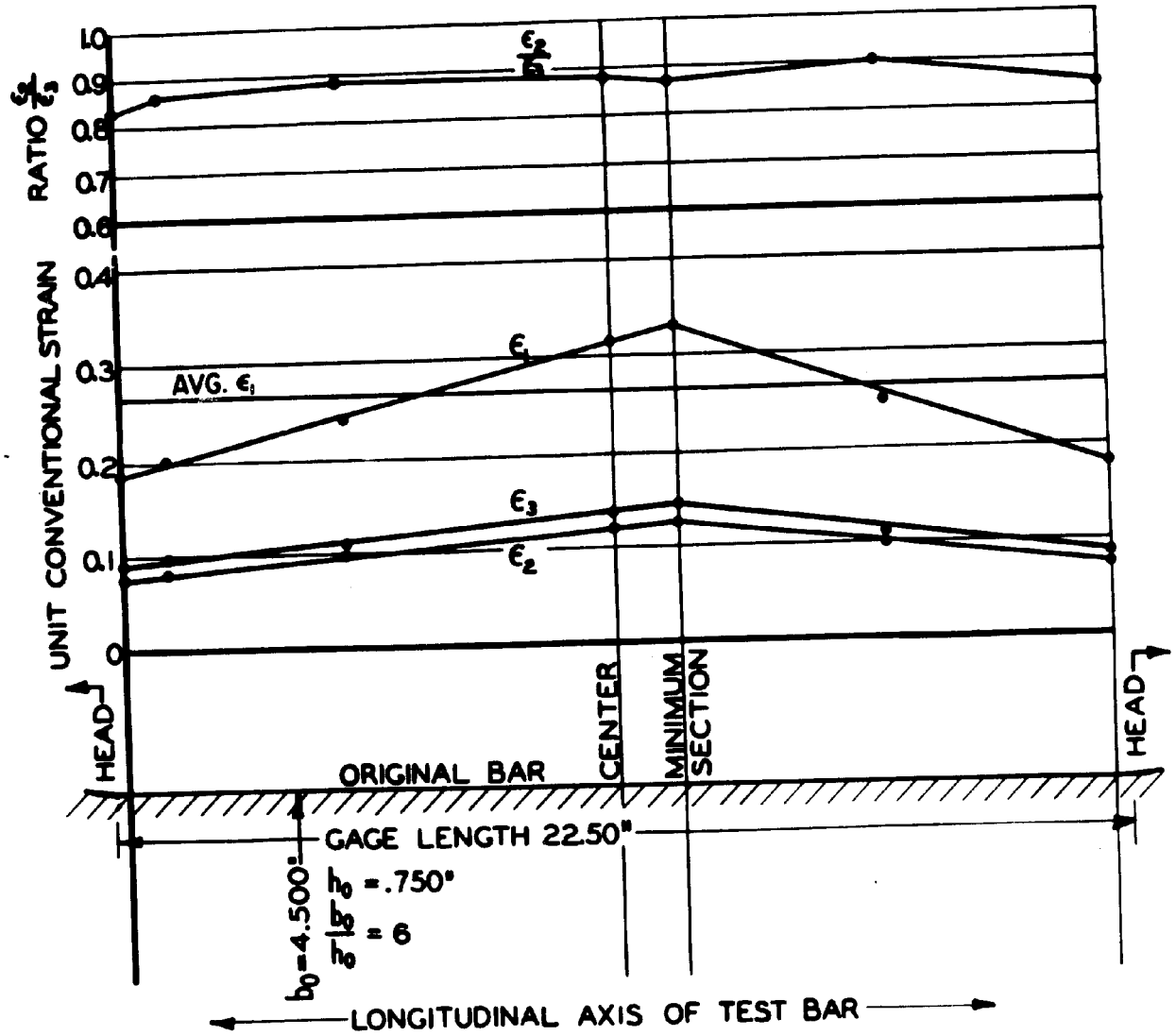

FIG. 7 VARIATION OF $\epsilon_1, \epsilon_2, \epsilon_3$, AND $\frac{\epsilon_2}{\epsilon_3}$ WITH LONGITUDINAL AXIS OF TENSILE BAR

[SPECIMEN 6A. VALUES COMPUTED FOR BAR AT AVG. ϵ_1 = 0.26 (ULT LOAD)]

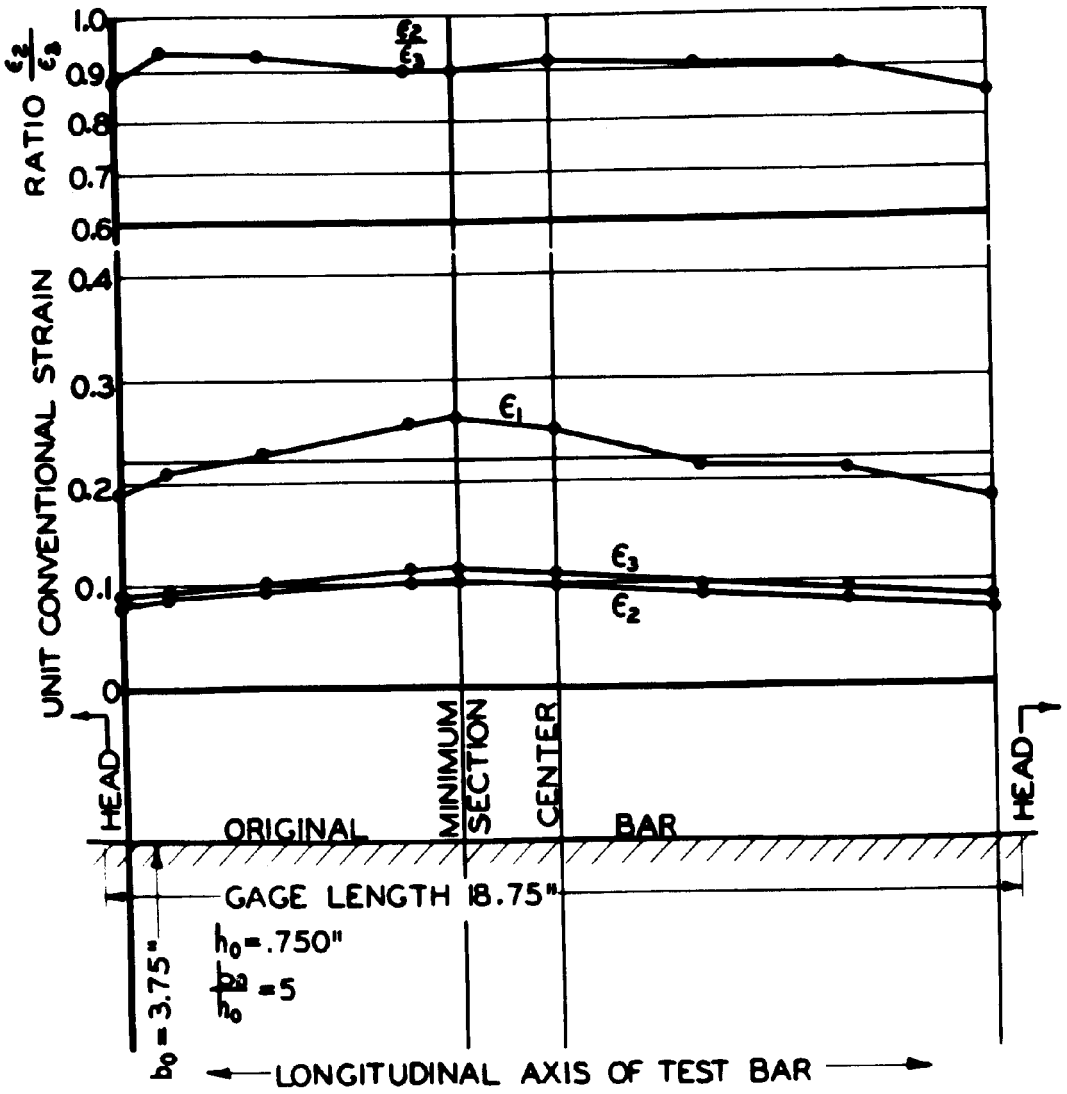

FIG. 8 VARIATION OF $\epsilon_1, \epsilon_2, \epsilon_3$, AND $\frac{\epsilon_2}{\epsilon_3}$ WITH LONGITUDINAL AXIS OF TENSILE BAR

[SPECIMEN 5A. VALUES COMPUTED FOR BAR AT AVG. ϵ_1 =0.225(ULT. LOAD)]

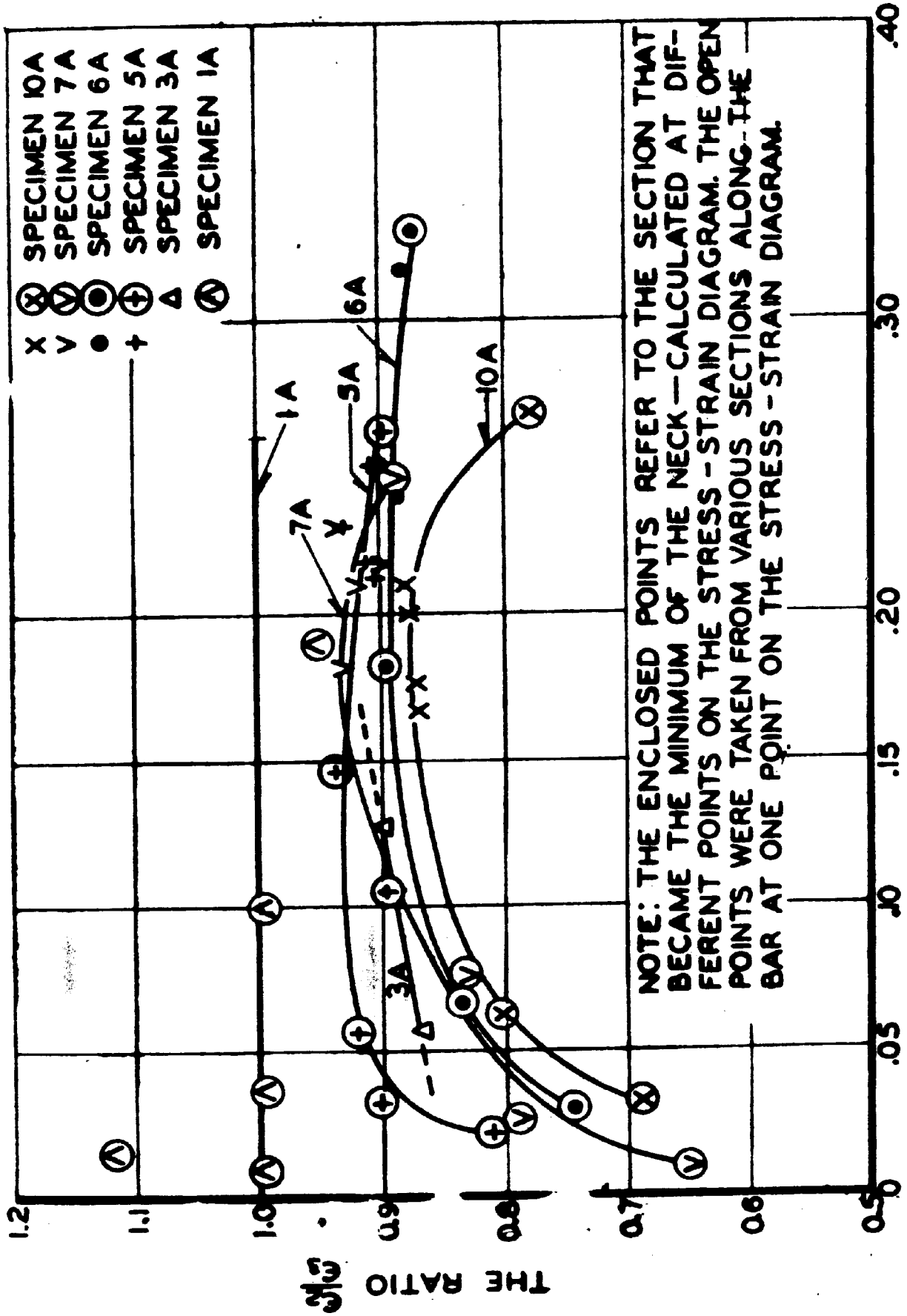

Fig. 9 The Variation of Ratio $\frac{\varepsilon_2}{\varepsilon_3}$ with ε_1 (Series "A" $h_0 = \frac{3}{4}$", b_0 from $\frac{3}{4}$" to $7\frac{1}{2}$")

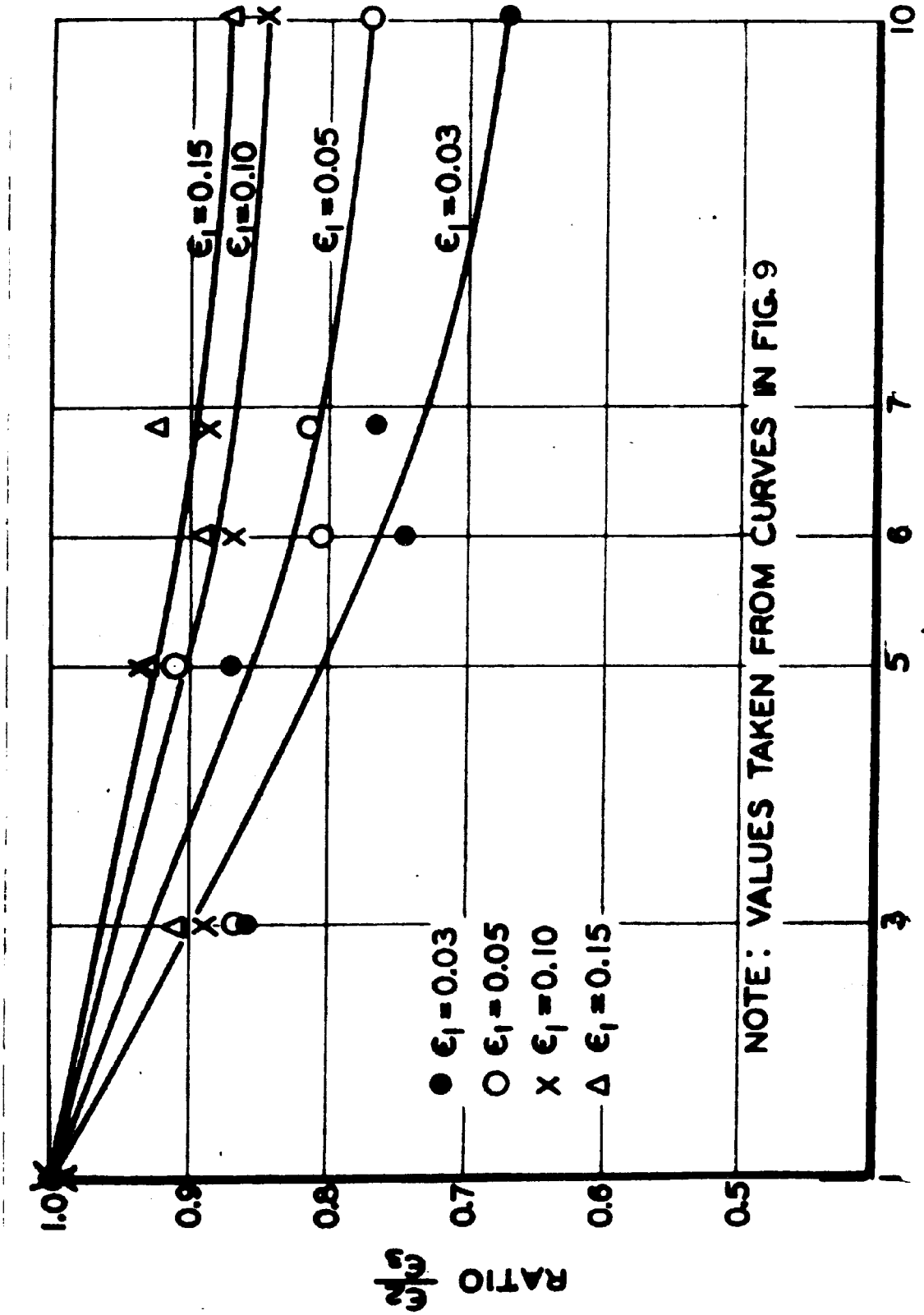

FIG. 10 THE VARIATION OF RATIO $\frac{\epsilon_2}{\epsilon_3}$ WITH GEOMETRY RATIO $\frac{b_0}{h_0}$

(SERIES 'A' $h_0 = \frac{3}{4}$", b_0 FROM $\frac{3}{4}$" TO $7\frac{1}{2}$")

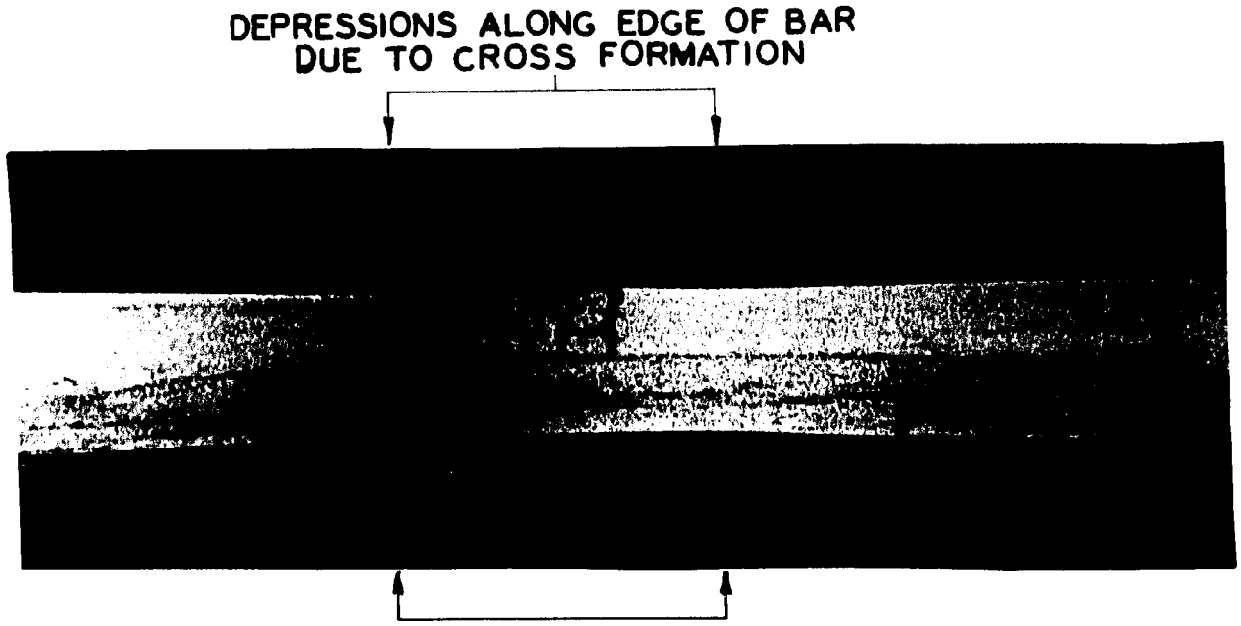

FIG.11 THE EDGE VIEW OF A FLAT TENSION BAR SHOWING THE CROSS EDGE DEPRESSIONS (SPECIMEN 5A)

SPECIMEN 10A

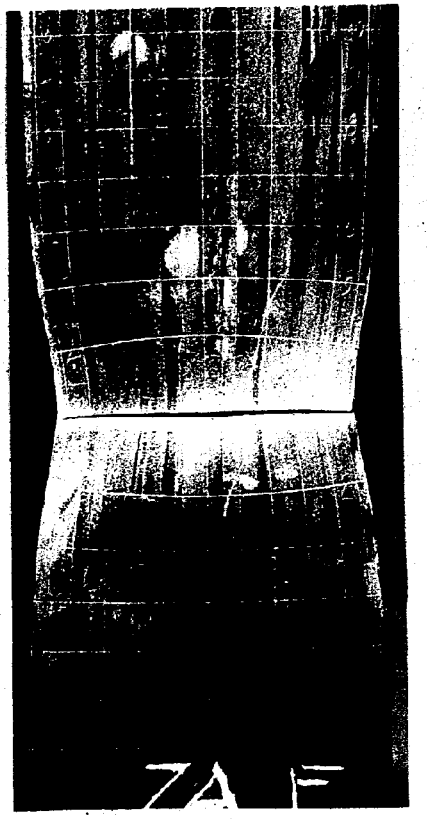

7A

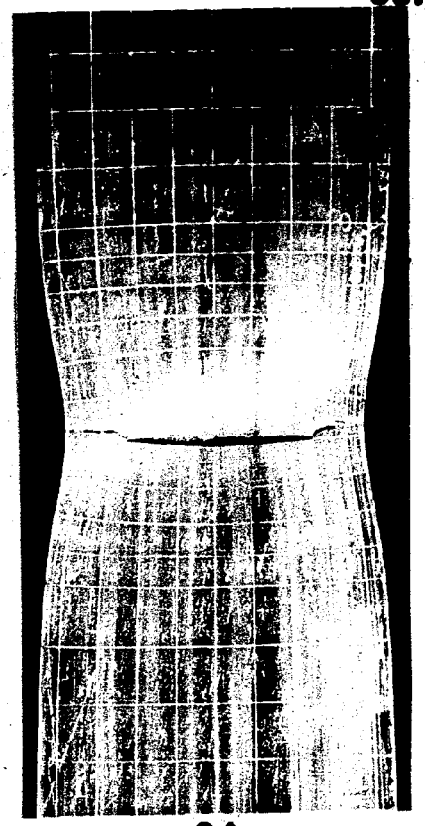

6A

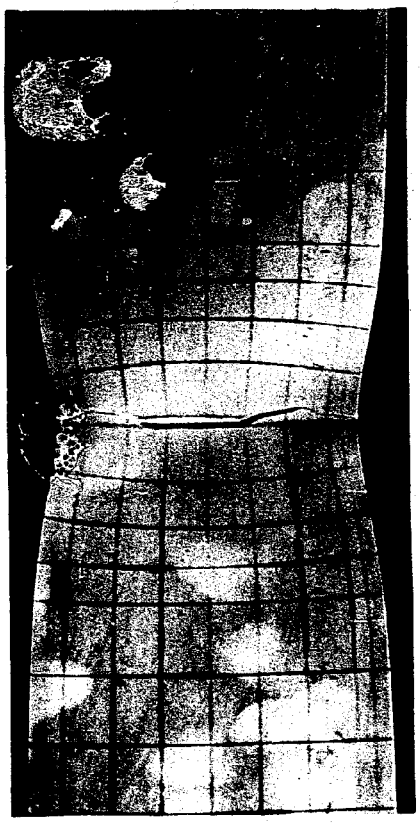

5A

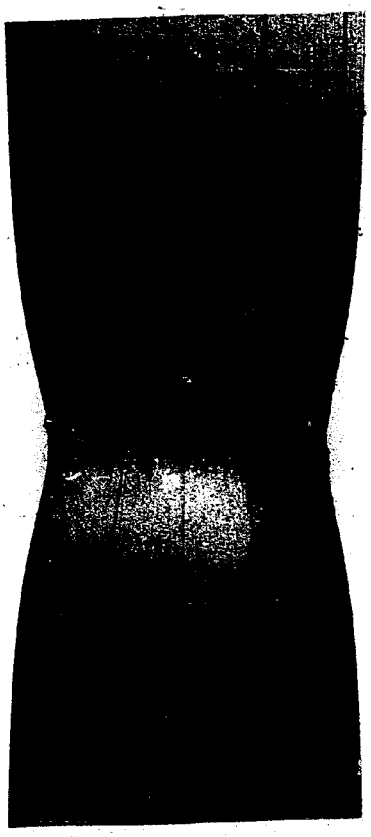

3A

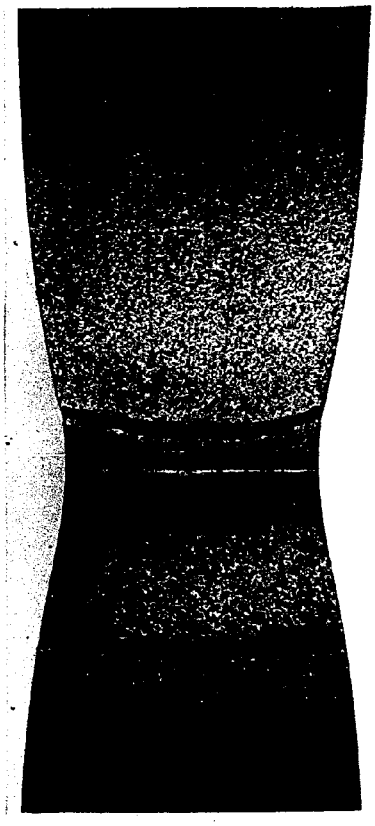

1A

FIG. 12 THE GEOMETRY INFLUENCE ON THE NECK AND FRACTURE OF THE FLAT TENSION BAR (SERIES A $h_0 = \frac{3}{4}$")

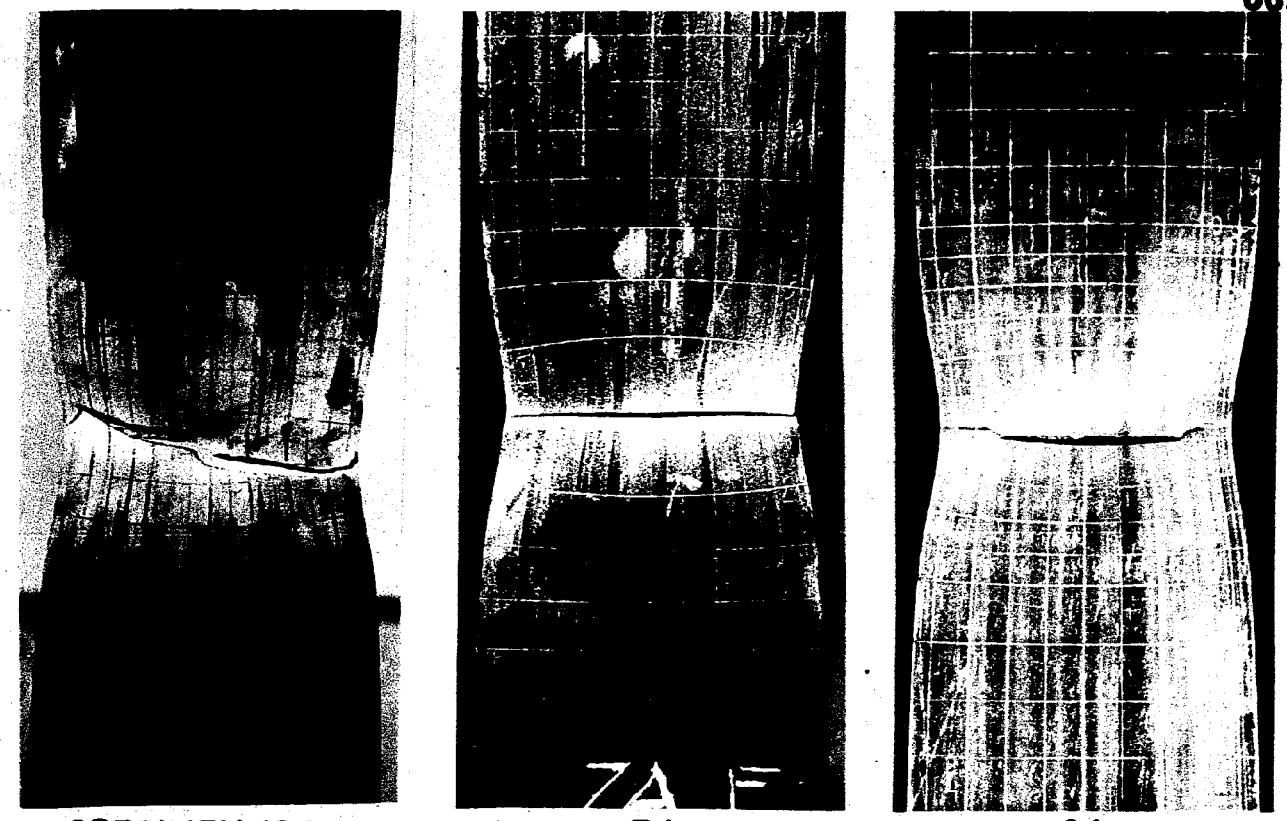

SPECIMEN 10A 7A 6A

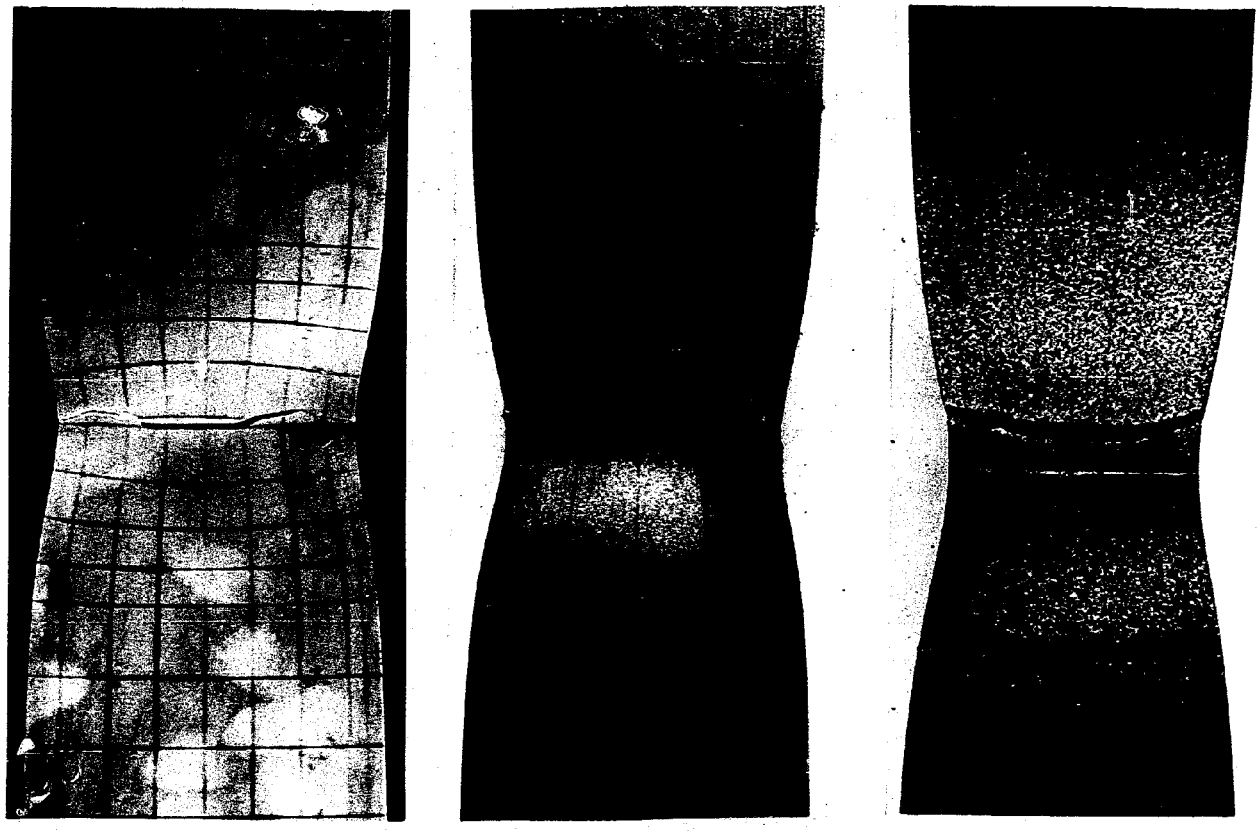

5A 3A 1A

FIG. 12 THE GEOMETRY INFLUENCE ON THE NECK AND FRACTURE OF THE FLAT TENSION BAR (SERIES A $h_0 = \frac{3}{4}$")

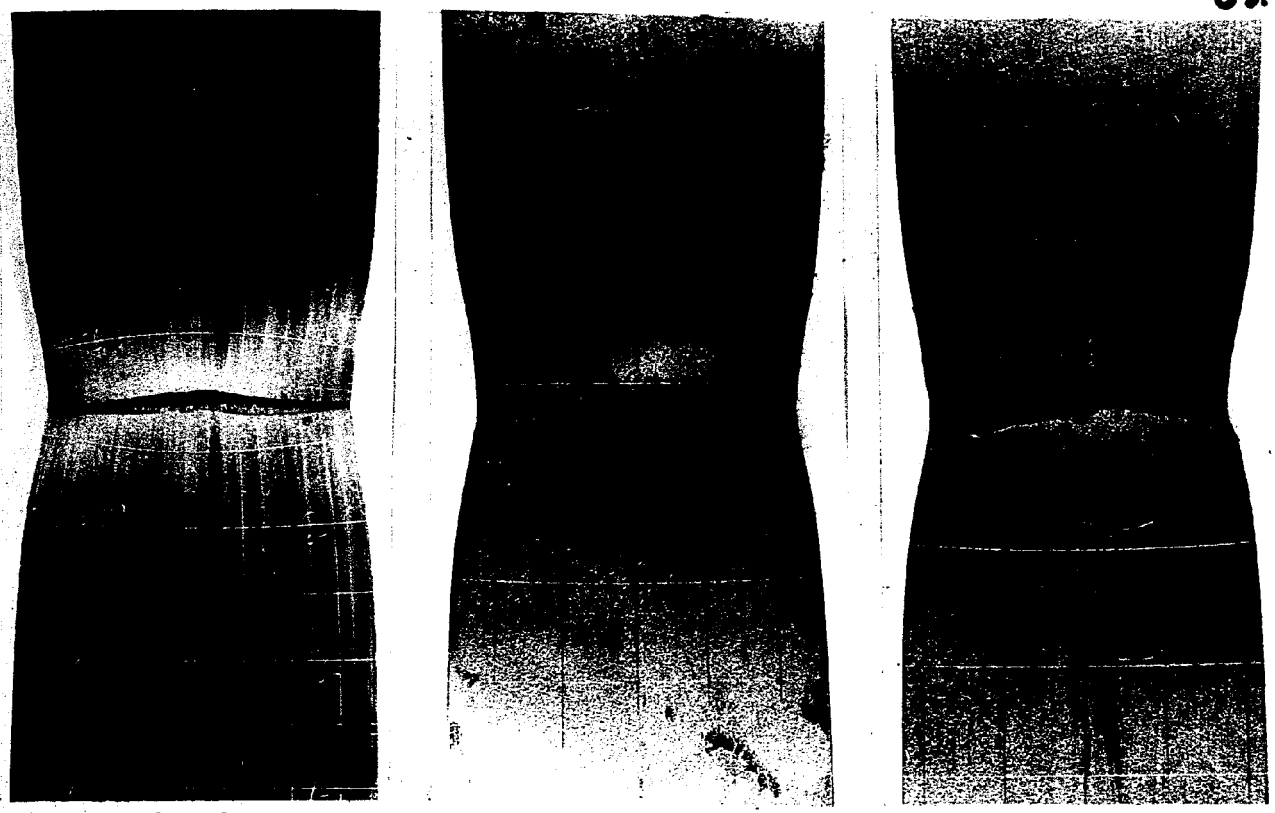

SPECIMEN 10B 7B 6B

5B 3B 1B

FIG. 13 ■ THE GEOMETRY INFLUENCE ON THE NECK AND FRACTURE OF THE FLAT TENSION BAR (SERIES B; $h_0 = \frac{3}{8}$")

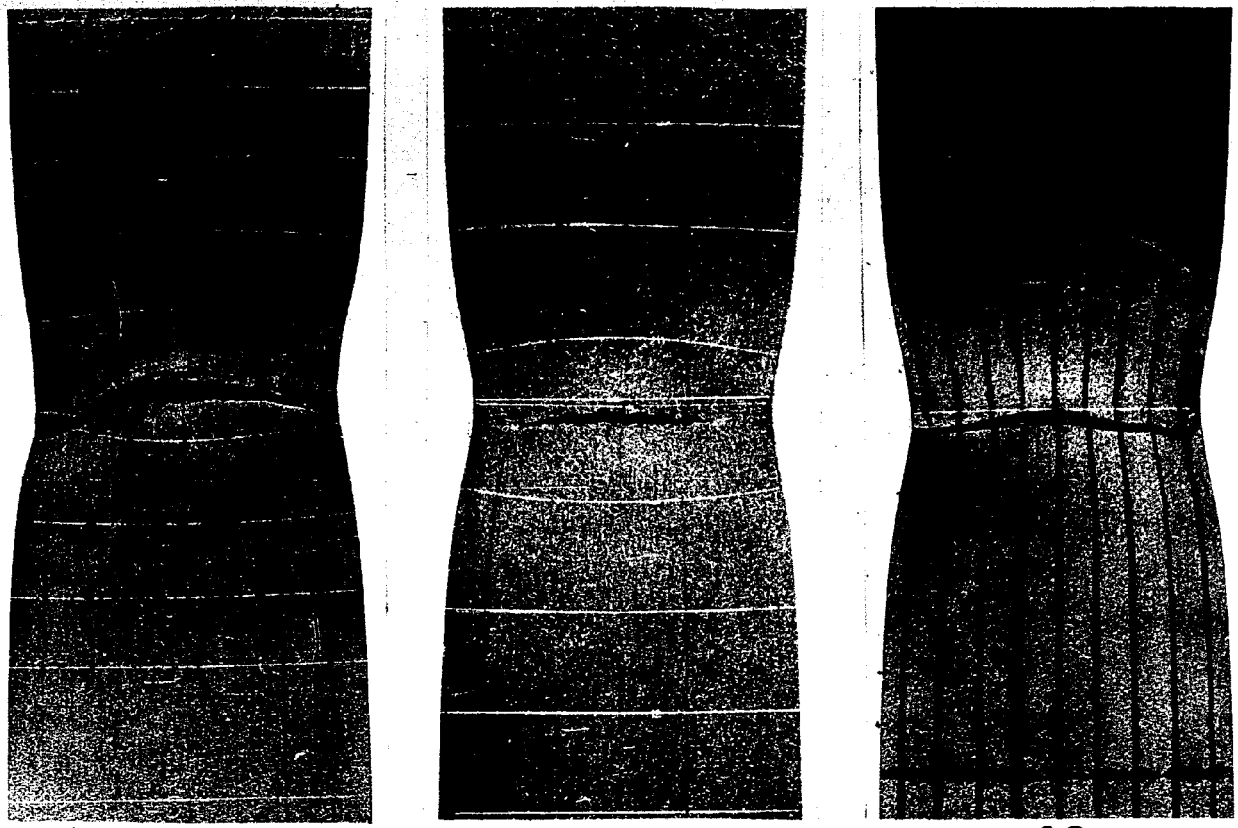

SPECIMEN 10C 7C 6C

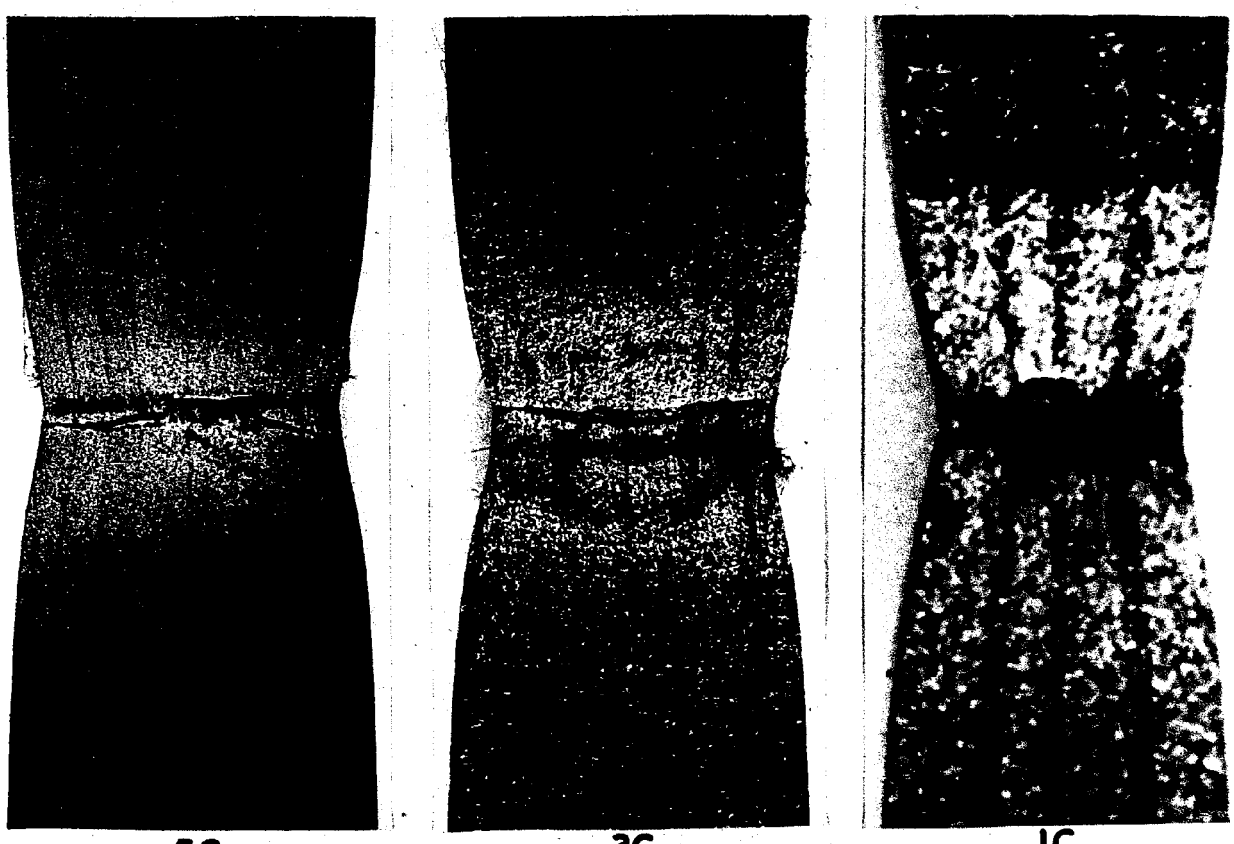

5C 3C 1C

FIG.14 ■THE GEOMETRY INFLUENCE ON THE NECK AND FRACTURE OF THE FLAT TENSION BAR (SERIES C $h_0 = \frac{3}{16}$") ■

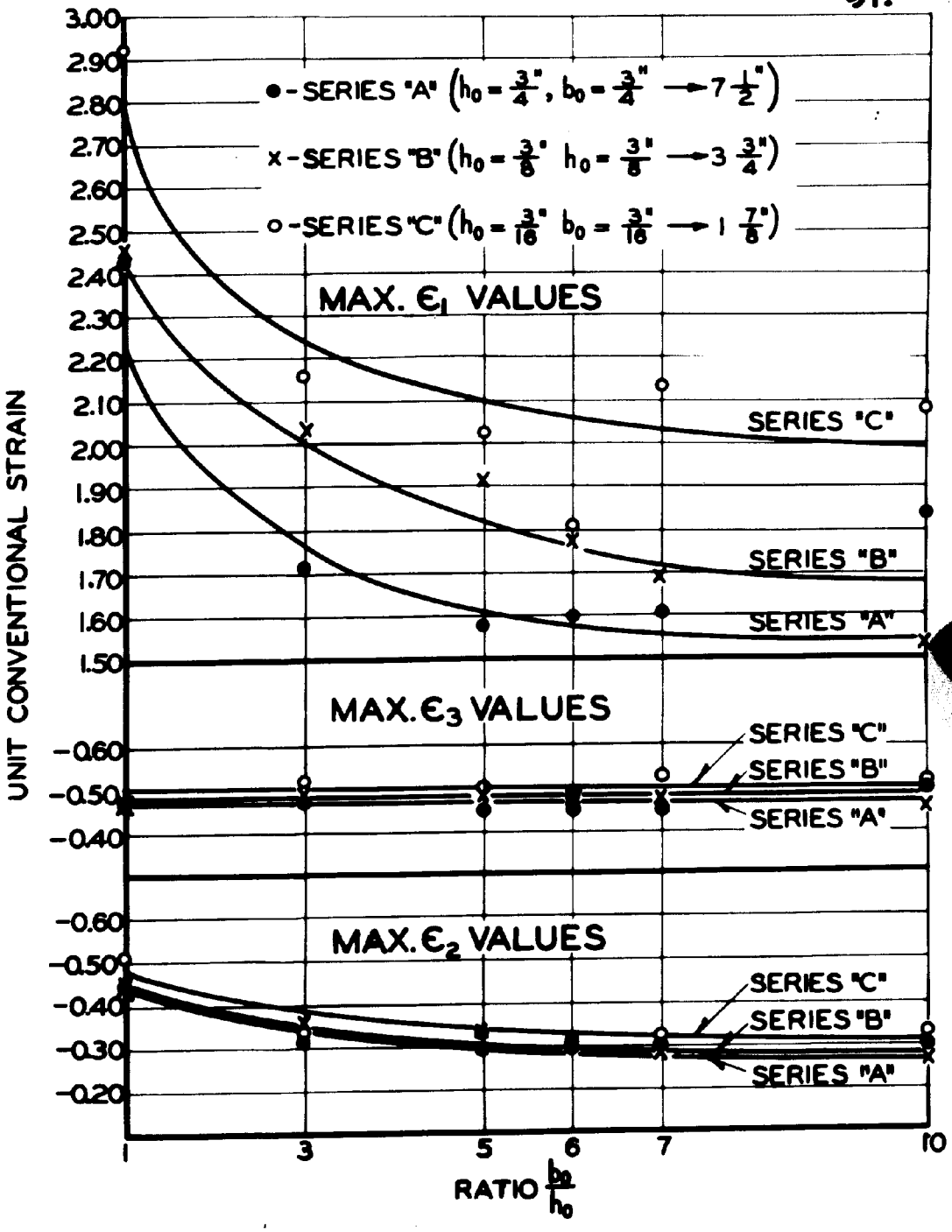

FIG. 15 VARIATION OF MAXIMUM VALUES OF ϵ_1, ϵ_2, AND ϵ_3 WITH SIZE AND GEOMETRY OF FLAT TENSION BAR
(ALL BARS AT FRACTURE)

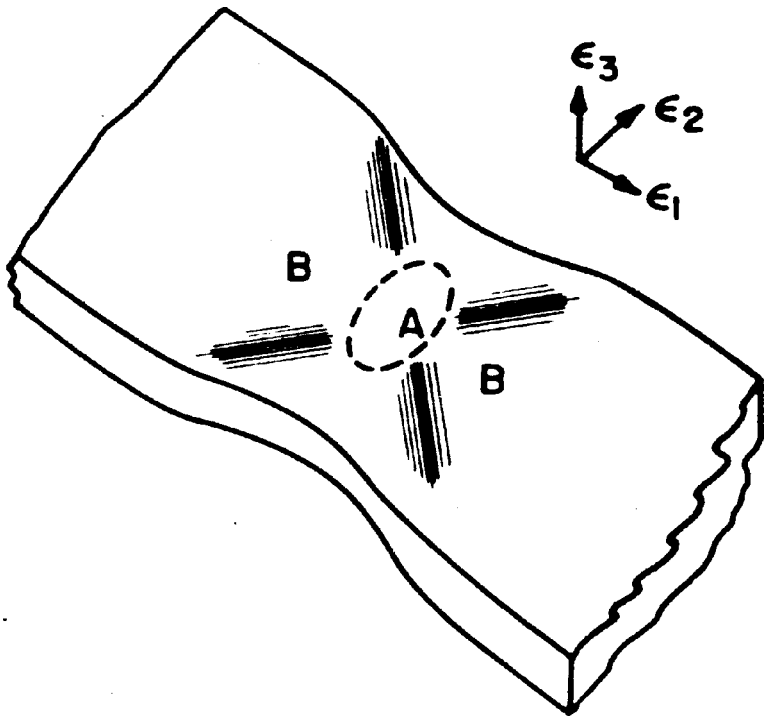

Fig. 16a

Division of the Stagnant (B) and Flowing Material (A)

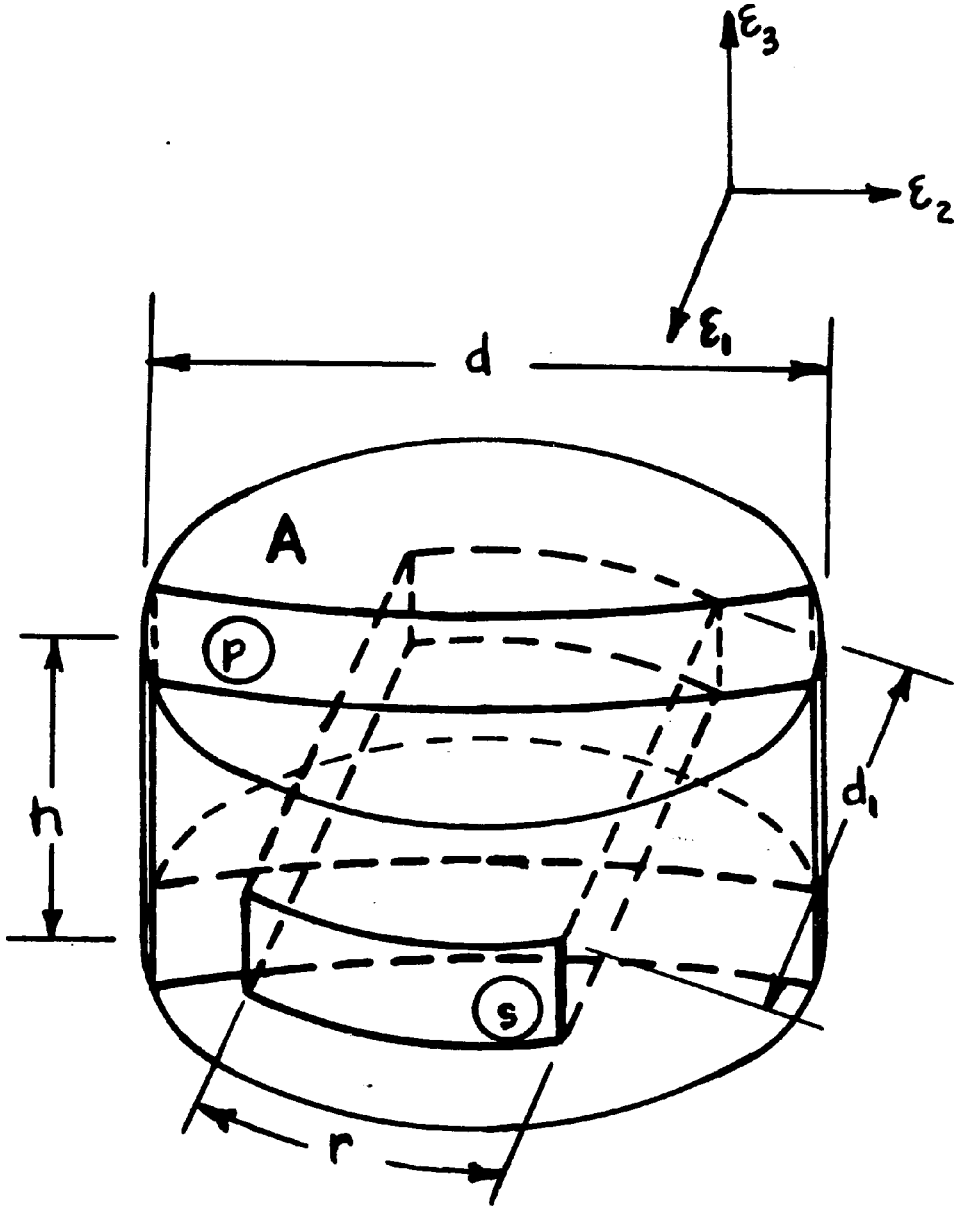

FIGURE 16(b)
CLOSEUP OF REGION "A" AND ITS SPECIMEN-LIKE ELEMENTS.

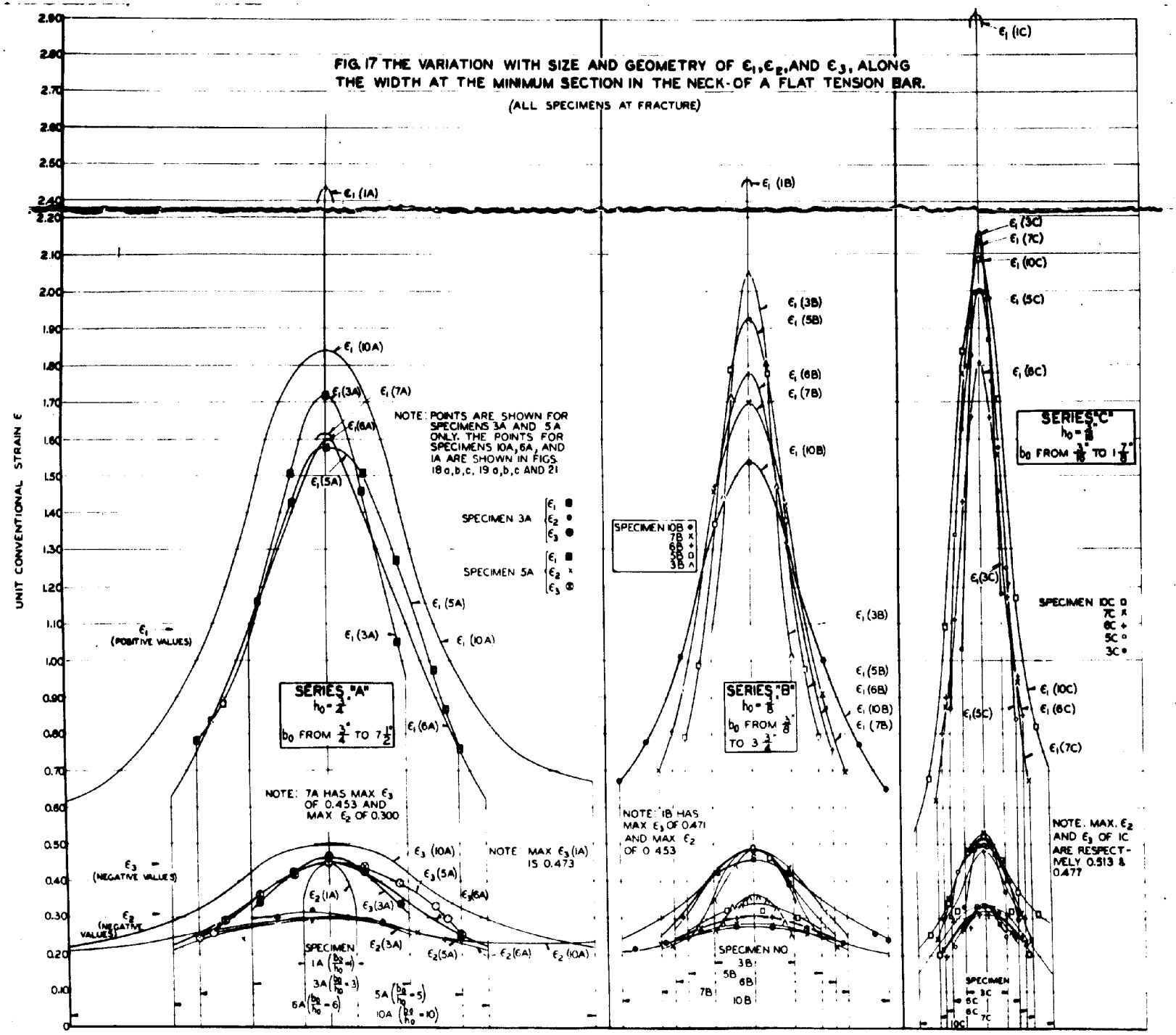
FIG. 17 THE VARIATION WITH SIZE AND GEOMETRY OF ϵ_1, ϵ_2, AND ϵ_3, ALONG THE WIDTH AT THE MINIMUM SECTION IN THE NECK OF A FLAT TENSION BAR.
(ALL SPECIMENS AT FRACTURE)
UNIT CONVENTIONAL STRAIN ε
ϵ_1 (1A)
ϵ_1 (1B)
ϵ_1 (1C)
ϵ_1 (10A)
ϵ_1 (3A)
ϵ_1 (7A)
ϵ_1 (6A)
ϵ_1 (5A)
NOTE: POINTS ARE SHOWN FOR SPECIMENS 3A AND 5A ONLY. THE POINTS FOR SPECIMENS 10A, 6A, AND 1A ARE SHOWN IN FIGS. 18 a,b,c, 19 a,b,c AND 21
SPECIMEN 3A ϵ_1 ϵ_2 ϵ_3
SPECIMEN 5A ϵ_1 ϵ_2 ϵ_3
ϵ_1 (POSITIVE VALUES)
ϵ_3 (NEGATIVE VALUES)
ϵ_2 (NEGATIVE VALUES)
SERIES "A" $h_0 = \frac{1}{4}$" b_0 FROM $\frac{1}{4}$" TO $7\frac{1}{2}$"
NOTE: 7A HAS MAX ϵ_3 OF 0.453 AND MAX ϵ_2 OF 0.300
NOTE MAX ϵ_3 (1A) IS 0.473
ϵ_3 (10A)
ϵ_3 (5A)
ϵ_3 (6A)
ϵ_3 (3A)
ϵ_2 (1A)
ϵ_2 (3A)
ϵ_2 (5A)
ϵ_2 (6A)
ϵ_2 (10A)
SPECIMEN 1A $\left(\frac{b_0}{h_0}=1\right)$ 3A $\left(\frac{b_0}{h_0}=3\right)$ 5A $\left(\frac{b_0}{h_0}=5\right)$ 6A $\left(\frac{b_0}{h_0}=6\right)$ 10A $\left(\frac{b_0}{h_0}=10\right)$
ϵ_1 (3B)
ϵ_1 (5B)
ϵ_1 (6B)
ϵ_1 (7B)
ϵ_1 (10B)
SPECIMEN 10B 7B 6B 5B 3B
SERIES "B" $h_0 = \frac{1}{8}$" b_0 FROM $\frac{1}{8}$" TO $3\frac{1}{4}$"
NOTE: 1B HAS MAX ϵ_3 OF 0.471 AND MAX ϵ_2 OF 0.453
SPECIMEN NO 3B 5B 6B 7B 10B
ϵ_1 (3C)
ϵ_1 (7C)
ϵ_1 (10C)
ϵ_1 (5C)
ϵ_1 (6C)
SERIES "C" $h_0 = \frac{1}{16}$" b_0 FROM $\frac{1}{16}$" TO $1\frac{7}{8}$"
SPECIMEN 10C 7C 6C 5C 3C
NOTE. MAX. ϵ_2 AND ϵ_3 OF 1C ARE RESPECTIVELY 0.513 & 0.477
SPECIMEN 3C 5C 6C 7C 10C
ORIGINAL WIDTH OF TEST BAR

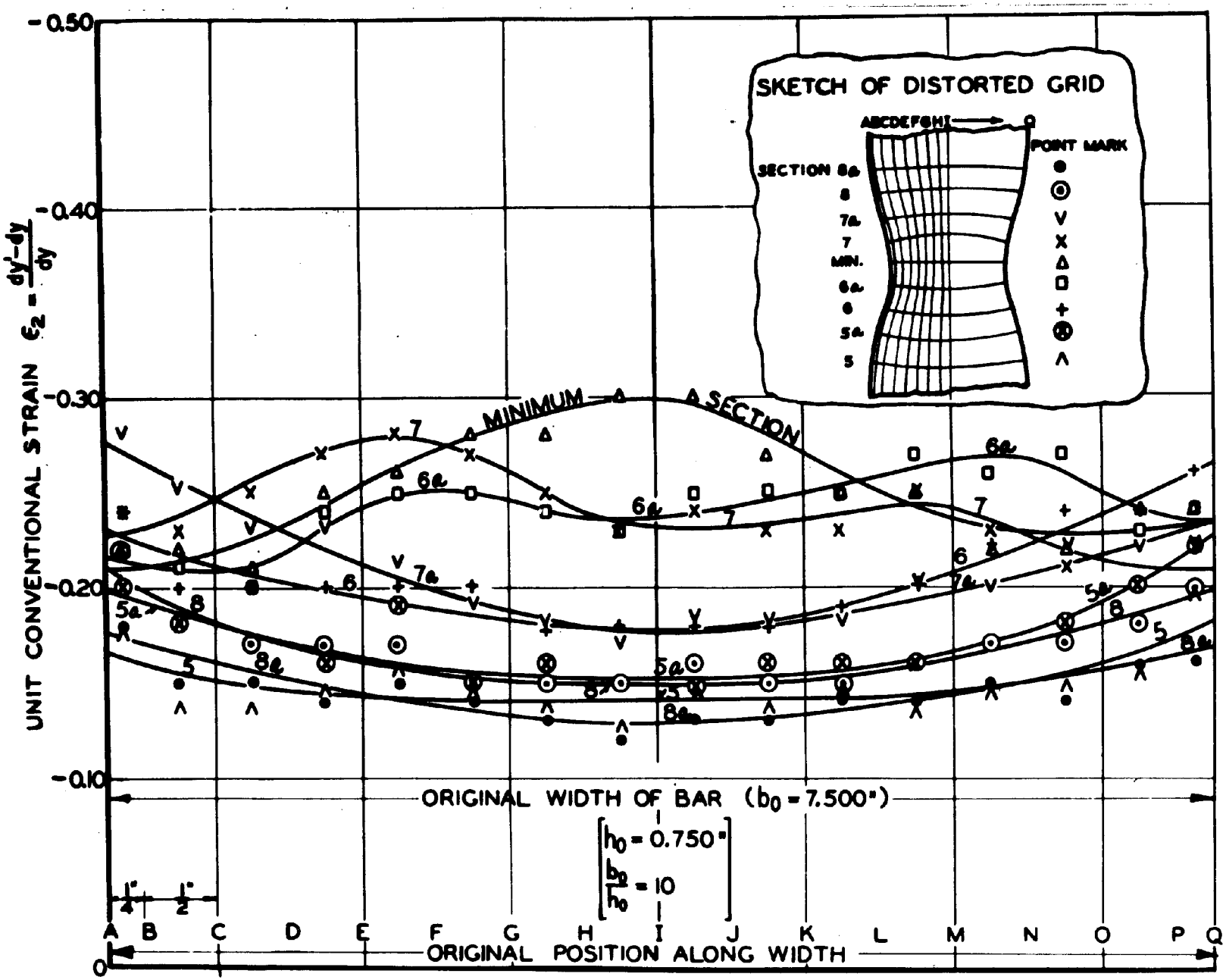

FIG.18a THE VARIATION OF ϵ_2 ALONG THE WIDTH IN THE NECK OF A FLAT TENSION BAR
SPECIMEN 10A $\left(\frac{b_0}{h_0} = 10\right)$ AT FRACTURE

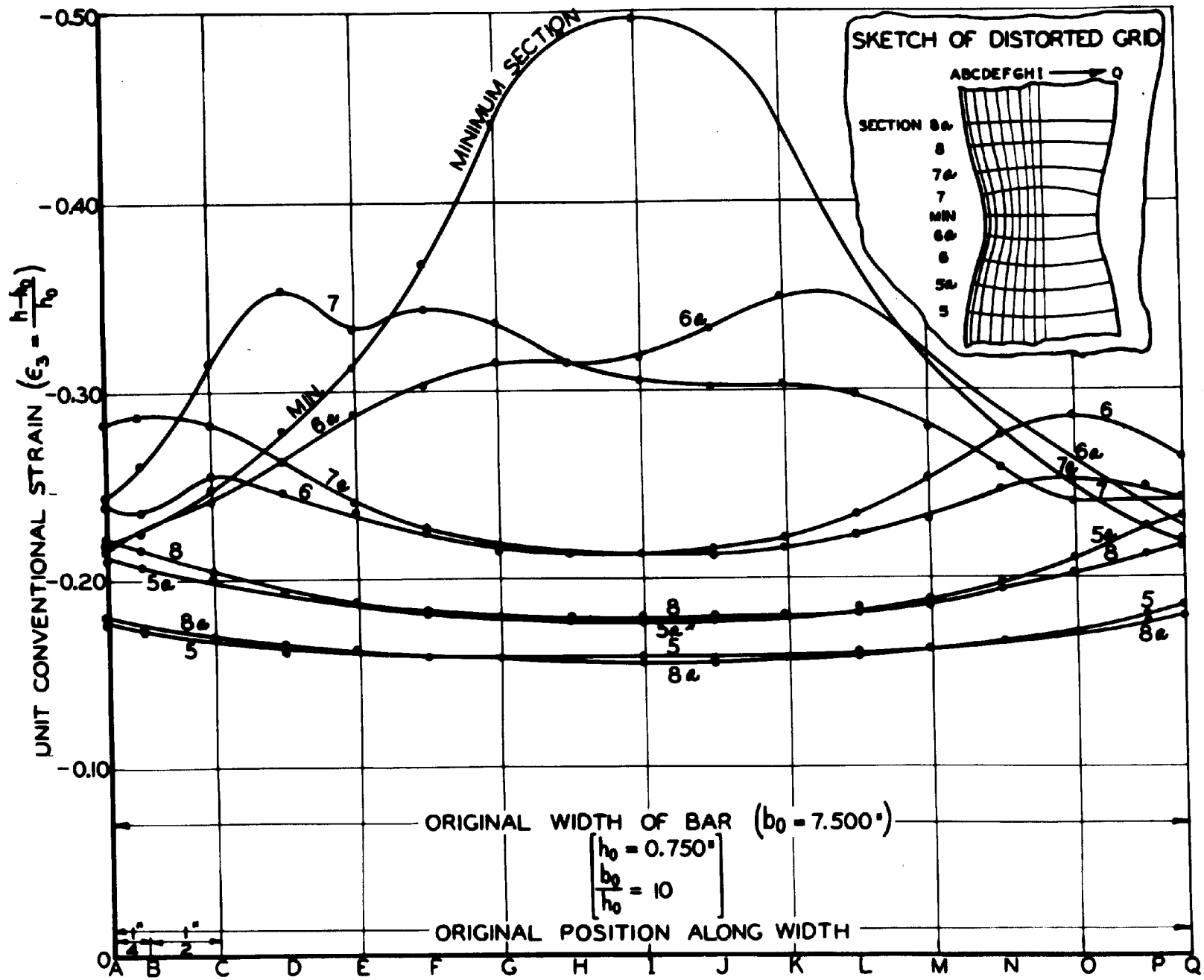

FIG. 18b THE VARIATION OF ϵ_3 ALONG THE WIDTH IN THE NECK OF A FLAT TENSION BAR SPECIMEN 10A. $\left(\frac{b_0}{h_0} = 10\right)$ AT FRACTURE

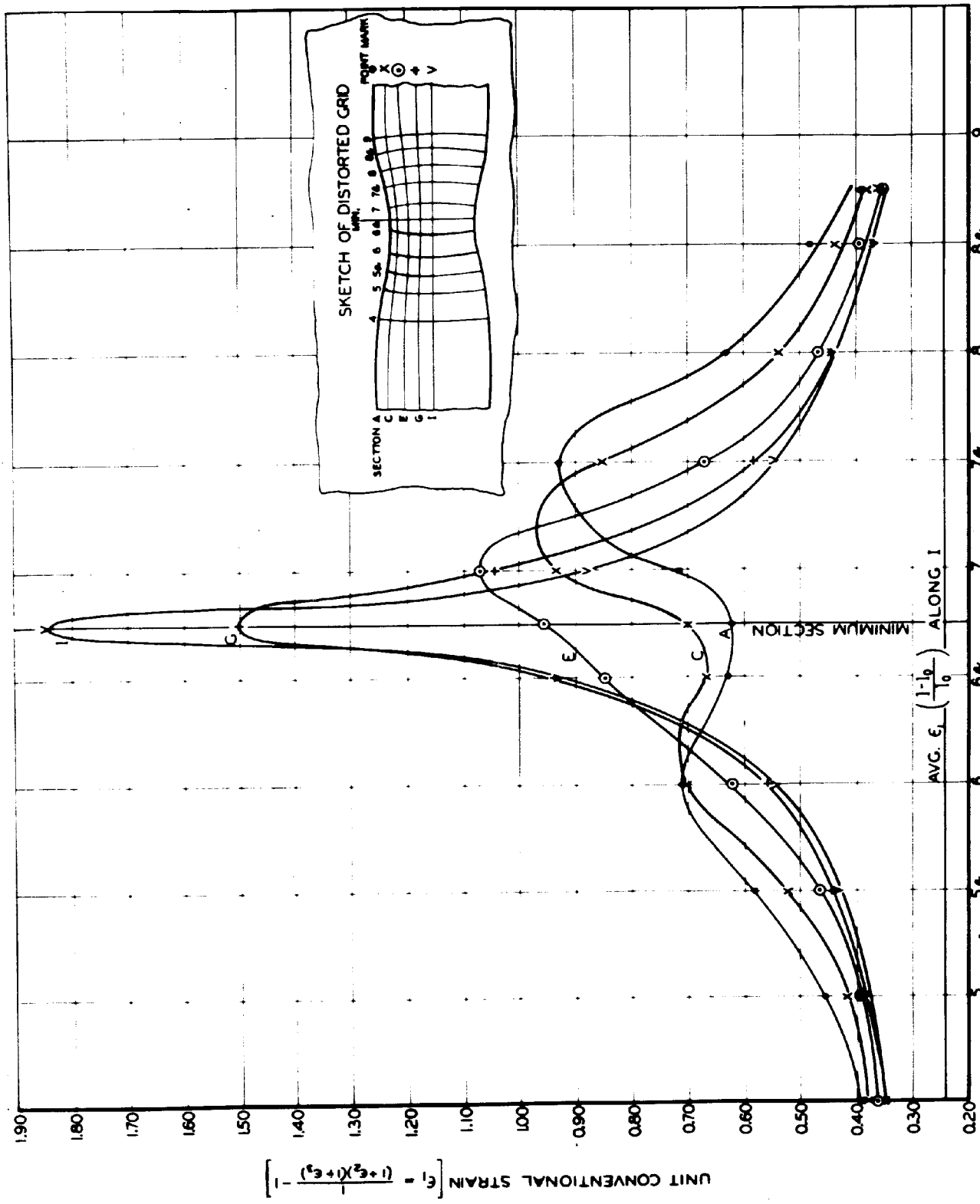

FIG. 18c THE VARIATION OF ϵ_1 ALONG THE LENGTH IN THE NECK OF A FLAT TENSION BAR

SPECIMEN 10A $\left(\frac{b_0}{h_0} = 10\right)$ AT FRACTURE

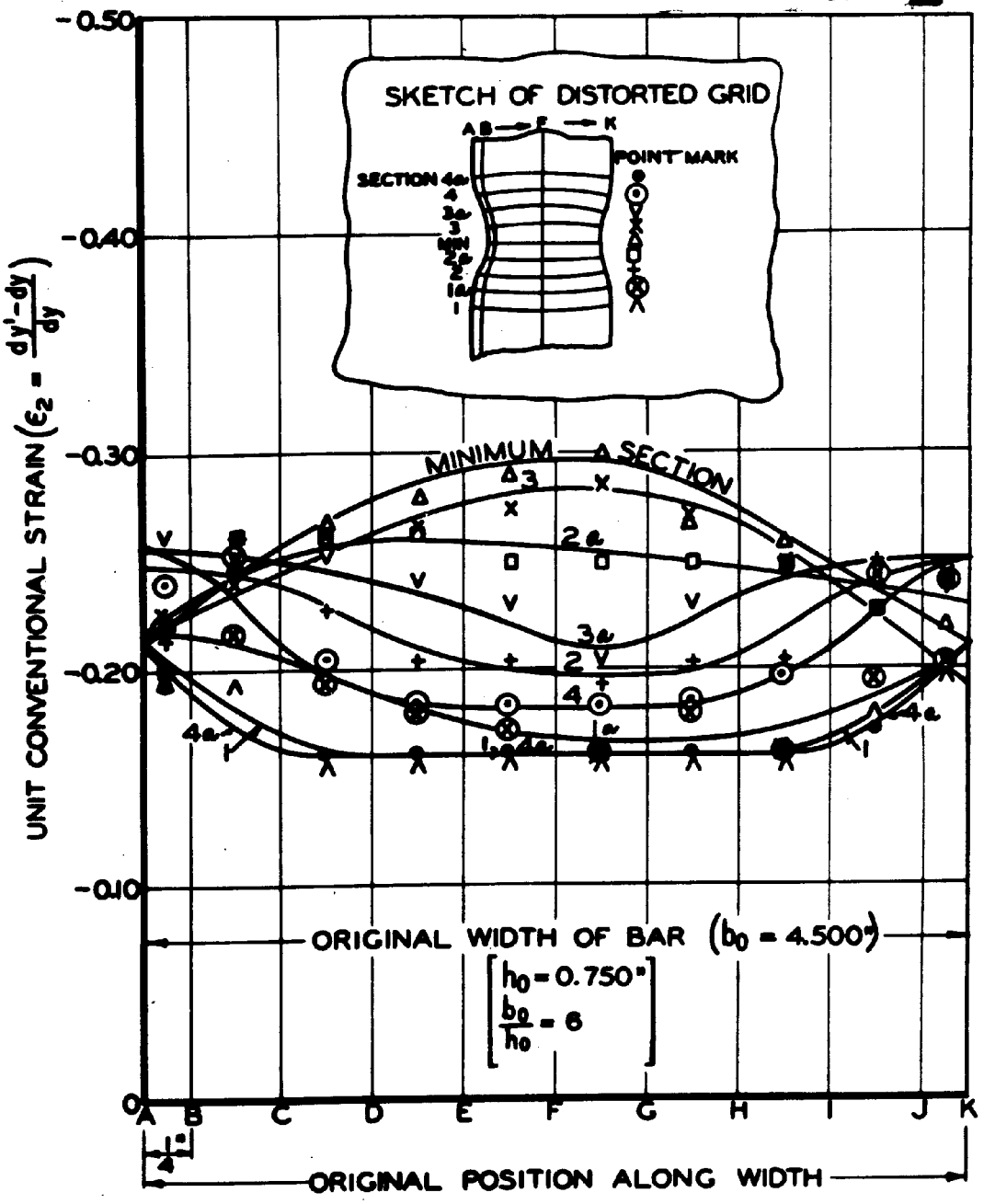

FIG. 19(a) THE VARIATION OF ϵ_2 ALONG THE WIDTH IN THE NECK OF A FLAT TENSION BAR

SPECIMEN 6A $\left(\frac{b_0}{h_0} = 6\right)$ AT FRACTURE

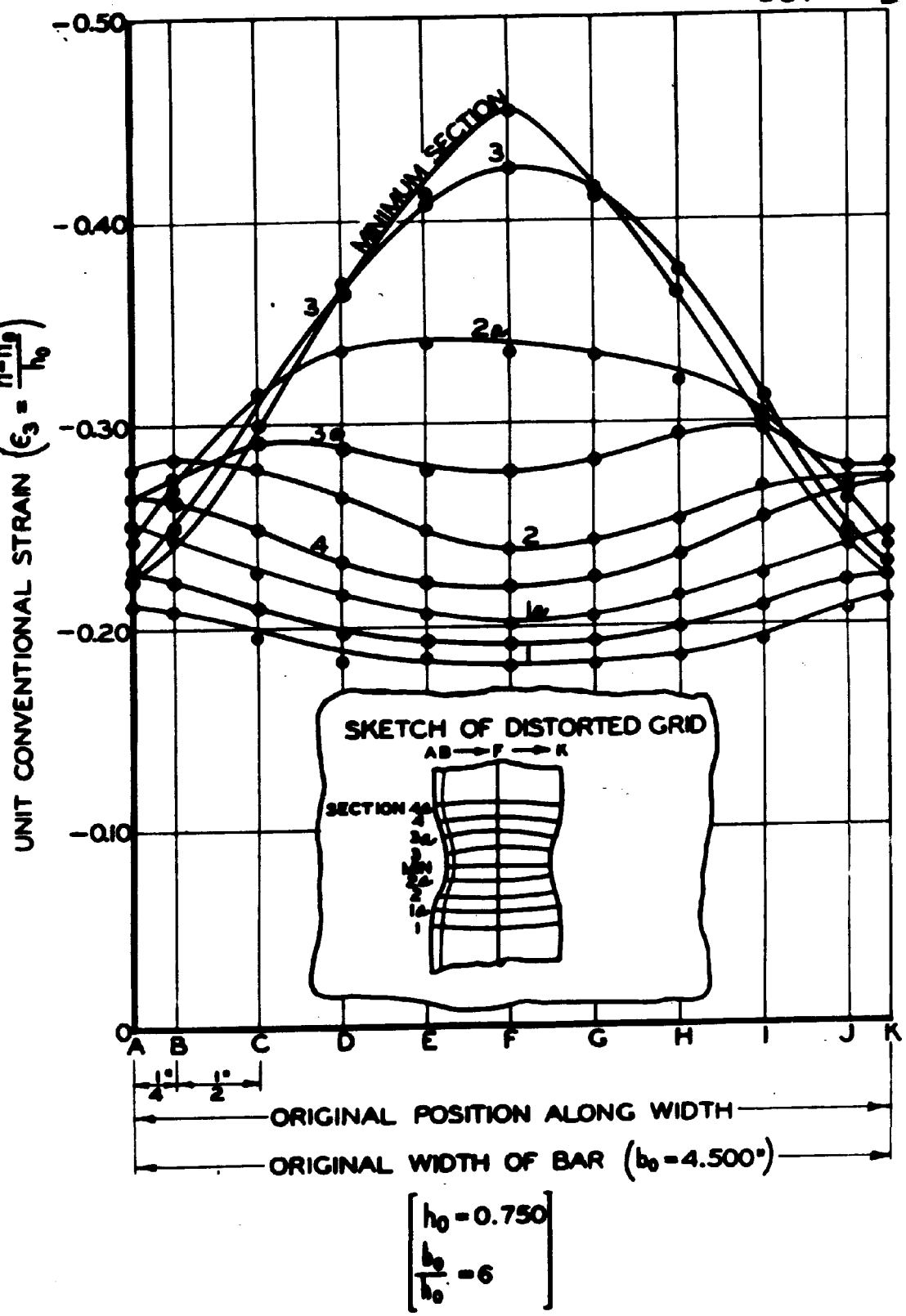

FIG. 19b THE VARIATION OF ϵ_3 ALONG THE WIDTH IN THE NECK OF A FLAT TENSION BAR

[SPECIMEN 6A $\left(\frac{b_0}{h_0} = 6\right)$ AT FRACTURE]

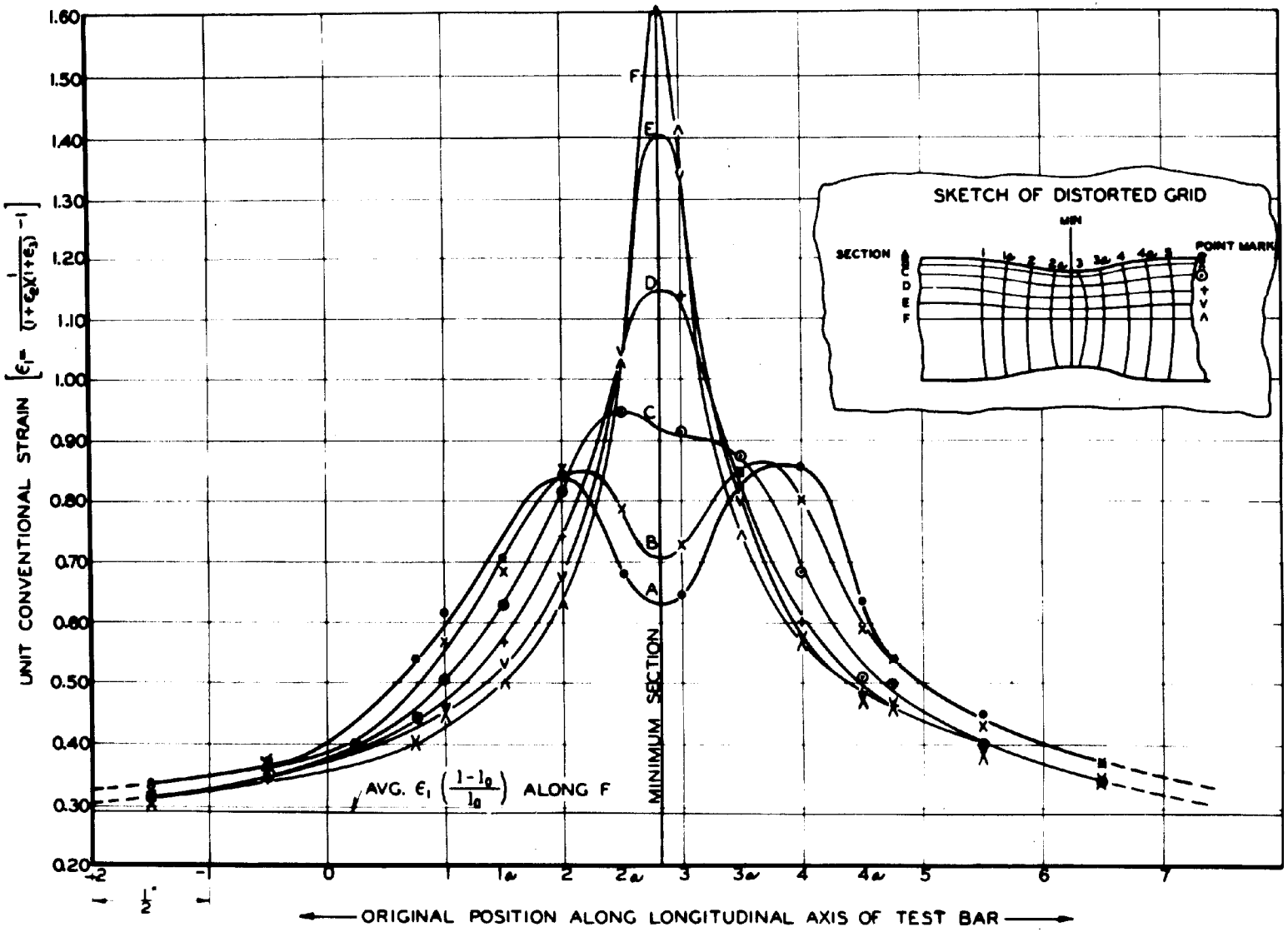

FIG. 19c THE VARIATION OF ϵ_1 ALONG THE LENGTH IN THE NECK OF A FLAT TENSION BAR

SPECIMEN 6A. $\left(\frac{b_0}{h_0} = 6\right)$ AT FRACTURE

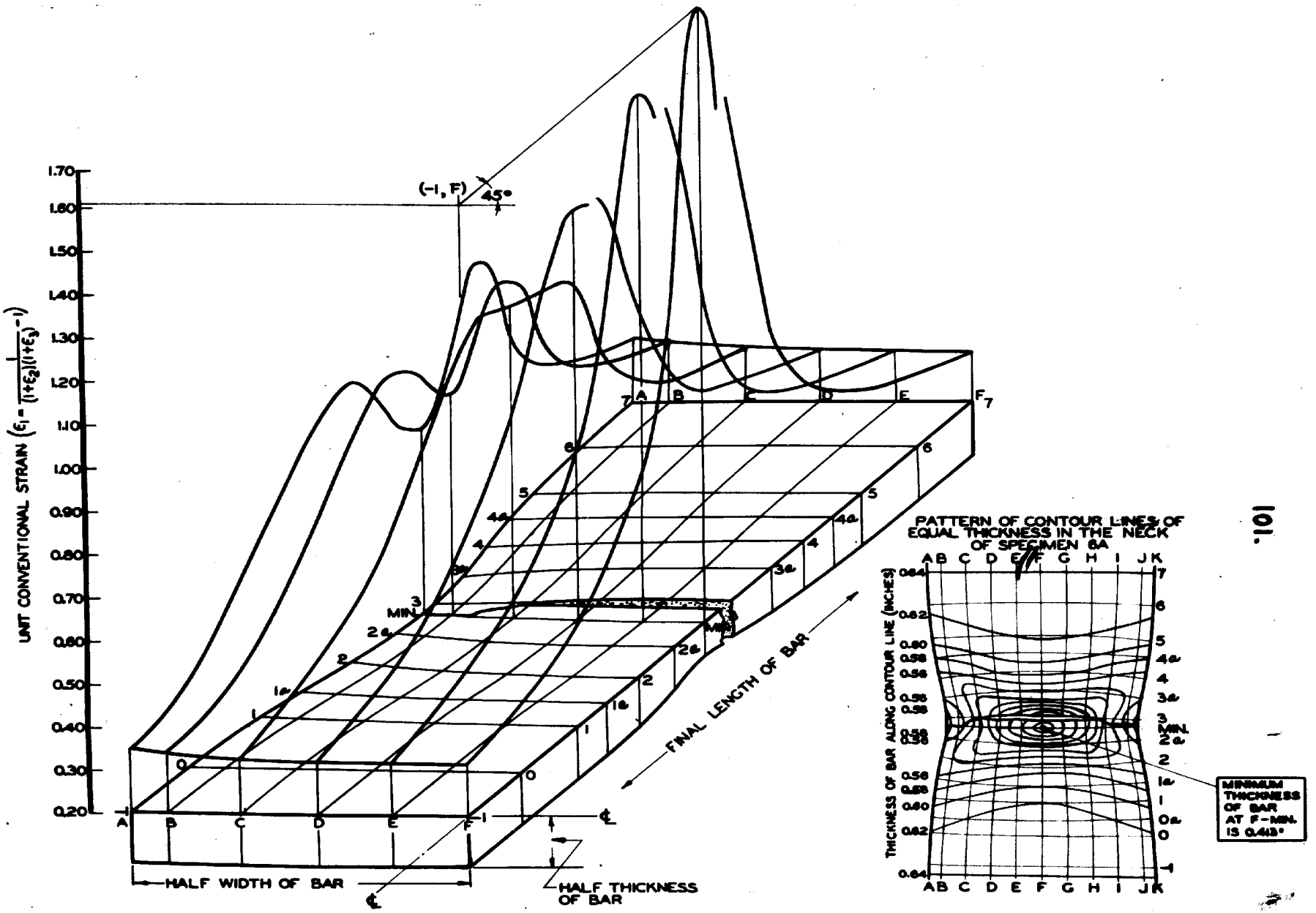

FIG. 20 PERSPECTIVE REPRESENTATION OF THE VARIATION OF THE AXIAL STRAIN ϵ_1 IN THE NECK OF A TENSION BAR AT FRACTURE
(SPECIMEN 6A ($\frac{2a}{D}$ = 6)) (SEE FIG. 19c FOR PLOT OF THESE STRAINS OVER ORIGINAL BAR)

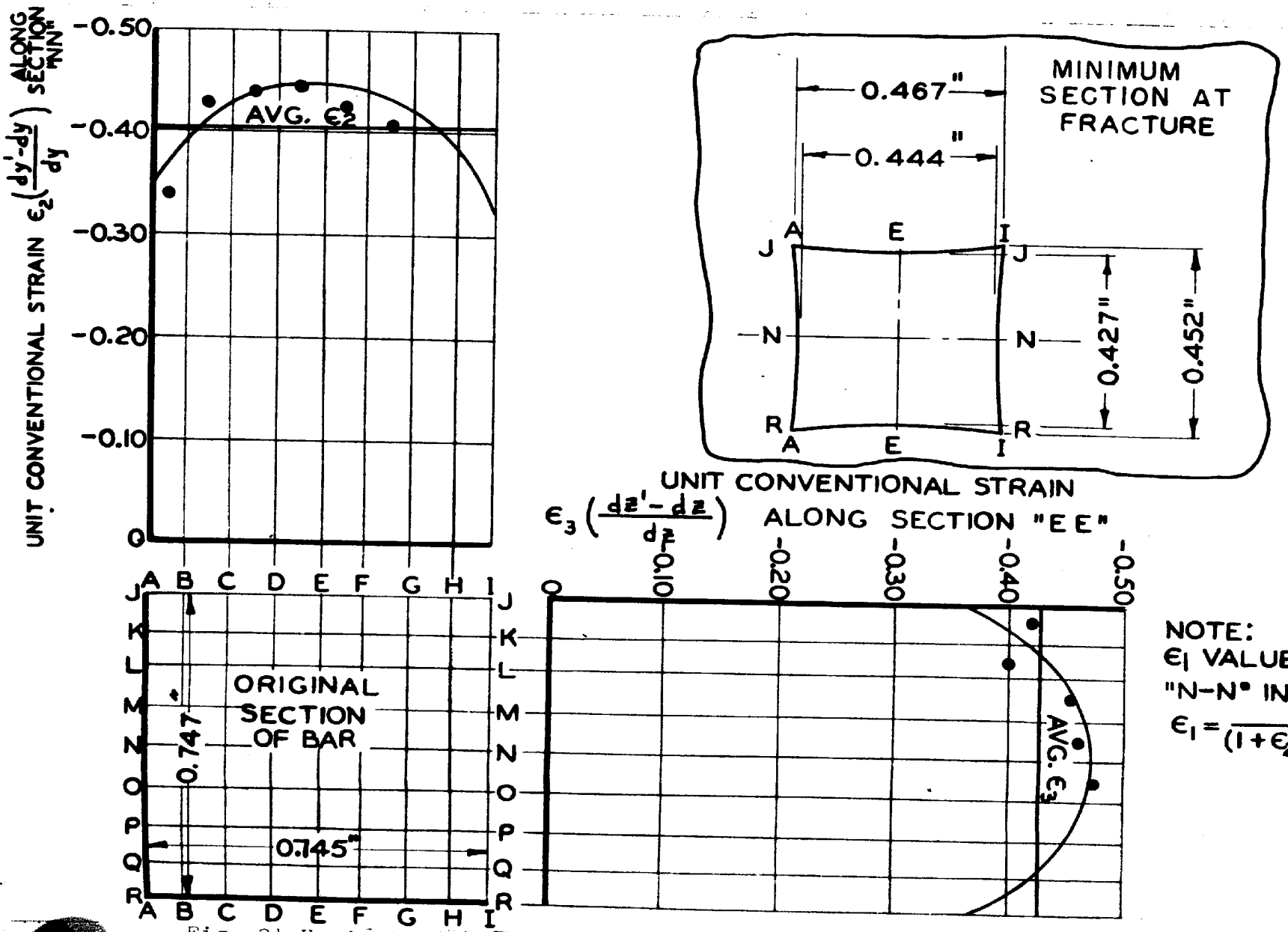

NOTE:
ϵ_1 VALUE AT "E-E"
"N-N" INTERSECTION

$$\epsilon_1 = \frac{1}{(1+\epsilon_2)(1+\epsilon_3)} - 1 = 2.43$$

Fig. 21 Variation of ϵ_2 and ϵ_3 with Their Respective Directions in the Min. Section of Neck of Square Tension Bar. (Specimen 1A ($\frac{b_o}{h_o}=1$) at Fracture)

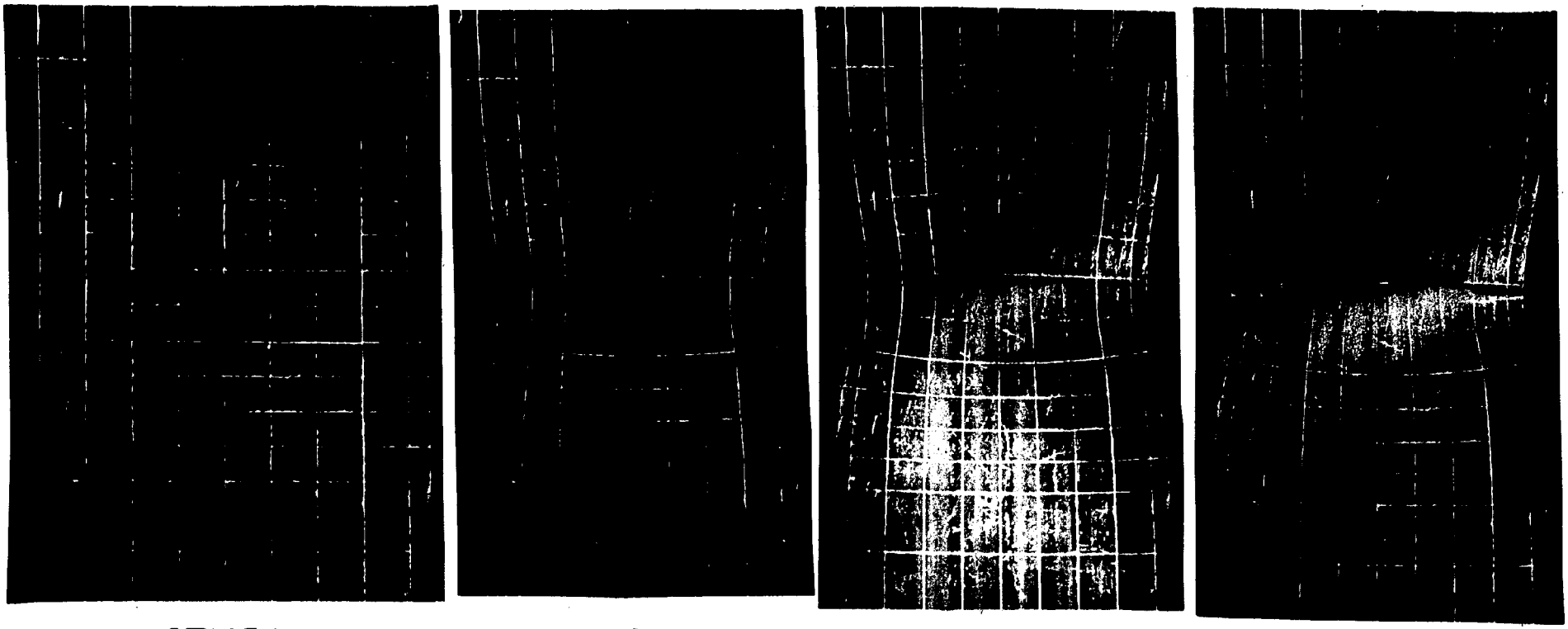

STAGE 1
(AT ULTIMATE LOAD OF 207,800LB.)

2

3

4
(AT FRACTURE LOAD OF
178,000 LB.)

FIG. 22 GRID DISTORTION IN THE DIFFERENT STAGES
OF NECKING IN THE FLAT TENSION BAR
(SPECIMEN 6A)

FIGURES 1 - 13 PART II

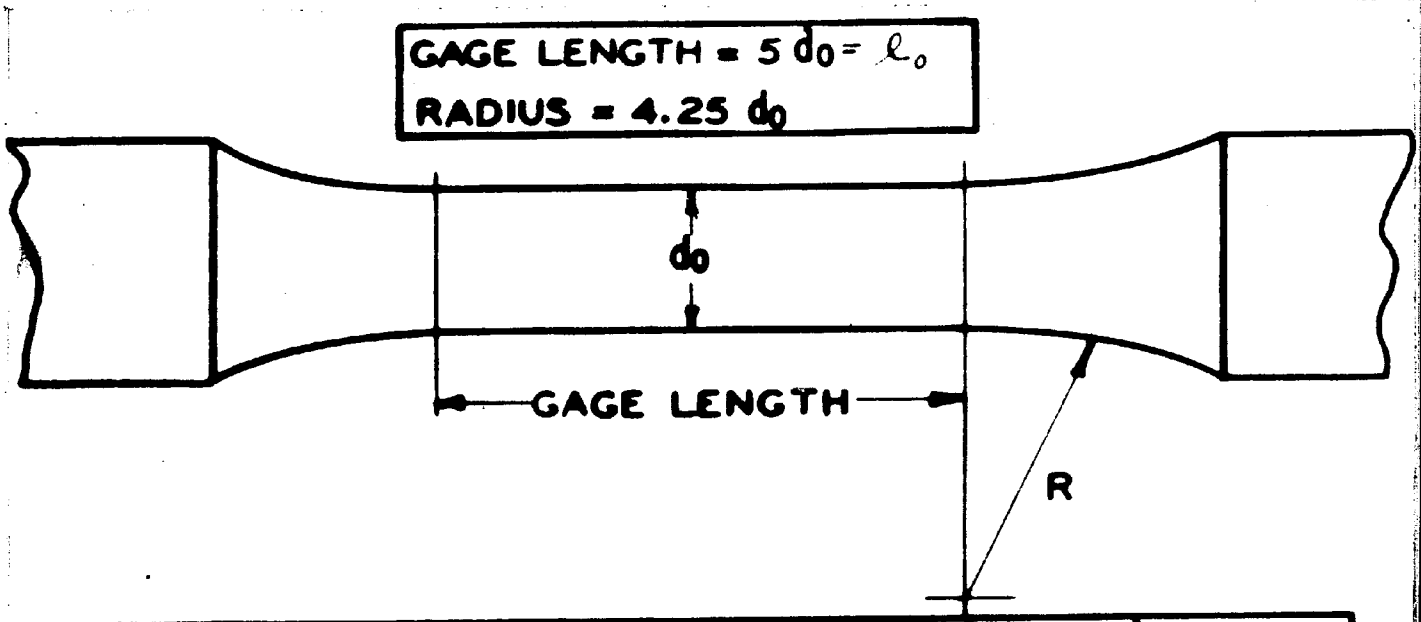

SPECIMEN NO.	DIMENSIONS (INCHES)		
	d_0	ℓ_0	RADIUS
9 10	3.000	15.000	12.750
7 8	1.500	7.500	6.375
1 2	0.750	3.750	3.188
3 4	0.375	1.875	1.594
5 6	0.188	0.938	0.797

THE LARGER SPECIMENS WERE UNDER CUT 1% IN DIA. AT THE CENTER OF THE GAGE TO CONTROL THE FRACTURE LOCATION.

Fig. 1 The Round Bars for the Series on Size Variation

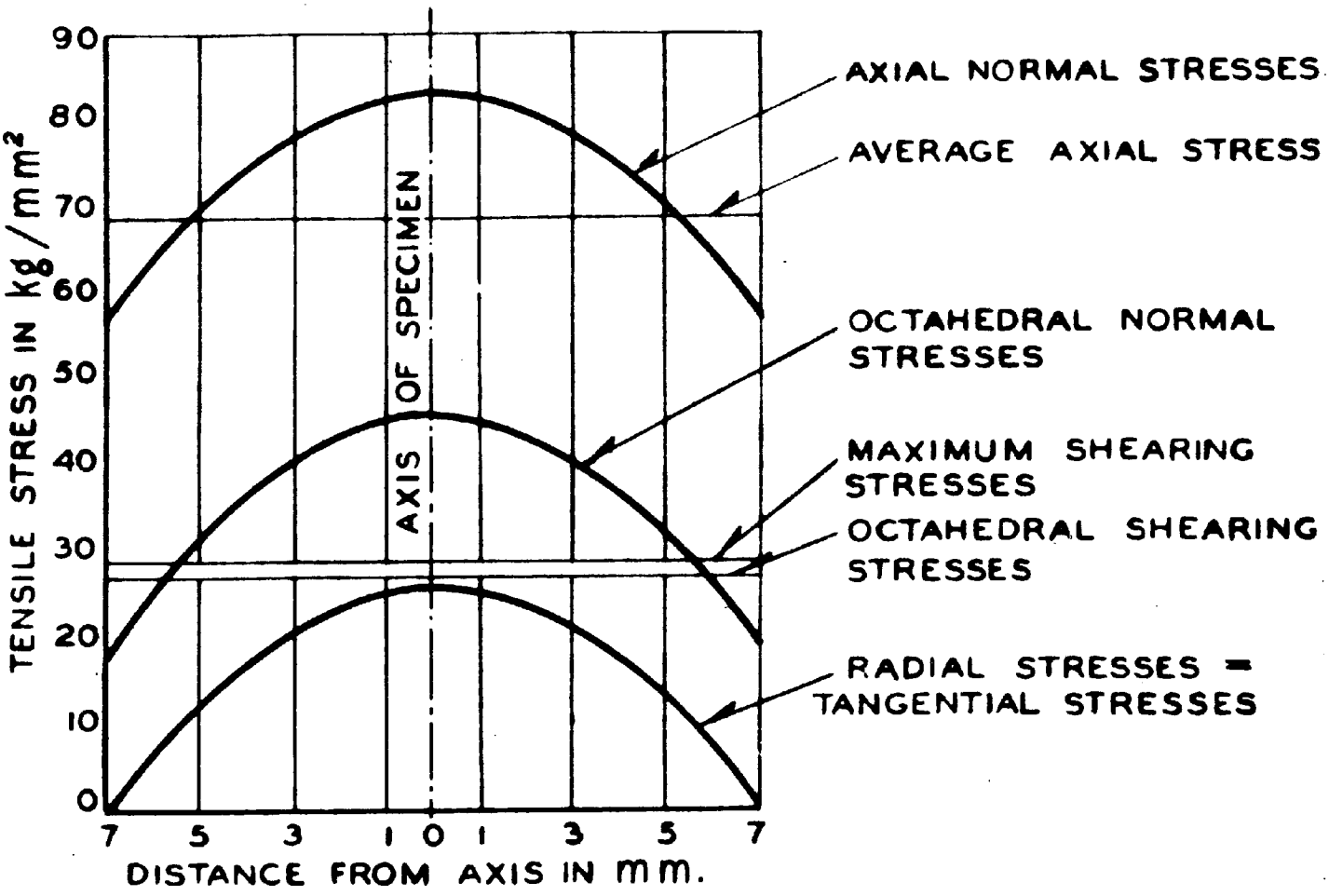

Fig. 2 Distribution of Stresses in the Minimum Section of the Neck of a Round Tensile Specimen According To Davidenkov and Spiridonova (1)

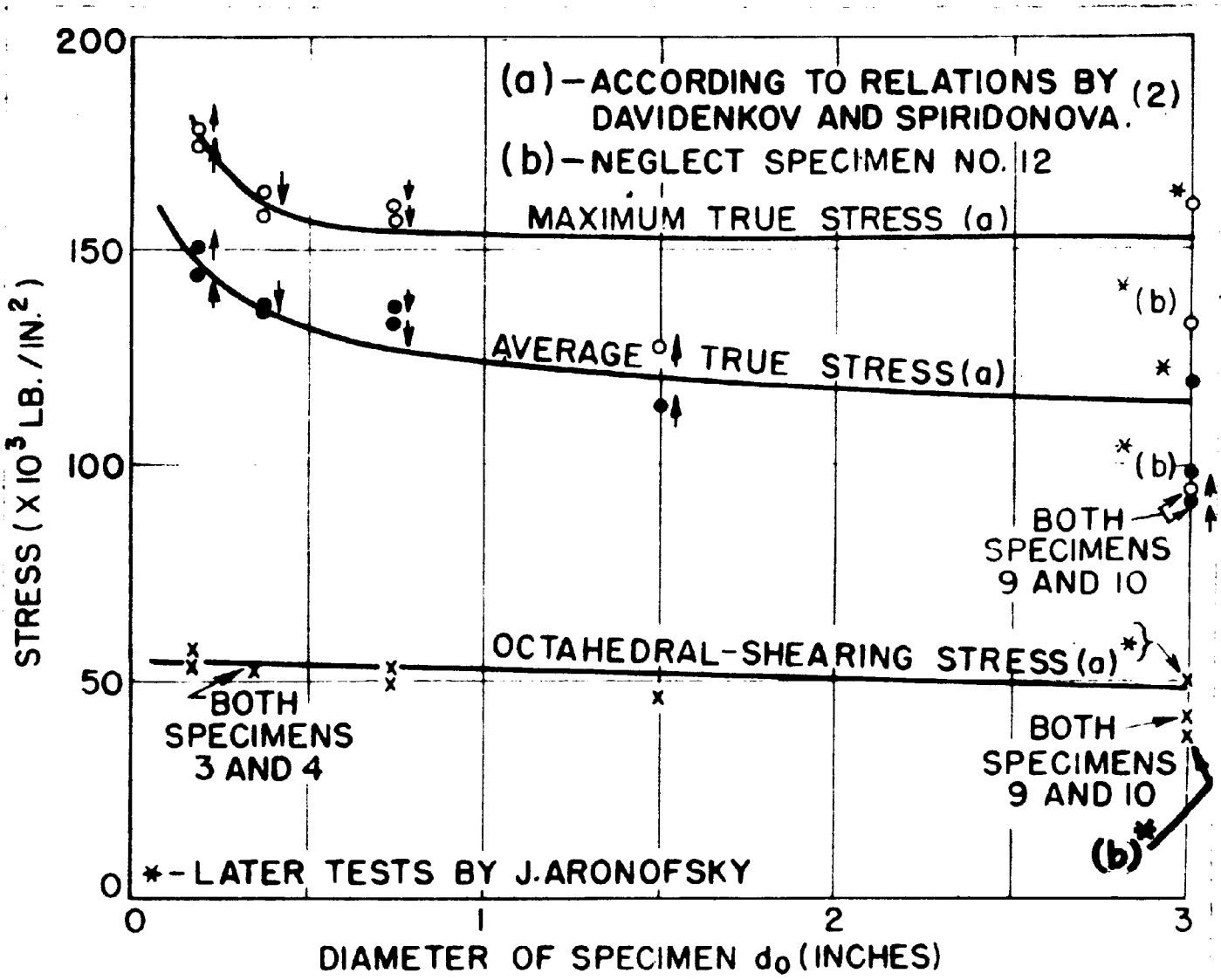

Fig. 3 The Influence of Size of Specimen on Stress in Minimum Section of Neck of a Round Tension Bar at Fracture

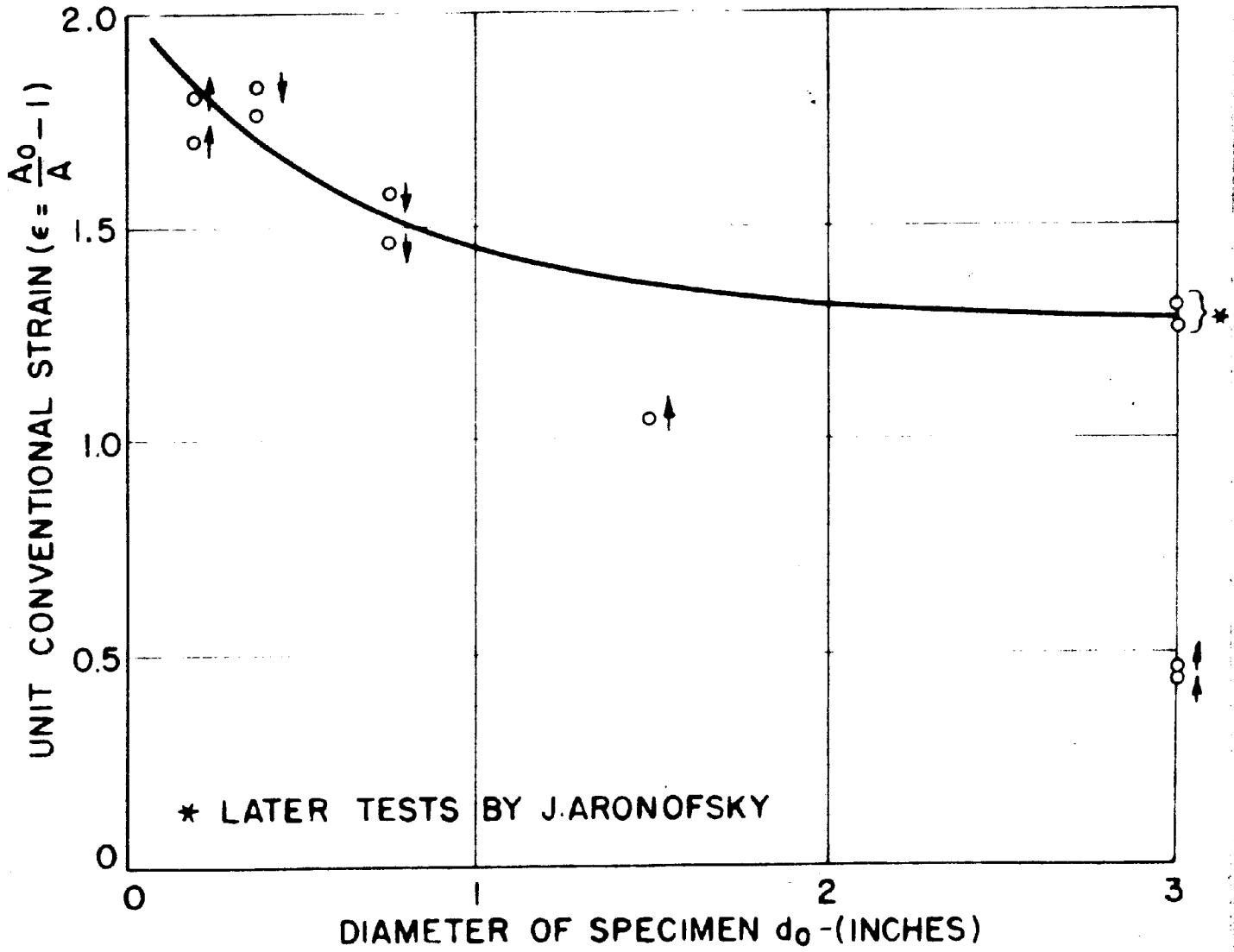

Fig. 4 Maximum Strain at Fracture in Minimum Section of Neck as a Function of Specimen Size

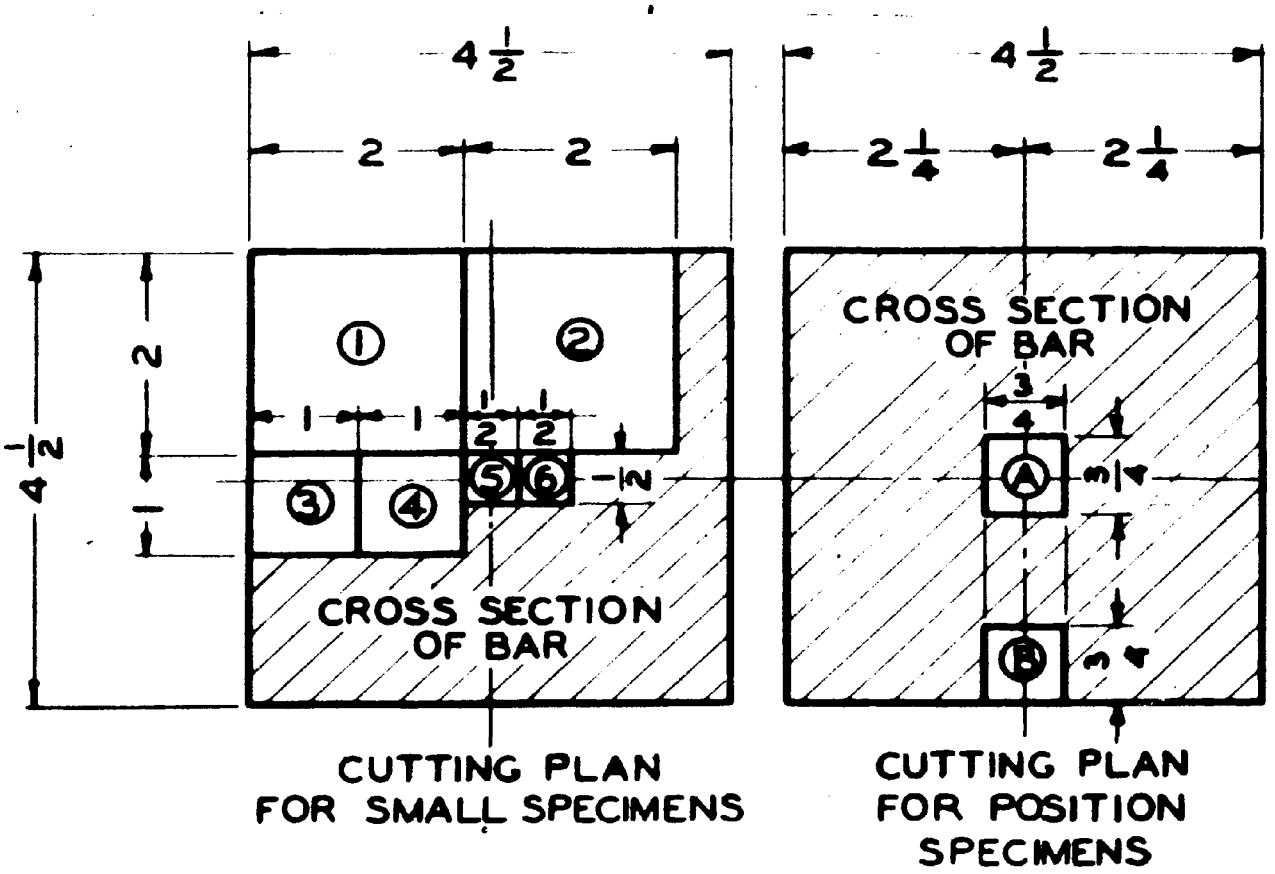

Fig. 5 Cutting Plans for Small Specimens in Round Bar Series

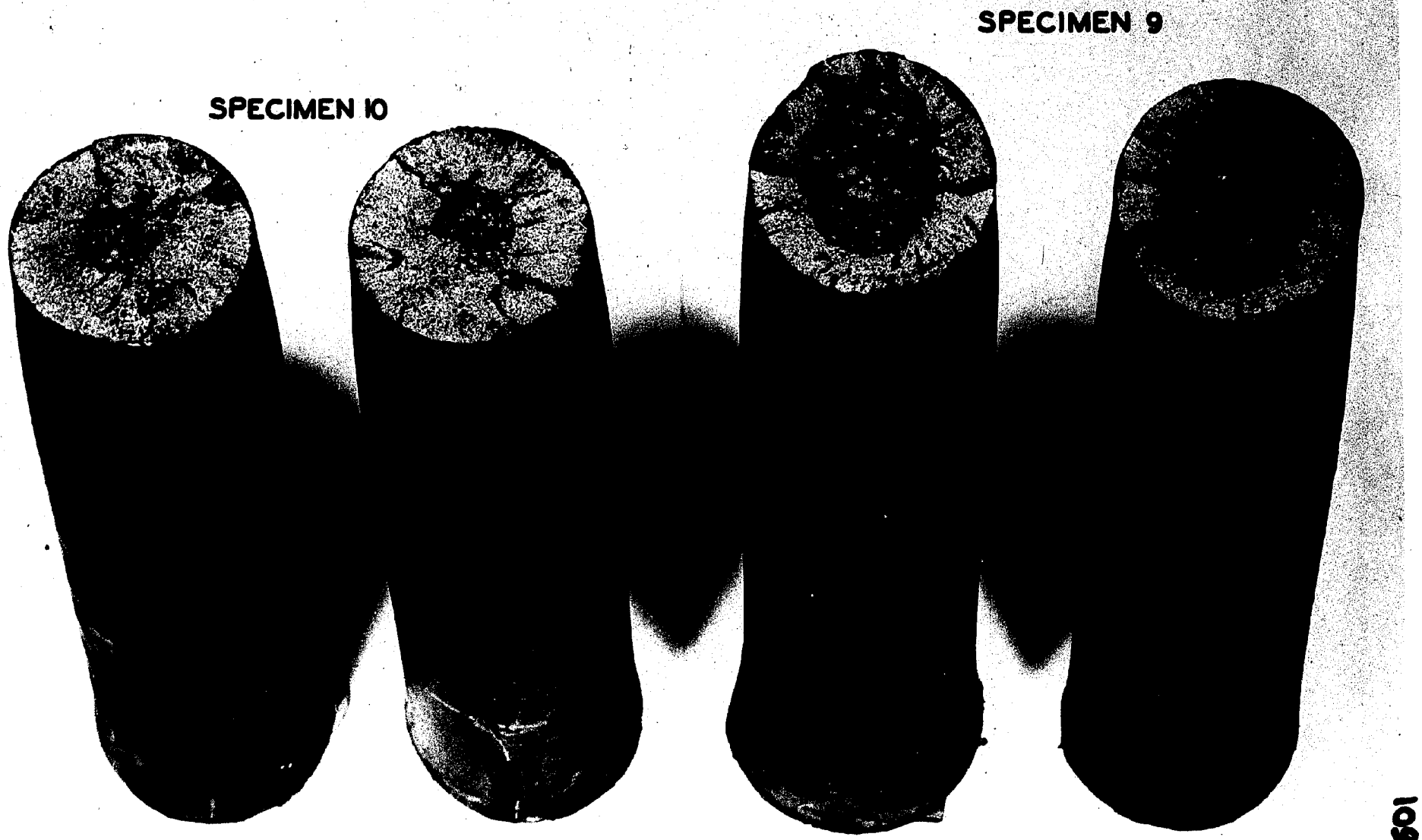

FIG.6 THE FRACTURE SURFACES OF TWO 3" DIAMETER TENSILE SPECIMENS (GAGE LENGTH 15")

FIG. 7

ENLARGED VIEW OF FRACTURE SURFACE OF SPECIMEN NO. 11

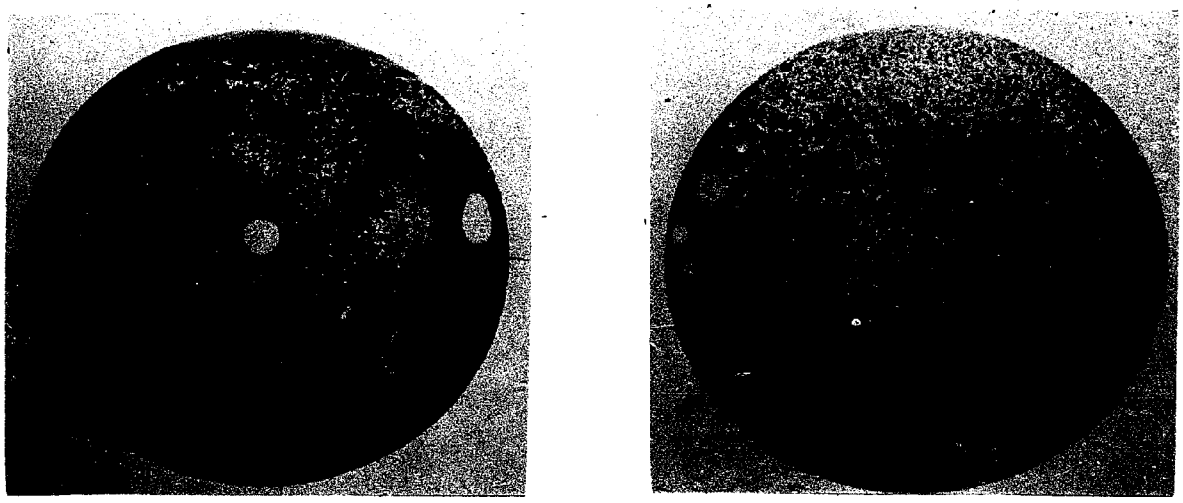

Spec. No. 10 Spec. No. 11

Fig. 8a. Comparison of Sulfur Prints of Cross Sections of Large Bars.

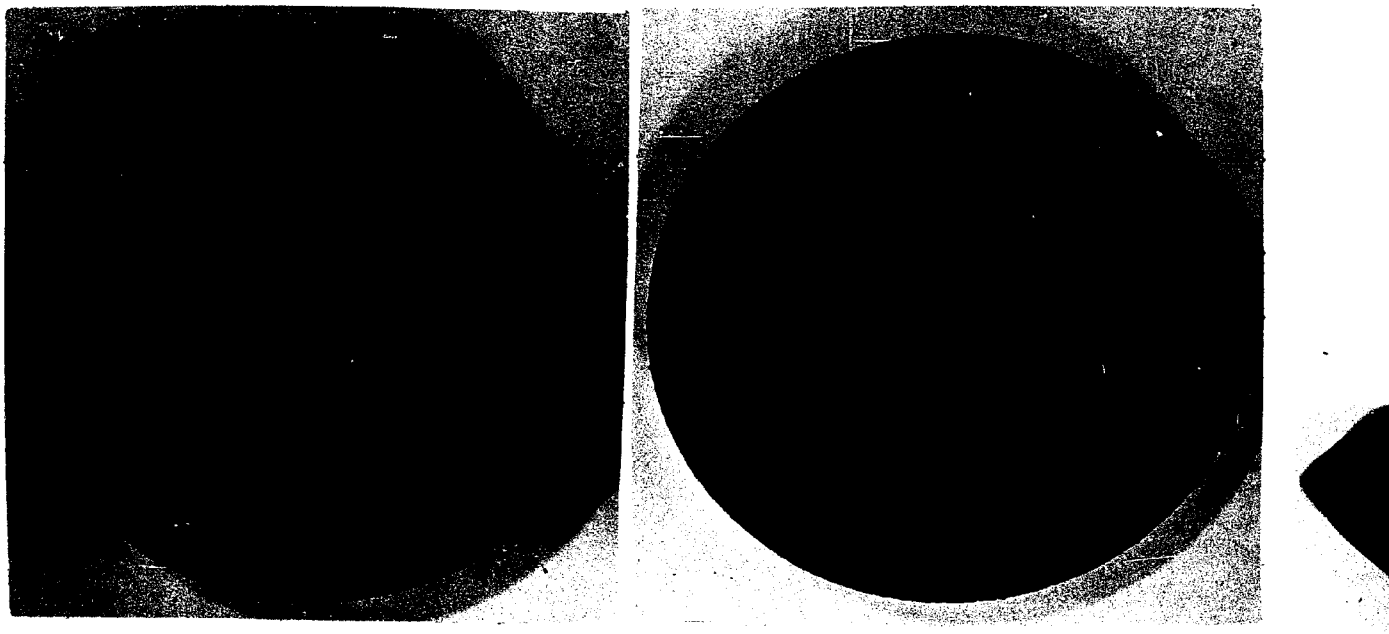

Spec. No. 10 Spec. No. 11

Fig. 8b. Comparison of Macroetches of Cross Sections of Large Bars.

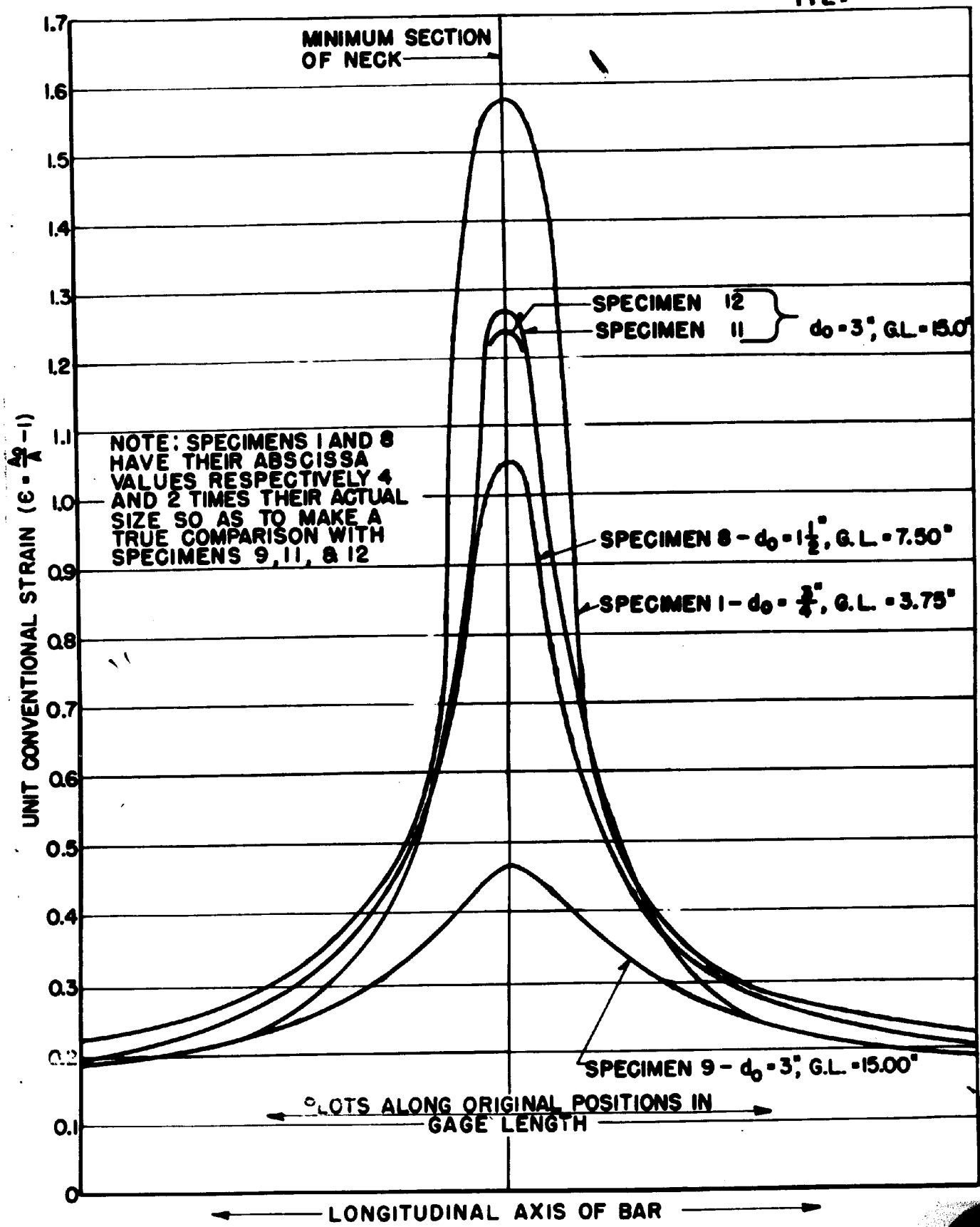

FIG. 9 DISTRIBUTION OF AXIAL STRAIN IN NECK OF A ROUND TENSION BAR AS A FUNCTION OF SIZE OF BAR
(ALL BARS AT FRACTURE)

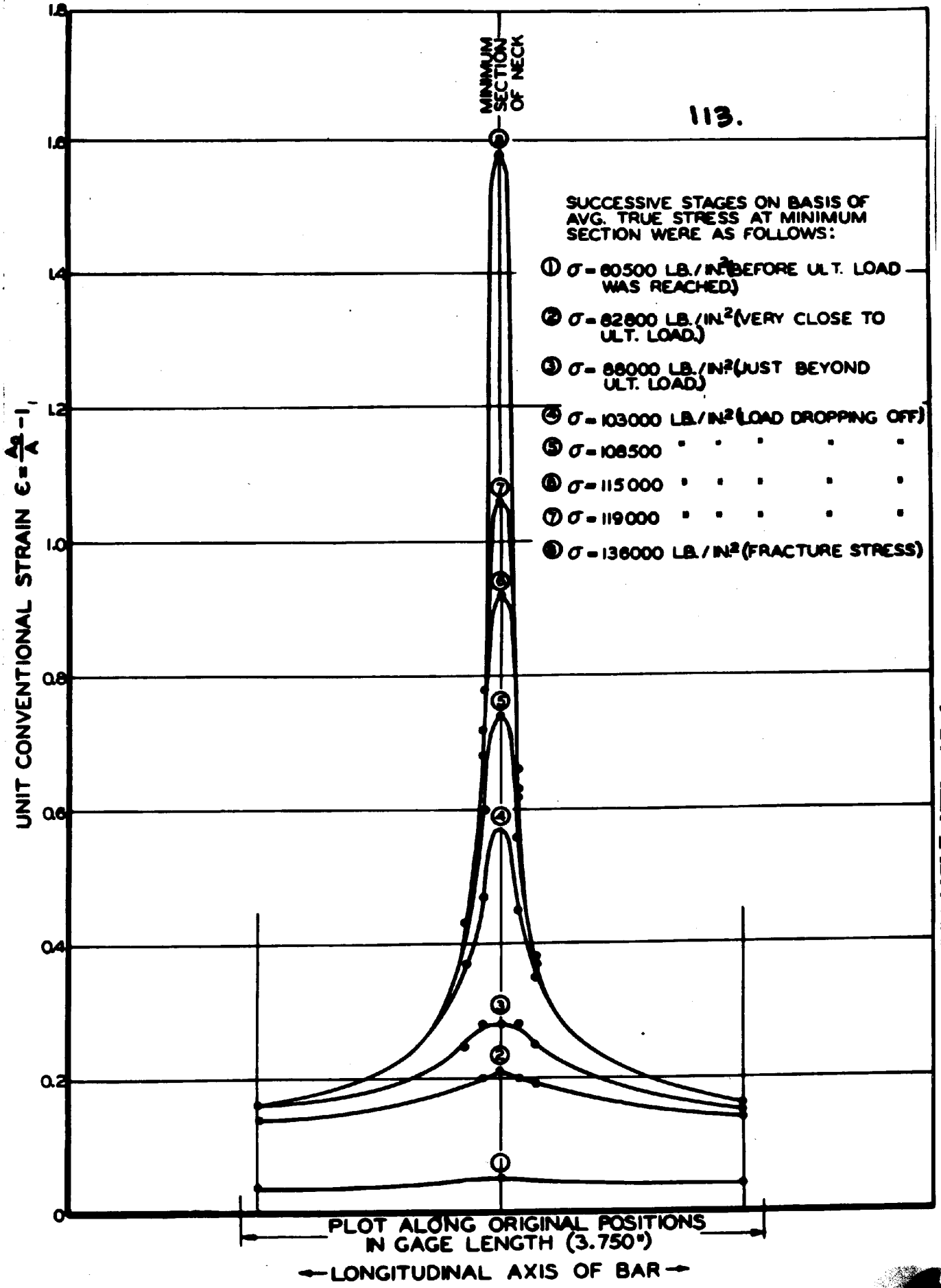

FIG. 10 PROGRESSIVE AXIAL STRAIN DIAGRAMS IN THE NECK OF A ROUND TENSION BAR
(SPECIMEN NO. 1 $d_0 = \frac{3}{4}$")

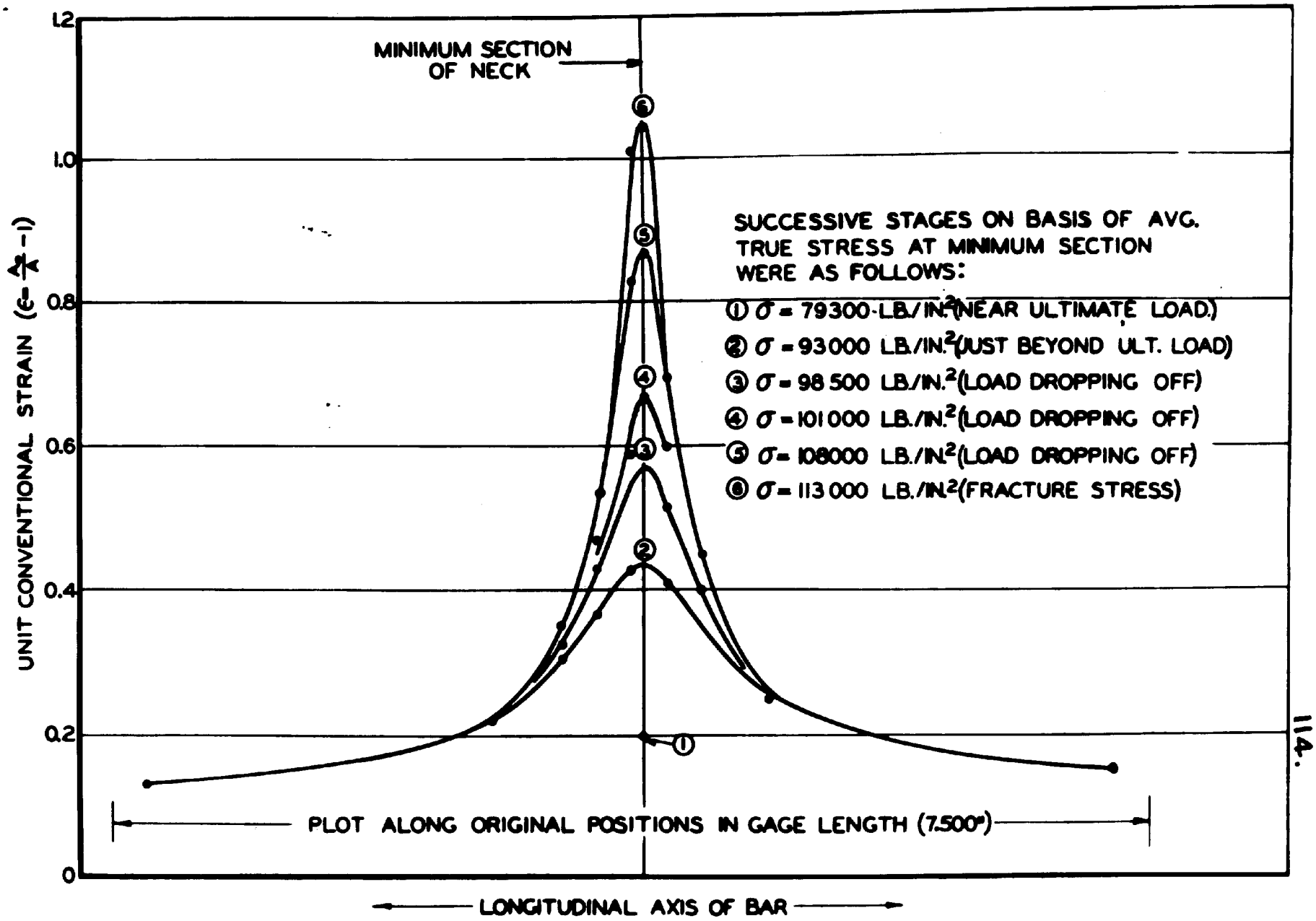

FIG.11 PROGRESSIVE AXIAL STRAIN DIAGRAMS IN THE NECK OF A ROUND TENSION BAR. SPECIMEN NO. 8 ($d_0 = 1\frac{1}{2}$")

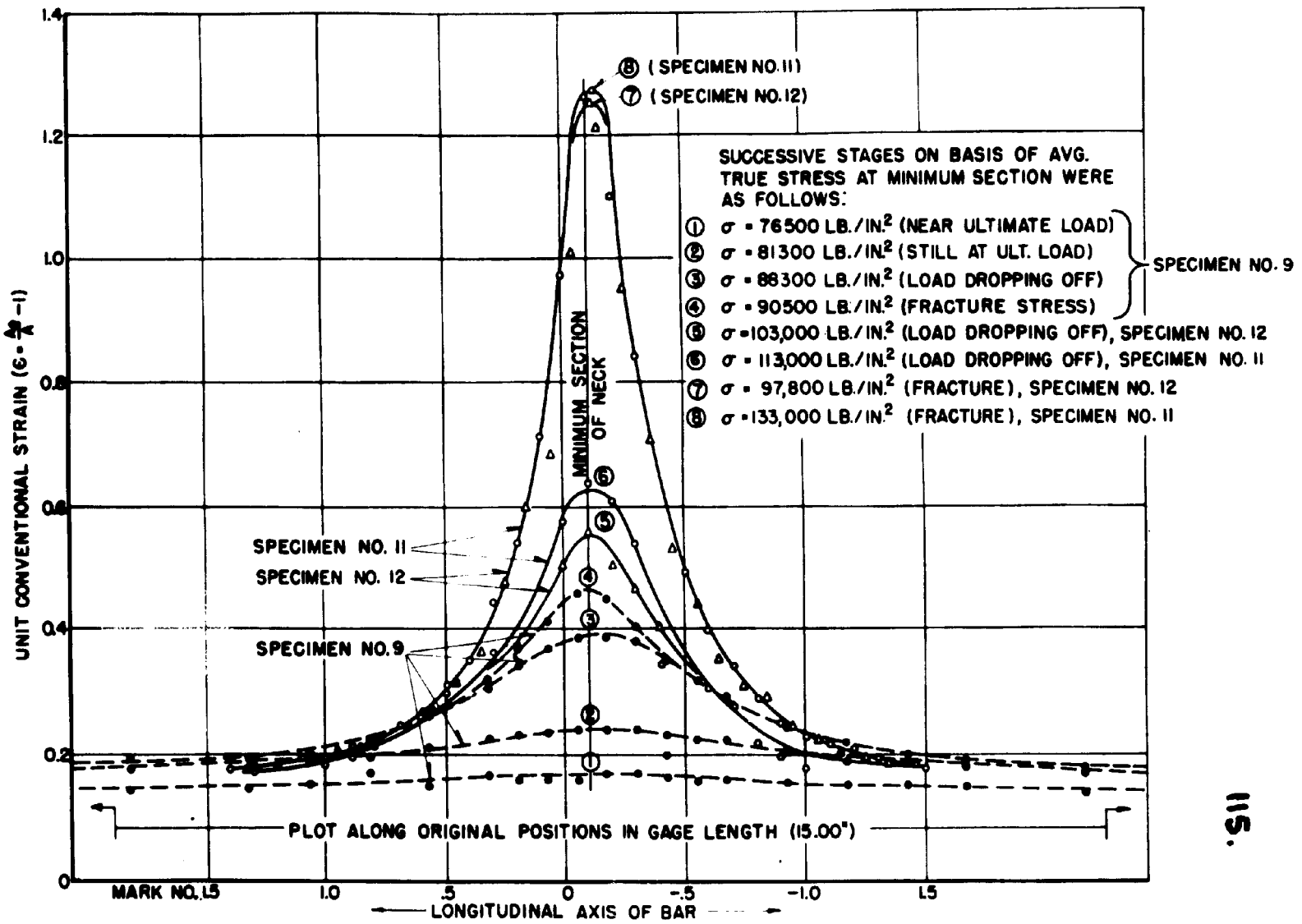

FIG. 12 PROGRESSIVE AXIAL STRAIN DIAGRAM IN THE NECK OF A ROUND TENSION BAR SPECIMEN NO. 9, 11 & 12

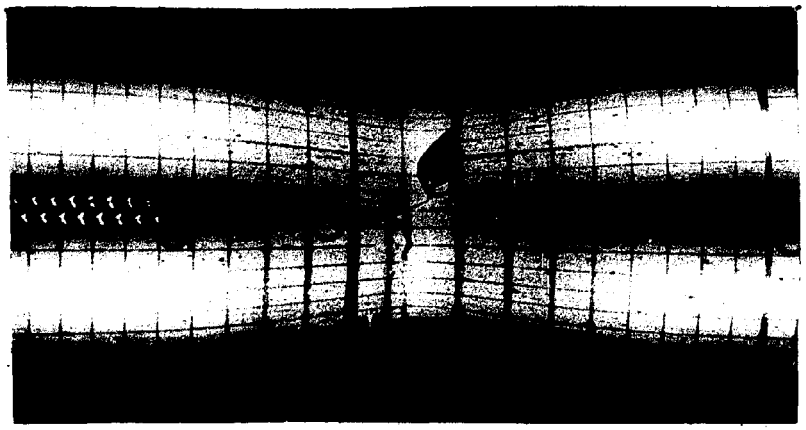

Spec. #11, Orig. Dia. 3", Gage Length 15".

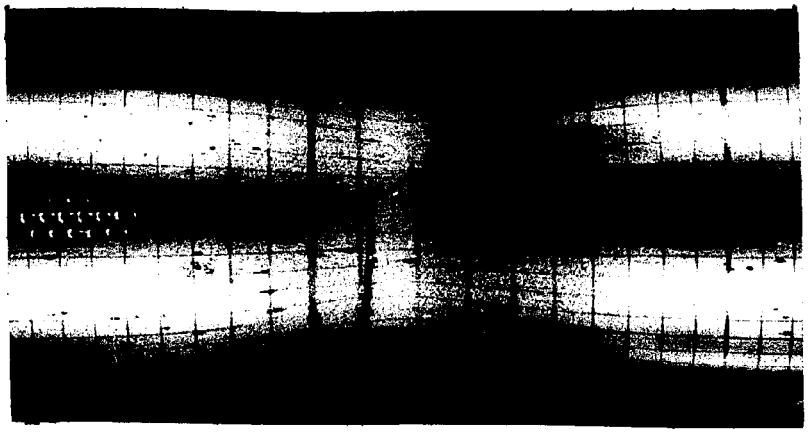

Spec. #12, Orig. Dia. 3", Gage Length 15"

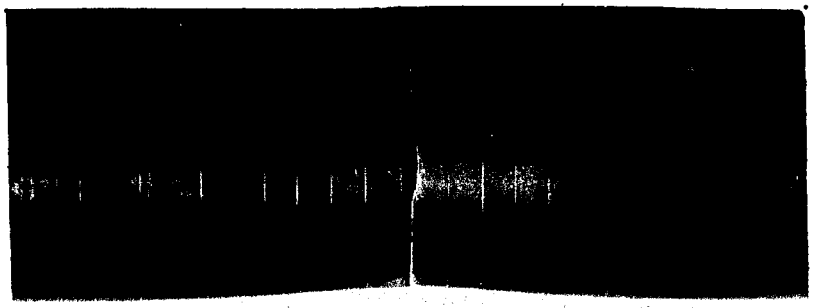

Spec. #10, Orig. Dia. 3", Gage Length 15".

Spec. #9, Orig. Dia. 3", Gage Length 15"

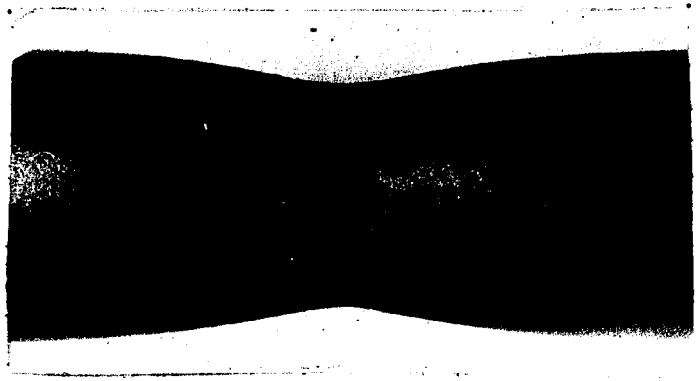

Specimen No. 8. Original Dia. $1\frac{1}{2}$" - Gage Length $7\frac{1}{2}$"

Fig. 13a. The Shape of the Neck of a Round Tensile Bar as Influenced by the Size of the Bar.

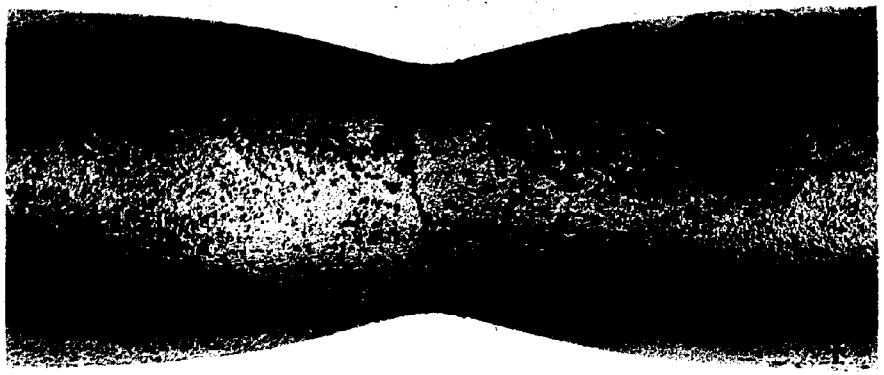

Spec. #1, Orig. Dia. 3/4", Gage Lgth. 3-3/4"

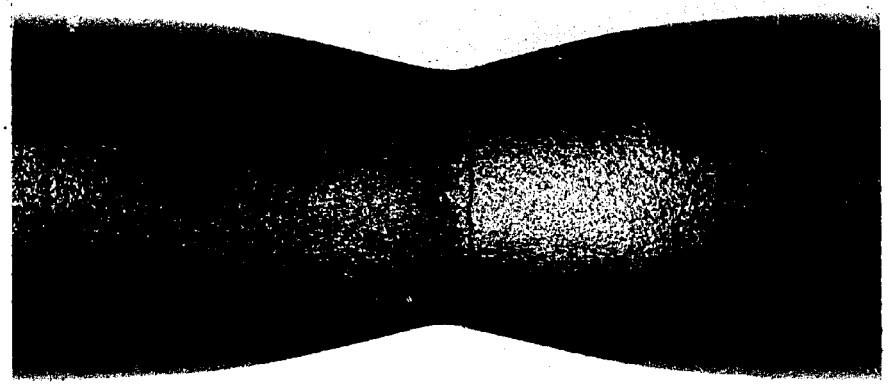

Spec. #2, Orig. Dia. 3/4", Gage Lgth. 3-3/4"

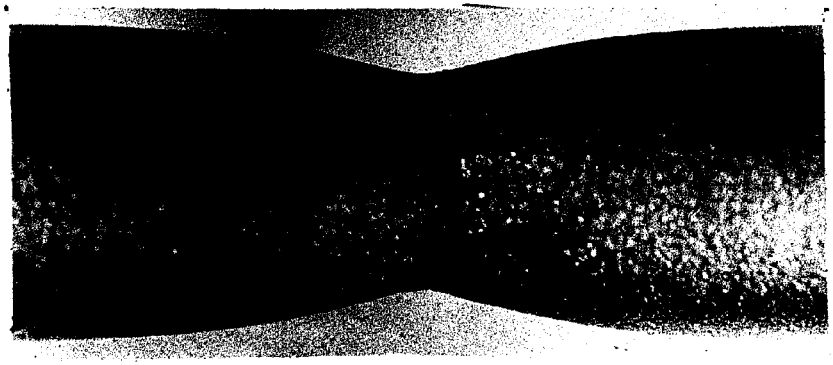

Spec. #3, Orig. Dia. 3/8", Gage Lgth. 1-7/8"

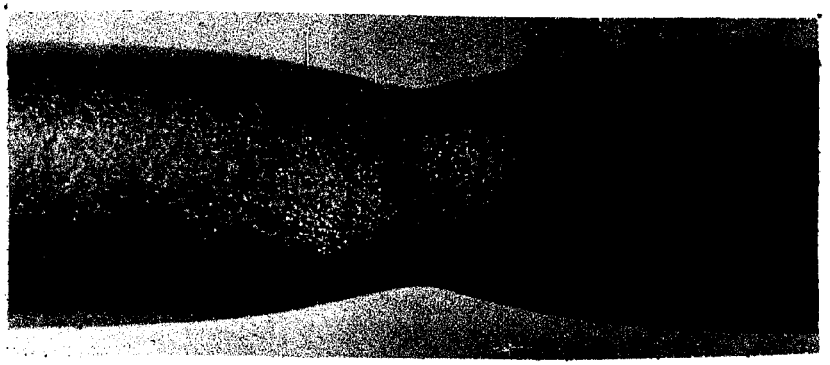

Spec. #4, Orig. Dia. 3/8", Gage Lgth. 1-7/8"

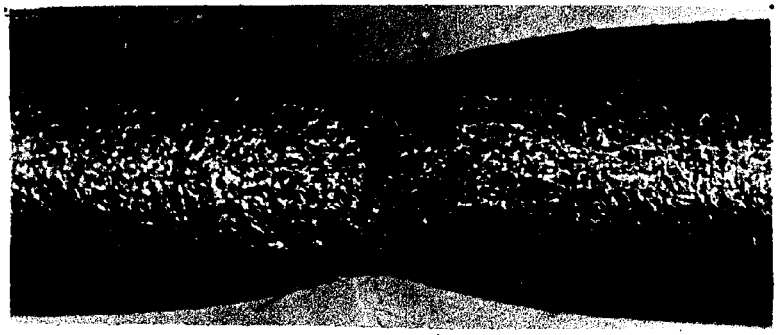

Spec. #5, Orig. Dia. 3/16", Gage Lgth. 15/16"

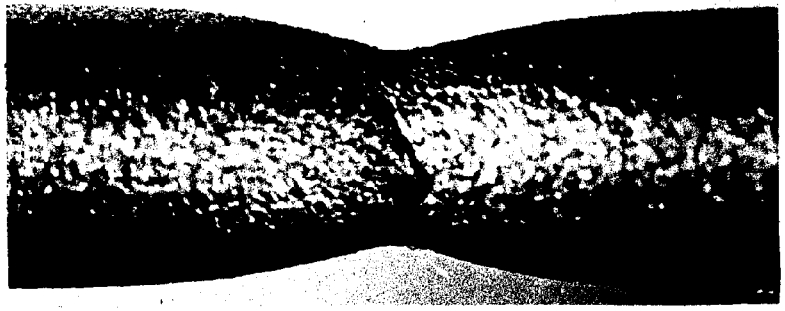

Spec. #6, Orig. Dia. 3/16", Gage Lgth 15/16"

Fig. 13b. The Shape of the Neck of a Round Tensile Bar as Influenced by the Size of the Bar.